AN EXAMINATION OF SOME AROMATIC MOLECULES BY THE METHOD OF ELECTRON IMPACT

Allan Norman Hamer

A Thesis Submitted for the Degree of PhD
at the
University of St Andrews

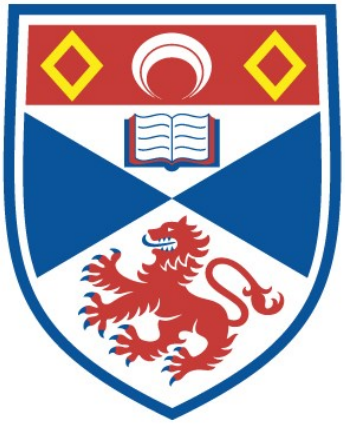

1957

AN

EXAMINATION OF SOME AROMATIC MOLECULES BY THE METHOD OF ELECTRON IMPACT.

Being a thesis presented by Allan Norman Hamer to St. Andrews University, in application for the Degree of Doctor of Philosophy.

MS 2020

DECLARATION.

I hereby declare that, this thesis is a record of my own experimental work, it is my own composition, and it has not been presented previously for a higher degree. The investigation was carried out in the Chemical Research Laboratories of the United College, St. Andrews University, under the supervision of Dr. Charles Horrex.

Allan N. Hamer.

CERTIFICATE.

I hereby certify that Allan Norman Hamer was engaged upon research work for thirteen terms under my supervision; he has fulfilled the conditions of Ordinance No.16(St.Andrews), and is qualified to submit the accompanying thesis in application for the degree of Doctor of Philosophy.

C. Horrex, Ph.D.,
Director of Research.

UNIVERSITY CAREER.

I entered the United College, St. Andrews University in October 1948 and graduated B.Sc. with First Class Honours in Chemistry in July 1952.

The work described in this thesis was carried out in the United College under the direction of Dr. Charles Horrex during the period July 1952 - November 1955, inclusive.

ACKNOWLEDGEMENTS.

In the first place I am indebted to Dr. Charles Horrex for the services which he rendered as Director of Research, and to Professor John Read for the provision of facilities which enabled this work to be carried out. My thanks are due also to the Carnegie Trust for the Universities of Scotland, for the award of a research scholarship, and to Shell Research Ltd., for a small grant which allowed me to complete the investigation.

The amount of work involved in building the mass spectrometer demanded some co-operation with others, to which reference is made in the relevant place. In particular I wish to thank Mr. D. Calvert for his interest and assistance on many occasions, also Mr. G.U. Ferguson and members of the Physics and other departments for advice on electronic matters, and Mr. G.W. Downs who acted as scribe during most of the measurements of appearance potentials. I am grateful also to Dr. J.Y. Macdonald and Messrs. R. Morris and G. Wood who produced the photographs.

SUMMARY

The thesis begins with an account of the behaviour of molecules on electron impact, and explains how bond dissociation energies may be deduced from a study of ionization processes.

The experimental work was carried out with a mass spectrometer designed and built for the purpose, and a full description of this instrument is provided, together with an account of the problems which arose during its construction and development, and the performance of which it was ultimately capable.

After the reliability of the instrument had been tested by investigating some simple ionization processes, it was used to study the formation of benzyl ions from a number of related aromatic compounds. When the appearance potentials obtained in this way are combined with the ionization potential of the benzyl radical (which is the subject of a separate and direct determination) it is possible to make provisional estimates of the benzyl-X bond energy in dibenzyl, benzyl chloride, and benzyl iodide. The derived value of $D(PhCH_2-CH_2Ph)$ is used to verify Szwarc's value of 77.5 kcal for $D(PhCH_2-H)$. From this quantity, the following bond energies may be deduced thermochemically: $D(PhCH_2-CH_2Ph) = 45 \pm 3$ kcal;/

45±3 kcal; $D(PhCH_2-CH_3)$ = 63±3 kcal; $D(PhCH_2-Ph)$ = 74.4±3 kcal, $D(PhCH_2-I)$ = 36.6±4 kcal; $D(PhCH_2-Cl)$ = 62±4 kcal. The last two values are confirmed by the direct electron impact data. Lastly, an indirect estimate of I(Ph) = 9.7 eV is based on a measurement of the appearance potential of this radical from benzene, and a thermochemical value for D(Ph-H).

The thesis ends with a description of how the instrument was modified by the inclusion of a reactor furnace in order to study the mechanisms of thermal decomposition reactions. Results are included of a brief experiment involving the pyrolysis of benzyl iodide carried out by this means.

CONTENTS.

LIST OF ILLUSTRATIONS.

FIGURE 1.

Fig. 1.

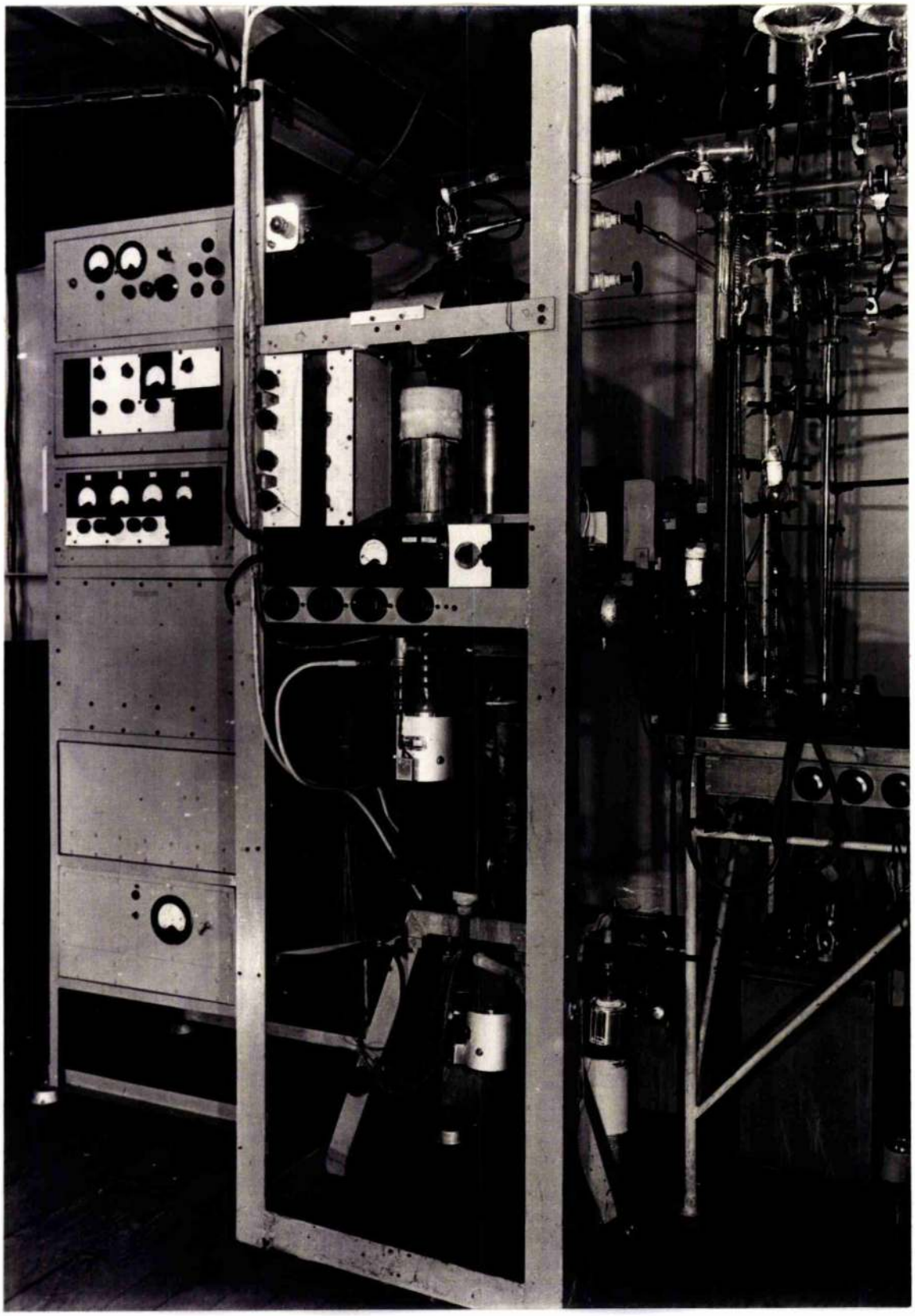

PART I

THE PRINCIPLES UNDERLYING THE DETERMINATION OF BOND DISSOCIATION ENERGIES BY THE METHOD OF ELECTRON IMPACT.

INTRODUCTION

Reactivity is a fundamental interest of the chemist. After characterisation, each new compound is examined with a view to understanding its behaviour in different environments, and this knowledge can be gained only by a study of dynamic as well as static systems. Even in the most simple cases, the experimental problems posed by the former type are the more difficult, and for this reason the complete investigation of the functioning of a living cell, whose metabolism consists of a complex balance of labile materials, is a problem which will tax all his available resources for many years.

A chemical change can be defined by the stoichiometry of the products and reactants, and its practicability assessed from their bulk properties. However, classical thermodynamics is unable to predict the rate of a permissible process, and this vital information must be sought elsewhere. A full appreciation of chemical reactivity requires a knowledge of molecular structure, and the mechanism of the change must be approached in terms of structural alterations governed by considerations of geometrical factors and fields of force. The geometry of molecules has been studied with increasing precision for several decades and stereochemistry now contains a large body of accurate data. By contrast, although thermochemistry could/

could supply precise information about the energy differences between initial and final states, little was known until recently of the energy required to extend or rupture individual links. Since chemical reactions occur by the breaking and making of bonds, a knowledge of these factors is of fundamental interest.

The practical determination of bond dissociation energies may be carried out in various ways. In a few cases the equilibrium between a molecule and its dissociated products can be studied over a range of temperatures and a heat of dissociation deduced. More often, dissociation is induced by the application of energy in a controlled way.

The use of the energy of light has allowed very accurate values of the dissociation energy of diatomic molecules to be deduced from molecular spectra. Occasionally, difficulties in the interpretation of a spectrum have resulted in a number of equally plausible values being produced, each of which is known to a high degree of precision, as in the case of carbon monoxide. Unfortunately the spectra of polyatomic molecules are too complex for reliable values of bond dissociation energies to be deduced.

In gas phase reactions, energy is supplied to the participants by molecular collisions, and the first step is often the dissociation of a weak bond. In kinetic work an attempt/

attempt is made to arrange conditions so that this process is the rate determining step, in which case the activation energy deduced from the kinetic data may be identified with the energy required to break the bond. In spite of the experimental difficulties the field has proved a fruitful one, and many data concerning bond dissociation energies have been deduced in this way.

Energy may be supplied to molecules in the gas phase by bombardment with electrons of controlled energy, and this direct and versatile technique forms the subject of the work described in this thesis.

A research team in St. Andrews has been engaged on a study of the behaviour of a variety of compounds during thermal decomposition, by the chemical kinetic method, and the choice of substances in the studies of the author was determined, in part, by a desire to supplement existing data on these compounds using an alternative technique. At the beginning of this work, no electron impact data were available for these molecules except for an early study of benzene (1) and some measurements of ionization potentials. During the course of the investigation several papers appeared dealing with the application of electron impact methods to various aromatic molecules, but some of the results were difficult to correlate with each other, and with existing thermal data.

An/

An effective study of the products of electron impact on polyatomic molecules requires some form of mass analyser, and a mass spectrometer is ideal in this respect. Although no electron impact work had been attempted previously in St. Andrews, a mass spectrometer had already been constructed, but it was adjudged unsuitable for this investigation. This thesis therefore contains details of the instrument which was designed and built by the author for this purpose.

In principle, the determination of ionization and appearance potentials by a mass spectrometer is not a very involved process, but in practice there arise a number of serious complications. Some of these factors are instrumental while others are peculiar to the substance under investigation. Most determinations have been made with one of a very few models of commercial instruments, the users of which have had the benefit of a wide range of manufacturers' operating experience. Since there are many points in mass spectrometry where optimum instrumental behaviour has been achieved semi-empirically, it is desirable to have these fundamental molecular quantities determined on instruments which are not identical. Even the small departures from conventional design which were made in our instrument resulted in considerable time being spent on preliminary adjustments and modifications. It was gratifying to find, as shown later,

that in the case of the inert gases, and some organic compounds where difficulties peculiar to the substance do not arise, the derived ionization potentials are in good agreement with those of other workers and with spectroscopic values. On the other hand the author has to conclude that the ionization and fragmentation processes are not simple in the case of other organic compounds, and unfortunately for the applicability of the method, this opinion is growing in recent publications on the technique.

THE IONIZATION OF MOLECULES BY ELECTRON IMPACT

A given molecule can possess electronic, vibrational, rotational and translational energies; the first three are quantised. Excitation by irradiation, or by collision with a high energy particle may induce permitted transitions between these quantised energy levels, which may be accompanied by a change in the kinetic energy of the system. The internal energy of a molecule is defined chiefly by its electronic state, while the vibrational and rotational levels provide decreasing contributions. Only certain transitions are likely to occur, in accordance with the Franck-Condon principle that vertical excitation has maximum probability. The rule implies that the time for a transition is small in comparison with the period of vibration, and was formulated

to/

FIGURE 2.

Fig. 2.

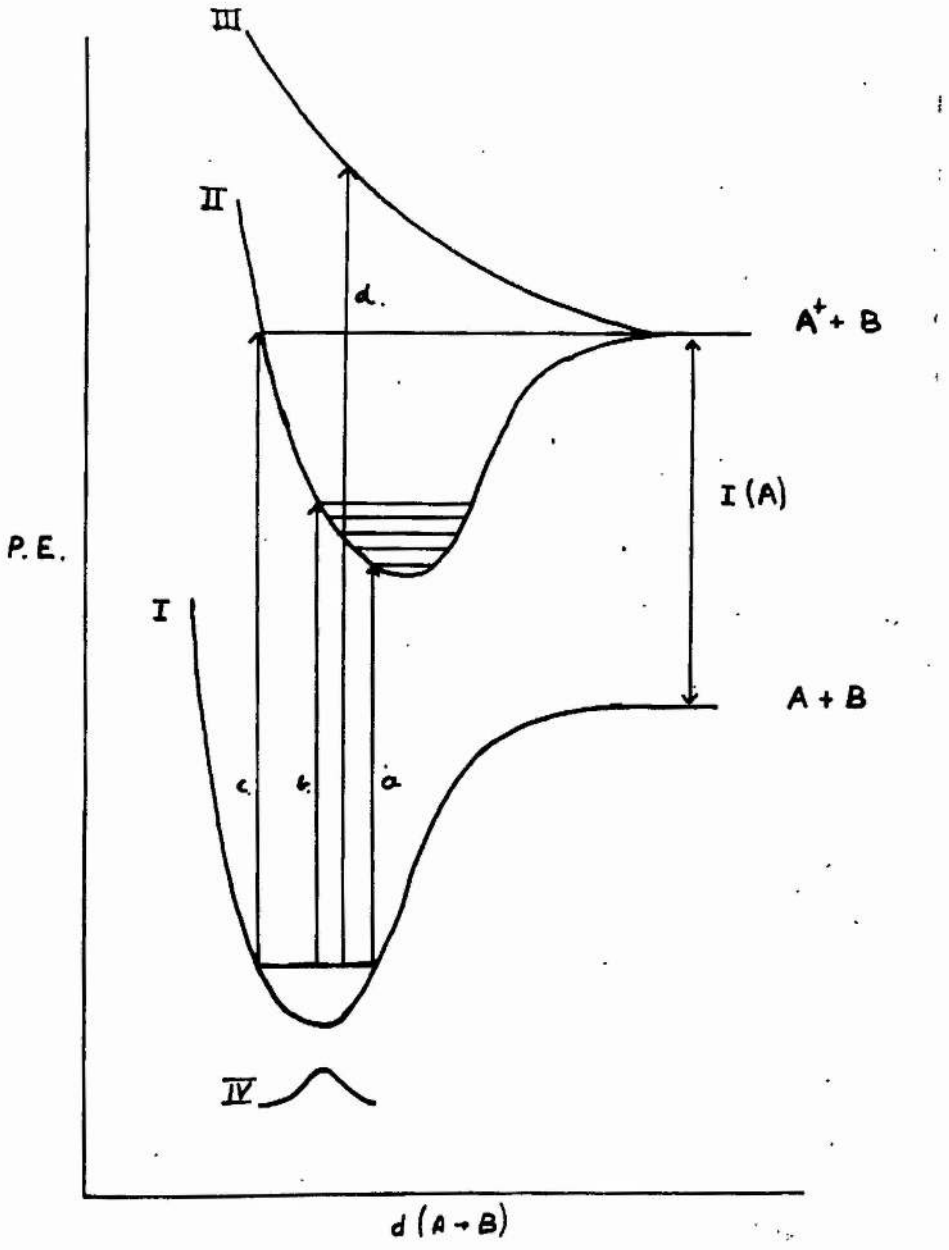

Potential energy diagram for a diatomic molecule.

to explain photochemical dissociation (2) (3). It was soon extended to include excitation by electron impact (4).

The possible situations which may exist during the bombardment of a diatomic molecule by an electron are shown in Fig. 2. The lowest curve I is the potential energy diagram for the molecule A-B in the ground state, while the behaviour of the ionized molecule is represented by curve II. The permitted levels of vibrational energy are shown in each case, and at room temperature most molecules are in the ground state. Gradual addition of energy to the molecule by means of low energy collisions excites each vibrational level in turn until the convergence limit is reached when dissociation occurs. This is the mechanism of thermal decomposition. Transitions to higher electronic states result from collision with energetic particles, such as electrons, suitably accelerated. Typical examples are shown in the diagram and their relative probabilities are governed by the appropriate eigen-functions (curve IV) for the molecule in the ground state. The consequences of the respective transitions depend on the relative positions of the two curves. Thus (a) represents the ionization potential of the molecule A-B, (b) is a transition in energy, greater than I(A-B) by several vibrational energy terms, while (c) corresponds to the appearance potential of the ion A. Ideally, the sensitivity/

sensitivity of the equipment should be great enough to detect transitions between the two ground vibrational states, but if the probability of this process is low, a more likely transition such as (b) may represent the limit of response. In this case the vertical ionization potential derived from the electron impact experiment will differ from the adiabatic ionization potential obtained from convergence limits in spectra. Claims have been made that significant differences have been observed in practice (5) (6). Some excited states may be unstable (curve III) in which the forces between the constituent atoms are always mutually repulsive. Any transition to such a state (d) would result in immediate dissociation.

Excitation of polyatomic molecules causes the perturbation of complex vibrational degrees of freedom, which results in the production of a variety of fragments whose abundance is determined by the shape of the appropriate potential energy surface. In such cases, the time which elapses prior to dissociation may increase sufficiently for hydrogen transfer to occur. Thus the principal fragment of butyric acid has been proved to be CH_3COOH^+ (7).

Electron impact phenomena may be classified into various types:-

$$A\text{-}B + e \longrightarrow A\text{-}B^+ + 2e/$$

$$A\text{-}B + e \longrightarrow A\text{-}B^{+} + 2e$$
$$\longrightarrow A^{+} + B + 2e$$
$$\longrightarrow A^{+} + B^{-} + e$$
$$\longrightarrow A + B^{-}$$

None of the first three processes is subject to a rigid energy restriction, any excess kinetic energy being disposed of by the electron. On the other hand, the last example is one of resonance capture, and occurs at a sharply defined electron energy.

Since the formation of an ion may take place in a number of different ways which are accompanied by dissimilar changes in energy, it is necessary to identify all the products if an unequivocal value for the bond energy is to be deduced. Negative ion formation is unimportant in electron impact work on most hydrocarbon compounds, as its occurrence is usually confined to molecules containing many electronegative atoms. Thus although carbon tetrachloride dissociates to $CCl_3^+ + Cl^-$, methyl iodide yields $CH_3^+ + I$. On the other hand a positive ion may arise by either of two processes of differing endothermicity, and these must be distinguished from one another. Methane may yield the methylene radical ion in either of the following ways:- (8)

$$CH_4 \longrightarrow CH_2^+ + H_2 + e \quad A(CH_2^+) = 15.3 \text{ e.V.}$$
$$\longrightarrow CH_2^+ + 2H + e \quad A(CH_2^+) = 20.1 \text{ e.V.}$$

THE ELECTRON IMPACT METHOD

The basic operation consists of the ionization of an injected stream of molecules by a collimated electron beam whose energy is closely controlled. The resulting ions are removed from the ionization chamber and accelerated through several kilovolts to minimise the effects of inequalities in initial energy. They are identified according to their e/m ratio by the action of a magnetic field, and estimated quantitatively by some form of electronic detector. The ionization efficiency curve is determined by observing the change in ion current which results when the electron energy is varied, and the appearance potential of the ion is deduced from this curve by a suitable extrapolation procedure.

IONIZATION EFFICIENCY CURVES

The shape of a typical appearance potential curve is shown in Fig 3. Above the threshold voltage, the linear portion BC shows the dependence of ionization cross section on the electron energy. The foot of the curve DE is essentially logarithmic in character and in part is due to the thermal energy spread of the electron beam. At high collisional energies, the efficiency of the ionization process reaches a maximum and the curve levels off.

FIGURE 3.

Fig. 3.

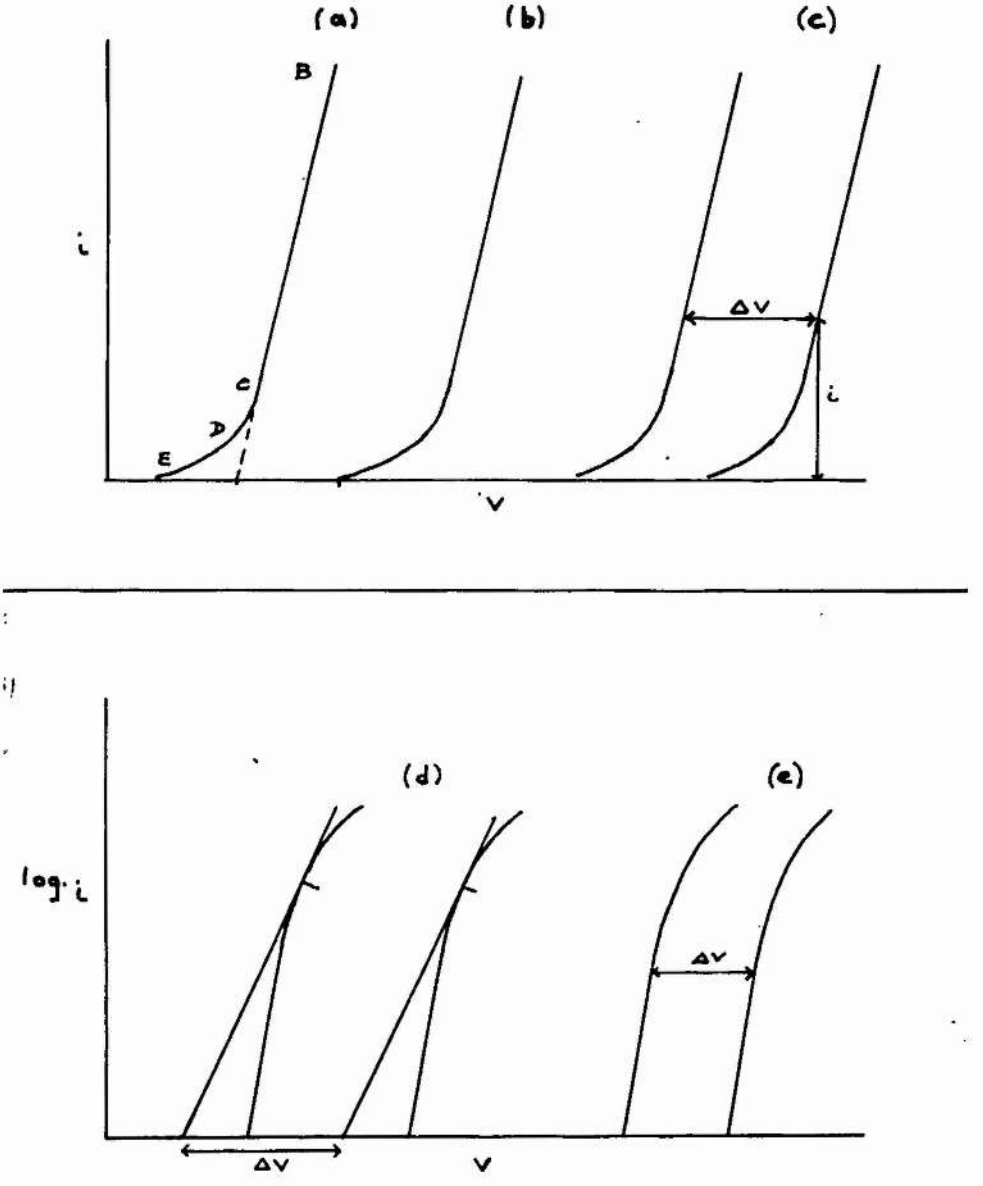

Methods of extrapolating I.E. curves.

(a) Linear extrapolation

(b) Initial upward break

(c) Warren's method

(d) Honig's critical slope

(e) Empirical treatment of semi-log plot.

Several theories have been put forward to account for the shape of the lower parts of these curves, which have met with varying degrees of experimental support. Robertson (9) assumes that the ionization probability is proportional to the difference between the electron energy and the ionization potential, whereas Honig (5) finds that the square of this parameter is in better accord with experimental data, for energies near the threshold voltage.

Other factors contribute to the overall shape of the curve. Kinetic energy possessed by the ion, other transitional processes, vibrational and rotational fine structure all affect the experimental relation. Oldenberg (10) and Morrison (11) have included a structural factor in the excitation function, while Long & Norrish (12) point out that it would be surprising if inelastic collisions produced unexcited fragments from large molecules, and that in any case there will he an energy corresponding to a change in the atomic arrangement between the parent molecule and the ion.

Normal techniques are not sufficiently sensitive to detect a fine structure, although this difficulty has been surmounted by two workers using suitable refinements. Morrison measures the second differential of the ion current-voltage relation, and has used this function to study various kinds of excitation (13) (14). A different approach to the problem/

problem has been made by Fox et al who have designed a most ingenious source which eliminates the effect of potential gradients in the ionization chamber by a pulse technique, and also the curvature due to the thermal energy of the electrons. (15) (16). The ionization efficiency curves of the rare gases have been shown to be essentially linear, but the corresponding relation for a more complex molecule such as benzene retains considerable curvature.

THE EVALUATION OF APPEARANCE POTENTIALS FROM IONIZATION EFFICIENCY CURVES.

For reasons outlined in Part 4, these measurements are made with reference to a calibrating gas which serves to fix the voltage scale. The appearance potential of the ion is determined by adding the extrapolated voltage difference to the ionization potential of the standard. The rare gases are used widely for this purpose. Several methods of manipulating these curves have been suggested by different workers and have been applied with varying degrees of success, the principal methods being illustrated in Fig.3.

Linear extrapolation (17) seeks to avoid the uncertainty associated with the foot of the curve by relying entirely on the well-defined linear portion of the curve. Simple cases such as those of the rare gases may be analysed occasionally

by/

by this method, but in most instances the derived energy terms have no obvious significance.

In the method of initial upward breaks, the linear parts of the curve are first of all made parallel by suitable adjustment of the intensity axis, (for which there is no theoretical justification) and are extrapolated by eye to zero ion current. Since measurements at high sensitivity (11) confirm that ionization efficiency curves approach the voltage axis asymptotically, the treatment is liable to subjective errors, although Stevenson has shown that in the hands of an experienced operator it is capable of yielding self-consistent results (18).

The treatment known as critical slope (5) springs from the theory which Honig developed to account for the exponential nature of the foot of the curve. It entails the construction of a tangent of prescribed slope which is produced to give an intercept on the voltage axis. It is debatable whether the accuracy of the results is comparable with their consistency, since the underlying theory has not been fully established.

In Warren's method (19) the slopes are adjusted for parallelism, after which the voltage differences corresponding to decreasing ion currents are plotted as a function of these currents./

currents. The procedure is empirical but gives good results whenever the curvature of the two tails is similar. If the curvature is very great, replotting the curves on an expanded voltage scale may bring to light the onset of an ionization process (20).

Another empirical method has been described by Lossing (21) (22) which bears a resemblance to that of Warren. The results are plotted on semi-log paper giving a series of nearly parallel lines when the plots are restricted to ion currents below 1% of the value corresponding to 50 e.V., and are finally extrapolated by Warren's method. The result is corrected from a calibration curve for the instrument based on its performance with gases of known ionization potential.

While investigating Honig's method, Morrison showed that comparable results were obtained by measurement of the separation of the semi-log plots at the end of the linear portion (11). This is in keeping with the earlier claim by Lossing that the voltage difference corresponding to ion currents 1% of those at 50 e.V., is itself adequate when measuring the ionization potentials of the rare gases (13). In (24) an attempt to derive the true ionization efficiency curve depends on a mathematical treatment of the experimental results to remove the effects of thermal energy spread.

In the case of curves corresponding to ions of very different/

different mass, errors can result from mass discrimination effects which may arise from potential gradients in the ionization chamber. Furthermore, if the threshold voltages for the two processes are very different, changes in filament temperature due to the operation of the emission stabilizer may alter the energy distribution of the electron beam, which in turn can affect the shape of the exponential foot of the curve. From this point of view, grid controlled emission has some advantages over the more common method of temperature limitation.

THE DERIVATION OF BOND DISSOCIATION ENERGIES FROM ELECTRON IMPACT DATA.

The various energy terms involved in the ionization process $X\text{-}Y + e \longrightarrow X^+ + Y + 2e$ are related by the equation:-

$$A(X^+) = D(X\text{-}Y) + I(X) + E(X^+) + E(Y) - E(X\text{-}Y) + K(X^+) + K(Y) - K(X\text{-}Y)$$

where E(R) and K(R) represent the internal and kinetic energies of the species R. In many cases the internal energy terms, together with K(X-Y) may be neglected (25) (26), and frequently the remaining kinetic energy terms are small. Stevenson claims that the necessary condition for the absence of kinetic energy in the products is that:-

$$I(X) < I(Y),$$

in/

in which case the expression reduces to the form:-

$$A(X^+)_{X-Y} = D(X-Y) + I(X)$$

which may be solved for D(X-Y) in two ways. In the direct method, I(X) is determined by a subsidiary experiment involving the subjection of free radicals, produced by thermal cracking or photolysis, to electron impact. In the case of simple species, such as atoms, I(X) might be determined spectroscopically. The practical difficulty of measuring I(X) directly, led to the adoption of an alternative procedure in which the need for this datum is eliminated by substitution from the equation

$$A(X^+)_{X-Z} = D(X-Z) + I(X)$$

which related to the corresponding process

$$X-Z + e \dashrightarrow X + Z + 2e.$$

If D(X-Z) is unknown, it may be obtained by manipulating the appropriate thermochemical equations, whereby it is expressed in terms of a known bond energy together with a number of thermochemical quantities.

The self-consistency among the results obtained from different methods for the determination of a bond energy is illustrated in the following table (18).

Method			$D(CH_3-H)$
Electron Impact Direct with	CH_3	$\rightarrow CH_3^+ + e$	
	CH_4	$\rightarrow CH_3^+ + H + e$	$4.4_4 \pm 0.2$
	CH_3OH	$\rightarrow CH_3^+ + OH + e$	$4.4_8 \pm 0.4$
Electron Impact Indirect	C_2H_6	$\rightarrow C_2H_5^+ + H + e$	
	C_3H_8	$\rightarrow C_2H_5^+ + CH_3 + e$	$4.3_8 \pm 0.2$
	C_3H_8	$\rightarrow C_3H_7^+ + H + e$	
	iC_4H_{10}	$\rightarrow C_3H_7^+ + CH_3 + e$	$4.3_4 \pm 0.2$
	C_3H_6	$\rightarrow C_3H_5^+ + H + e$	
	iC_4H_8	$\rightarrow C_3H_5^+ + CH_3 + e$	$4.4_8 \pm 0.2$
	nC_3H_7Cl	$\rightarrow C_3H_7^+ + Cl + e$	
	nC_4H_{10}	$\rightarrow C_3H_7^+ + CH_3 + e$	$4.4_2 \pm 0.2$
	CH_3OH	$\rightarrow CH_2OH^+ + H + e$	
	C_2H_5OH	$\rightarrow CH_2OH^+ + CH_3 + e$	$4.4_2 \pm 0.1$
		Average value	$4.4_2 \pm 0.04$
Photo-chemical	$CH_4 + Br$	$\rightarrow CH_3 + HBr$	
	HBr	$\rightarrow H + Br$	$4.4_3 \pm 0.04$
Pyrolysis	CH_3I	$\rightarrow CH_3 + I$	
	HI	$\rightarrow H + I$	$4.4_5 \pm 0.04$

The example chosen is particularly favourable, and such good agreement is not always obtained. The difficulty of extrapolating ionization efficiency curves which possess long tails, precludes anything like this accuracy being reached in such cases. The extension of electron impact studies to this/

this class of compound has received little attention in the past, and a number of discrepancies in the literature may be the result of a tacit assumption that the products are formed in the ground state. An example of this is the formation of CN^+ from C_2N_2 (27) (28). It is also doubtful whether Stevenson's rule for the production of ions without kinetic energy is obeyed in all cases.

MEASUREMENT OF THE KINETIC ENERGY OF IONS.

The presence of excess kinetic energy among ions has been known for some time and an early method of measurement was described by Lozier (29) in 1930. The technique is a powerful one for the examination of homonuclear diatomic molecules where the ion is unambiguous, but the absence of mass dispersion makes it ineffective for polyatomic molecules unless one ion predominates. It has been applied to heteronuclear diatomics however. Ions were produced by a magnetically collimated electron beam of controlled energy passing along the axis of two concentric cylinders. Slots in the thick inner cylinder allowed only those ions moving radially to escape to the outer collecting electrode in the face of a retarding potential. Measurement of the ion current received by the latter as the retarding potential is varied, gives the distribution of the kinetic energy of the ions./

FIGURE 4.

Fig. 4.

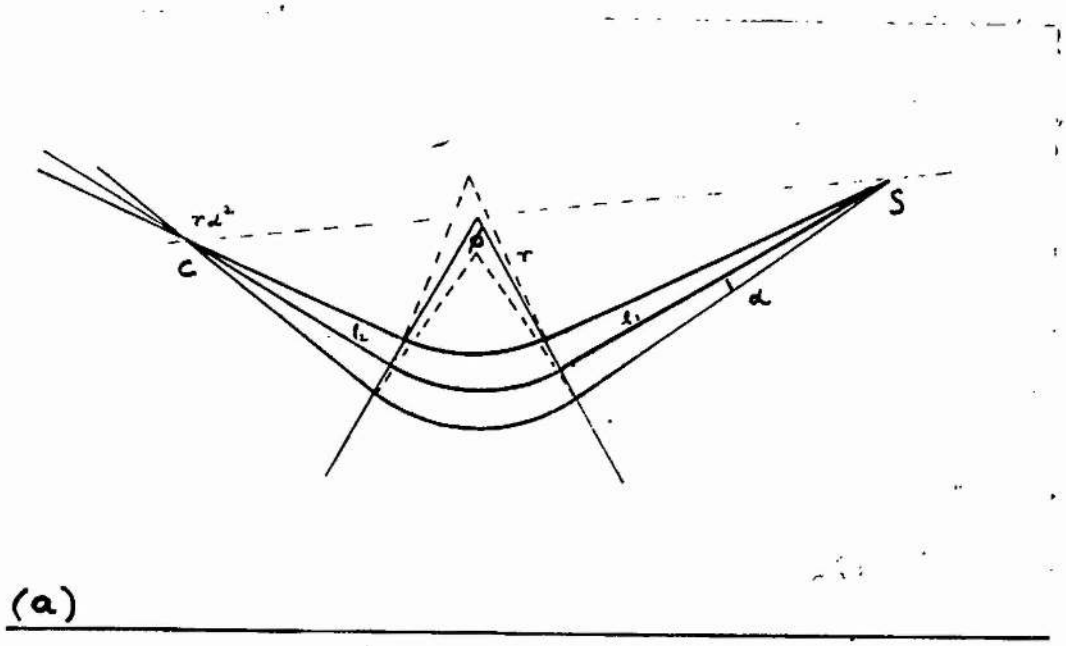

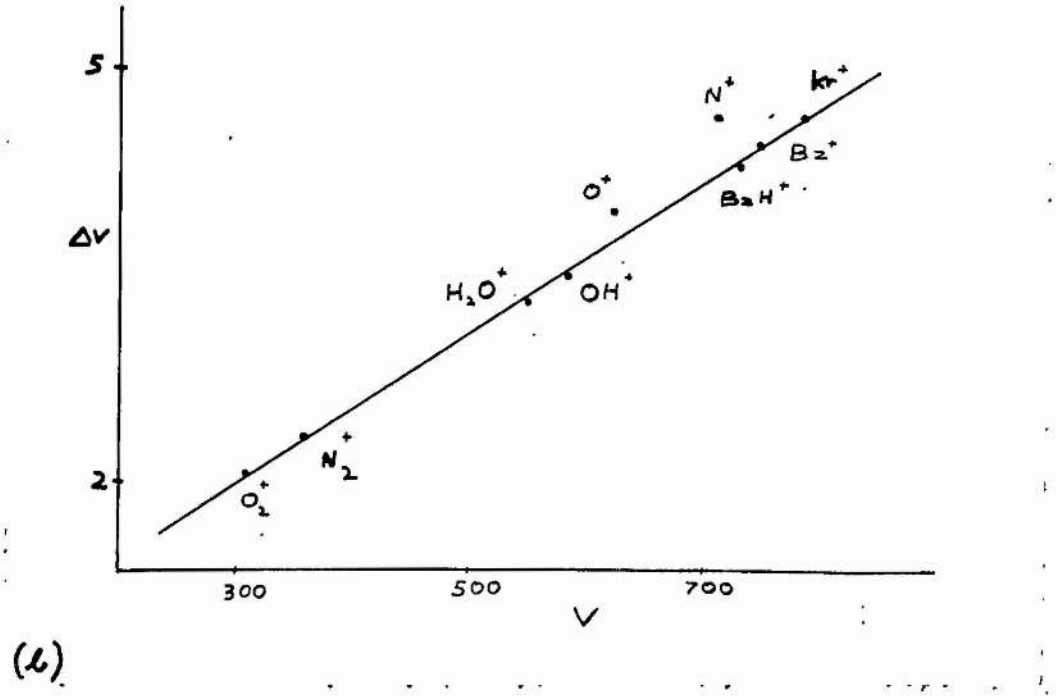

(a) Focussing action of a sector magnetic field.

(b) Presence of K.E. among ions; half peak width method.

the ions.

It is convenient to measure the kinetic energy on instrument by which the ionization is being studied, a several attempts have been made to modify mass spectro for this purpose. This usually involves the insertio a retarding potential between the analyser and collect that ions reach the latter with low energies. The va in ion current as this potential is altered gives the distribution across the ion beam. A general review c use of stopping potentials has been made by Hagstrum (with special reference to diatomic molecules. Kandel describes an application of stopping potentials which to a quantitative estimation of kinetic energy, while McDowell and Warren (8) show its presence qualitativel the basis of half peak widths. They found that this was proportional to the accelerating voltage for ions without kinetic energy, while its presence was indicat line broadening. The effect is shown in Fig 4(b) whi correlates the results obtained during the experiments toluene described in Part V. The ions O^+ and N^+ are to possess excess energy and do not fall on the line.

One serious limitation to all these methods of de kinetic energy is that only the fraction associated wi fragments/

fragments can be measured. Since the collisions are su
to the limitations of the conservation of momentum, the
energy will be distributed among the products in amounts
inversely proportional to their masses. Thus in the pr
$PhCH_3 \rightarrow PhCH_2 + H+e$, only 1% of any excess energy would
associated with the ion, and if the limit of detection w
0.03 eV as in Kandel's method, an energy term in the
dissociation process of less than 3eV would pass unnotic

THE DEVELOPMENT OF POSITIVE RAY ANALYSIS.

Since the study of electron impact processes has be
bound up so closely with the development of positive ray
analysis in general, and mass spectrometry in particular
it is useful to consider very briefly the steps through
the subject has evolved.

Positive rays were discovered by Goldstein in 1886
found that perforation of the cathode in a low pressure
discharge tube resulted in the transmission of a streamer
discharge. The behavious of these rays under the influ
of magnetic and electrostatic fields was examined by Wie
who showed them to consist of positively charged particl
The extensive investigations of Thomson yielded much mor
detailed knowledge of their nature, and his parabola
spectrometer was used to evaluate their e/m ratio. In
way he showed that polyatomic molecules gave rise to a
mass/

mass spectrum; thus $COCl_2$ yields C^+, O^+, Cl^+, CO^+, Cl_2^+, $COCl^+$, $COCl_2^+$ together with C^- Cl^- O^- ; (31) includes a survey of this early work.

In contemporary experiments by Franck and Hertz (32), various gases were subjected to electron impact under controlled conditions and evidence was obtained for the Bohr theory of stationary states. Later refinements to the method allowed the absorption of energy by a resonance process (critical potential) to be distinguished from an ionization porcess (ionization potential).

A year or two later Aston (33) built a spectrograph for mass determination, while in 1918 Dempster (34) described the first spectrometer designed specifically for the measurement of relative abundances; the subject of mass spectrometry springs from this work. These early instruments resembled one another inasmuch as the ions were produced in a spark discharge, or by thermal emission, but in 1922 Smythe coupled an electron impact source with a crude positive ray analyser (35).

At about this stage, mass spectrography and mass spectrometry parted company, and the next important development in the design of mass spectrometers was due to Bleakney (36) whose instrument employed the analysing property of a 180° magnetic field, coupled with an accurately constructed electron gun. It formed a model for most of the instruments built/

built during the following decade.

The growing interest in the behaviour of substances upon electron impact was stimulated further by Smith's classic paper on the ionization processes in methane (37) in which is derived a value for $D(CH_3-H)$. Since that time the subject has been developed and refined considerably by the efforts of Stevenson, Hipple, Honig, McDowell, Morrison and others. Many modern instruments are based on designs by Nier (38) (39) which employ the refocussing properties of a sector magnetic field.

Recently, interest has widened to include a study of negative ion formation, the estimation of kinetic energy among ions, and spontaneous dissociation phenomena.

Another ingenious application of mass spectrometers lies in the detection and study of free radicals and other reaction intermediates, and a summary of this work is included in Part 7.

Some attention has been paid to the measurement of ionization potentials, and their relation to other molecular properties. (11) (6) while attempts have been made to apply the theory of molecular orbitals to the calculation of ionization potentials for a number of paraffins (40)(41)(42). In a similar way Franklin (43) has calculated the ionization potentials of a large number of paraffins, olefins, aromatics, alkyl//

alkyl halides, amines and oxygenated compounds. With a few exceptions, the agreement between the calculated and measured values is excellent. A review dealing with the chemical significance of ionization potentials is given by Walsh (44).

PART 2

THE MASS SPECTROMETER.

BASIC PRINCIPLES

The motion of an ion of mass m, moving with a velocity v, perpendicular to a magnetic field of strength H, is represented by the equation

$$Her = mv$$

where e is the charge on the ion, and r is the radius of curvature of the resultant path. It follows that such a system will exhibit dispersion according to the momenta of the incident particles. If the energies of the incident ions are equalised by acceleration through a large potential V, the combination of electrostatic and magnetic fields becomes mass dispersive since

$$\tfrac{1}{2}mv^2 = eV$$

which, by substitution in the first equation yields the expression

$$\frac{e}{m} = \frac{2V}{r^2H^2}$$

in which case the radius of curvature is proportional to $\sqrt{m}$

Early instruments used magnetic fields of 180°, but the theoretical papers of Barber and Stevens describing the focussing properties of sector fields were soon applied in practice, (45)(46) the resulting economy in magnet construction being quite considerable.

If its boundaries are sharp the effect of a homogeneous magnetic/

magnetic field on an incident pencil of ions is represented by the equation:- (47)

$$r.\sin(D) + \frac{L_1.\cos(D-e_1)}{\cos(e_1)} + \frac{L_2.\cos(D-e_2)}{\cos(e_2)} - \frac{L_1.L_2.\sin(D-e_1-e_2)}{r.\cos(e_1).\cos(e_2)} = 0$$

where r is the radius of curvature of the principal ray as it traverses the field,

D the angle of deviation,

e_1 and e_2 the angles of incidence and emergence, and

L_1 and L_2 are the source and image distances respectively.

In a sector field instrument e_1 and e_2 are made zero when:-

$$r.\sin(D) + (L_1 + L_2).\cos(D) - L_1.L_2/r.\sin(D) = 0.$$

Under these conditions the ions are refocussed at a point collinear with the source and the apex of the sector field, as shown in Fig 4(a). Usually a symmetrical arrangement is chosen where $L_1 = L_2$, in which case the expression reduces to the form

$$L/r = \cot(D) + \operatorname{cosec}(D)$$

In the practical case the refocussing is not perfect, since the divergence of the ion beam leaving the source results in a spherical aberration of $2r(1 - \cos a)$ where a represents the half-angle of spread. This approximates to ra^2 when a is small. Many other aberrations affect the image/

image cross section and these have been dealt with fully by Barnard (48). The more important ones are discussed below in the appropriate place.

A sector field mass spectrometer is the practical realization of this focussing condition. In order that the correct geometry may be followed, the source, collector and intermediate ion path must be evacuated to such a degree that the mean free path is larger than the dimensions of the apparatus. In order to achieve this, the whole system is placed in a vacuum tight envelope and pumped until the pressure has been reduced below 10^{-6}mm.

BACKGROUND TO THE PRESENT INSTRUMENT

The design of the spectrometer was influenced by several important factors. Its resolving power must be adequate for the unequivocal detection of benzyl radicals, and ideally, of even higher masses. Eventually it was decided to aim at a figure of 150.mass units. Secondly, the associated electronic circuits must permit the measurement of ionization efficiency curves within an energy range of 5 - 20 eV. Lastly, it must incorporate a reactor in the vicinity of the source for the production of free radicals, and for the general study of reaction mechanisms. The variety of uses which was envisaged for the instrument meant that demountability

FIGURE 5.

Fig. 5.

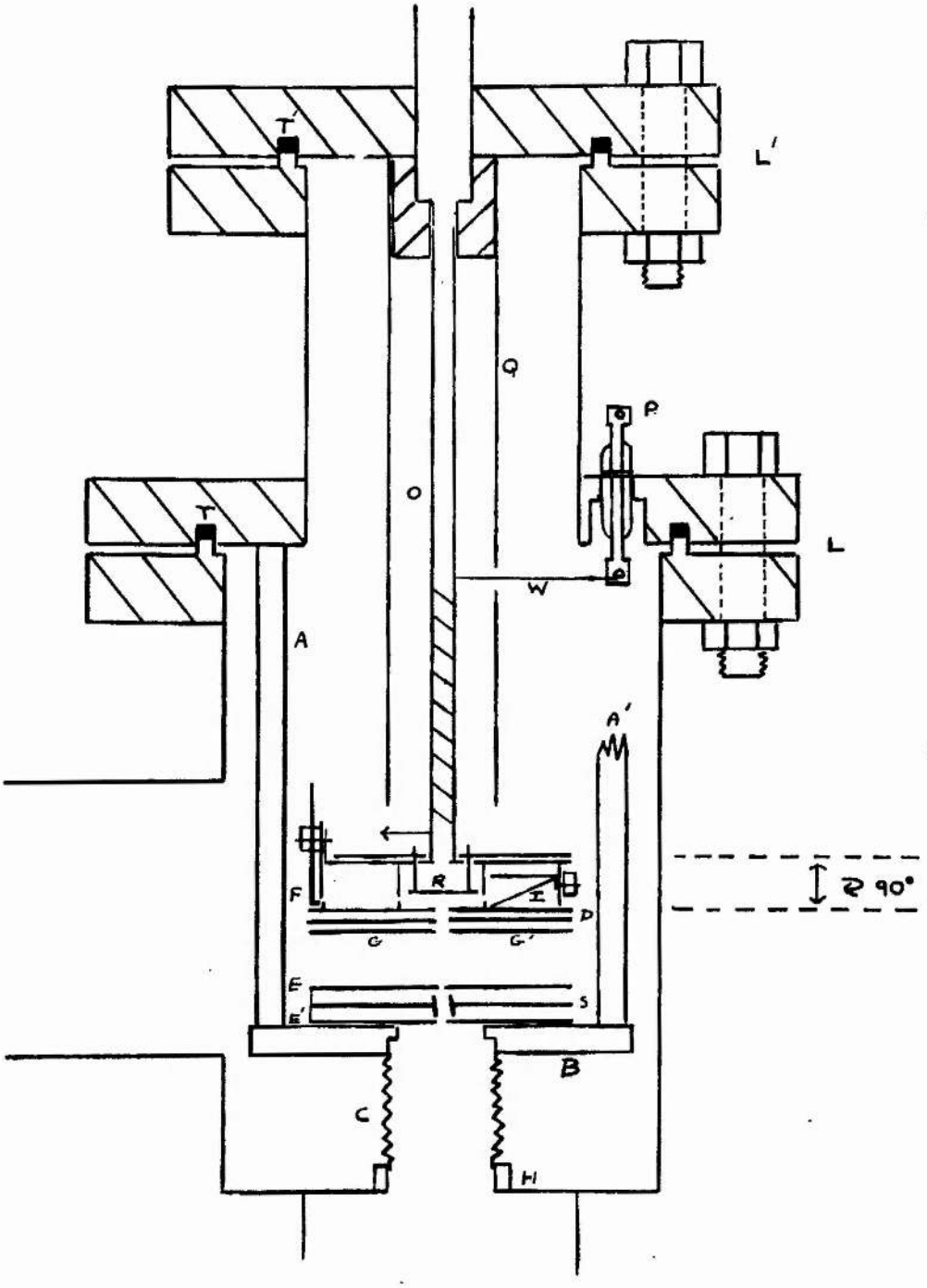

Diagram of source, including the reactor furnace used in the measurement of $I(PhCH_2)$. Section of drawing between the dashed lines is a side elevation

was an important aspect of the general design.

The mass spectrometer which existed already in the Chemistry Department at St. Andrews did not possess sufficient resolving power for the present investigation, nor could it have been adapted easily for use in conjunction with a reactor furnace. Consequently, the construction of a new instrument became essential.

THE SOURCE.

The most important, and yet in some ways the least satisfactory part of a mass spectrometer is the source, where electron impact occurs and the ions are formed into a geometrical beam prior to entering the analyser. The source used was basically of the Nier type and is illustrated in Fig. 5. Electrons are emitted from a filament F (0.4 x 0.03 x 0.001 in.) under temperature limited conditions, and are accelerated towards the box by means of a potential applied between the filament and the first slit. The emitter consists of a tungsten ribbon spot-welded to Nilo K rods which are held in position by insulating blocks of steatite. In order to accommodate the reactor immediately above the ion box, the filament assembly was moved back and the electrons made to traverse a second slit. The increased length of the electron gun was turned to good account by the provision/

provision of a hole in the top of the intermediate section by means of which improved differential pumping was obtained between the filament and the ionization chamber.

Collimation of the electron beam is achieved by means of an auxiliary magnet. The existence of this field in the source region is one of the causes of mass discrimination and the majority of workers strive to keep its value as small as possible although Thode et al (49) and Robertson (9) used strong fields. A range of magnets with field strengths of 100, 250 and 650 gauss was available, of which the second was found by experience to give the best compromise between effective collimation, good resolution and small mass discrimination. The mounting for this source magnet allowed motion both along and about the two axes at right angles to the direction of the electron beam. After traversing the ionization chamber, the electrons pass through a further slit and fall on a collector electrode I termed the trap. Its function is to monitor the intensity of the electron beam, secondary emission being prevented by maintaining it at a potential greater than that of the ion box.

The substance under examination is introduced through a hole in the top of the chamber and those ions which are not neutralised by collision with the wall are removed by the combined action of voltages applied to the repeller plate R and the draw-out plate D. The deflection which would otherwise/

otherwise be caused by the field of the collimating magnet, is counteracted by a small differential voltage applied to the focus plates G_1, G_2. In order to reduce the defocussing effect of the 'initial energy' of the ions, the beam is accelerated through about 2 kilovolts by raising the whole of the source assembly to this potential with respect to the earthed collector slit.

The resolution of the instrument is governed chiefly by the size of the exit slit, the voltages applied to the various electrodes in the ion gun being much less critical than might be imagined. Thus altering the mean operating potential of G_1 and G_2 from 1600v to 300v had small effect on the resolution. Very little information has been published on the focussing properties of this kind of slit system. Provision was made for variation of the width of the exit slit by forming it from two movable stainless steel knife edges bolted to the underlying plate E through elongated slots. For normal operation, a size of 0.2 mm was chosen.

The chief uncertainty in ionization efficiency curves arises from the existence of potential gradients in the source region. This has been removed by the technique of pulsed emission, to which brief reference has already been made. Ions are produced under field free conditions by a pulsed electron/

electron beam, and are withdrawn from the box by voltage pulses which are out of phase with the former. Another uncertainty arises from the Maxwell-Boltzmann energy distribution of the electrons leaving the filament. Since this is temperature dependent, the emission regulator would itself introduce errors in a system relying upon the condition of temperature limitation. Space charge limitation has been used in a few cases (50) but the complexity of the attendant grid structure is a disadvantage where space is limited. If the filament is directly heated by A.C. the electron energy is modulated by twice this frequency and further errors are introduced. The circuit used in this work supplies the filament with D.C., the energy of the electrons being measured by a valve voltmeter.

The walls of the ionization chamber consisted of solid blocks of Nichrome V to achieve temperature uniformity, provision being made for outgassing and temperature control by a coil of 40 S.W.G. nichrome wire and a thermocouple, insulated from the source potential by glass tubing. The plates were made of stainless steel 0.025 in thick, and were separated by glass spacing rings, cut from glass sheet by a cylindrical brass tool, used in conjunction with an aqueous suspension of carborundum powder. By this means, the provision of a bellows C at the foot of the stack effectively sealed/

FIGURE 6.

Fig. 6.

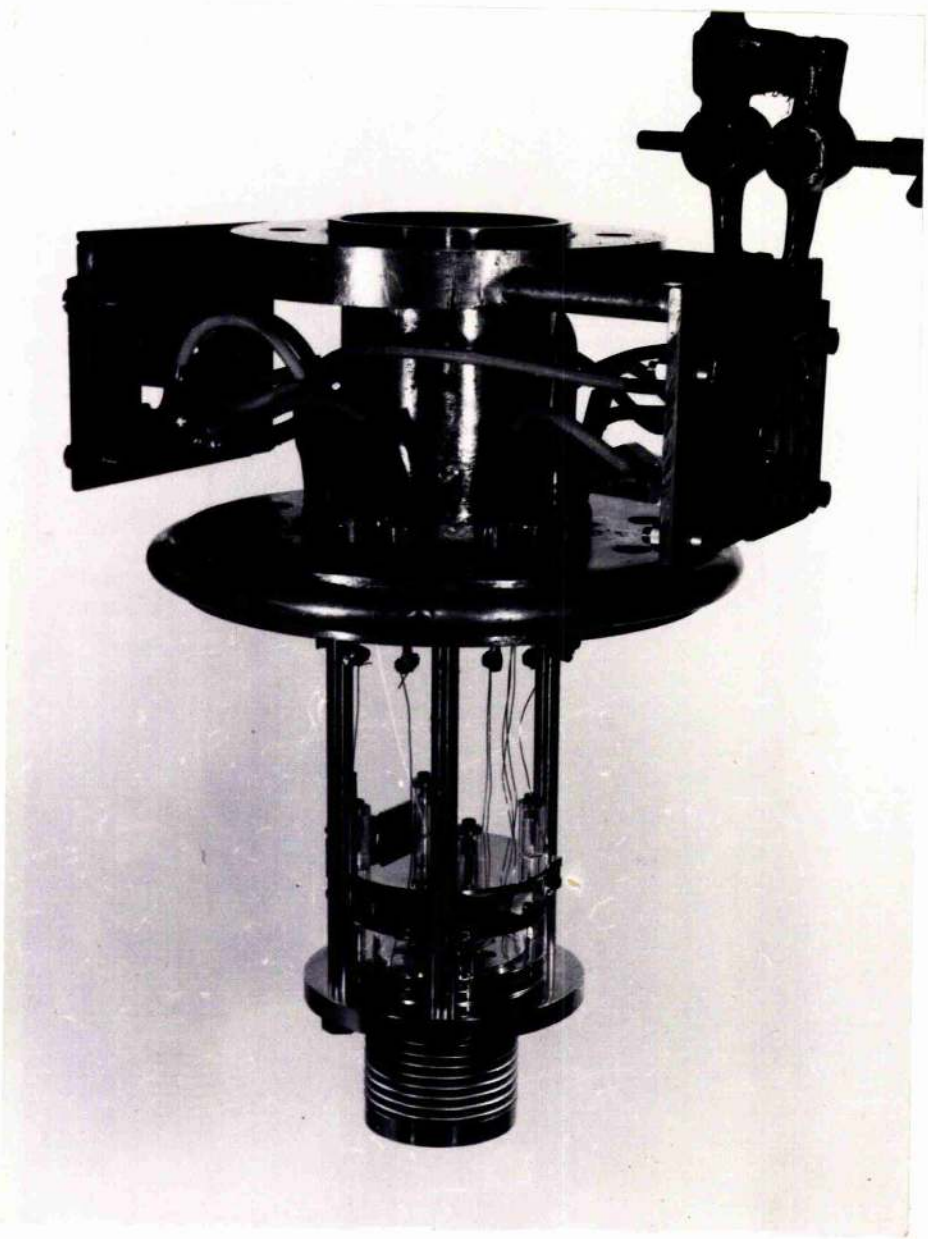

The complete source.

FIGURE 7.

Fig.7.

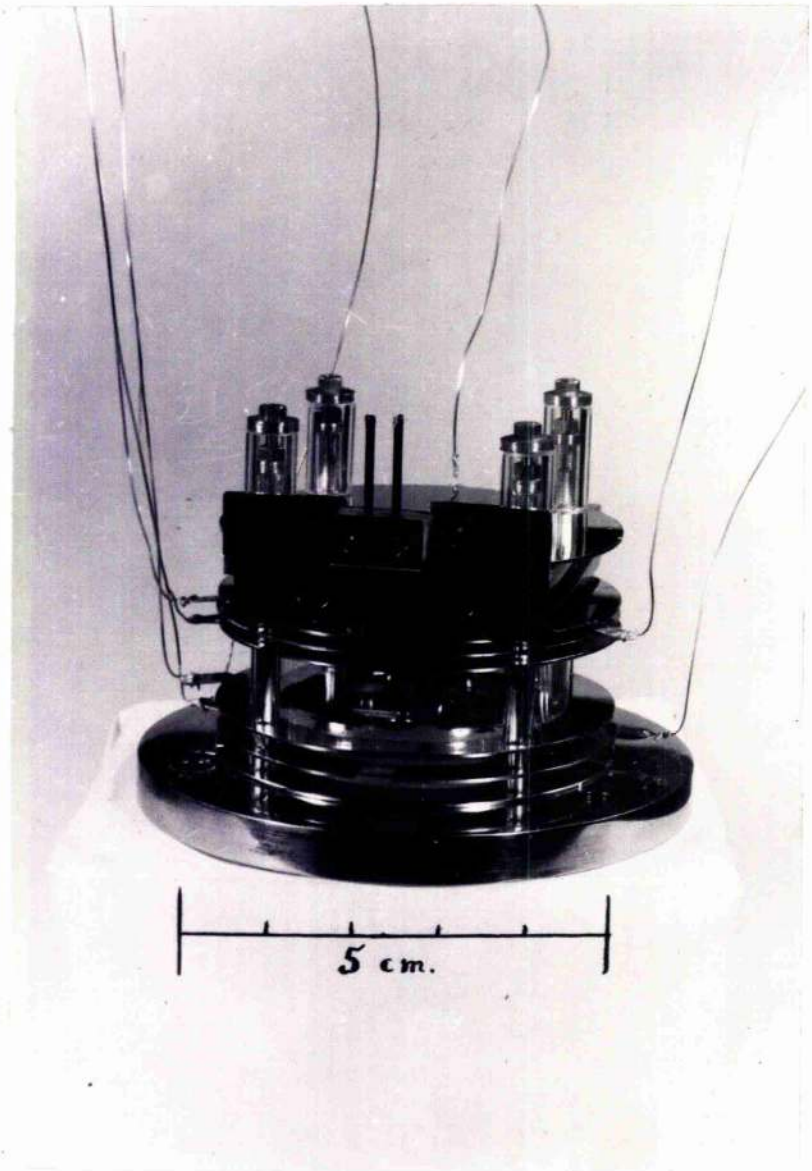

The stack, comprising the electron and ion guns.

FIGURE 8.

Fig. 8.

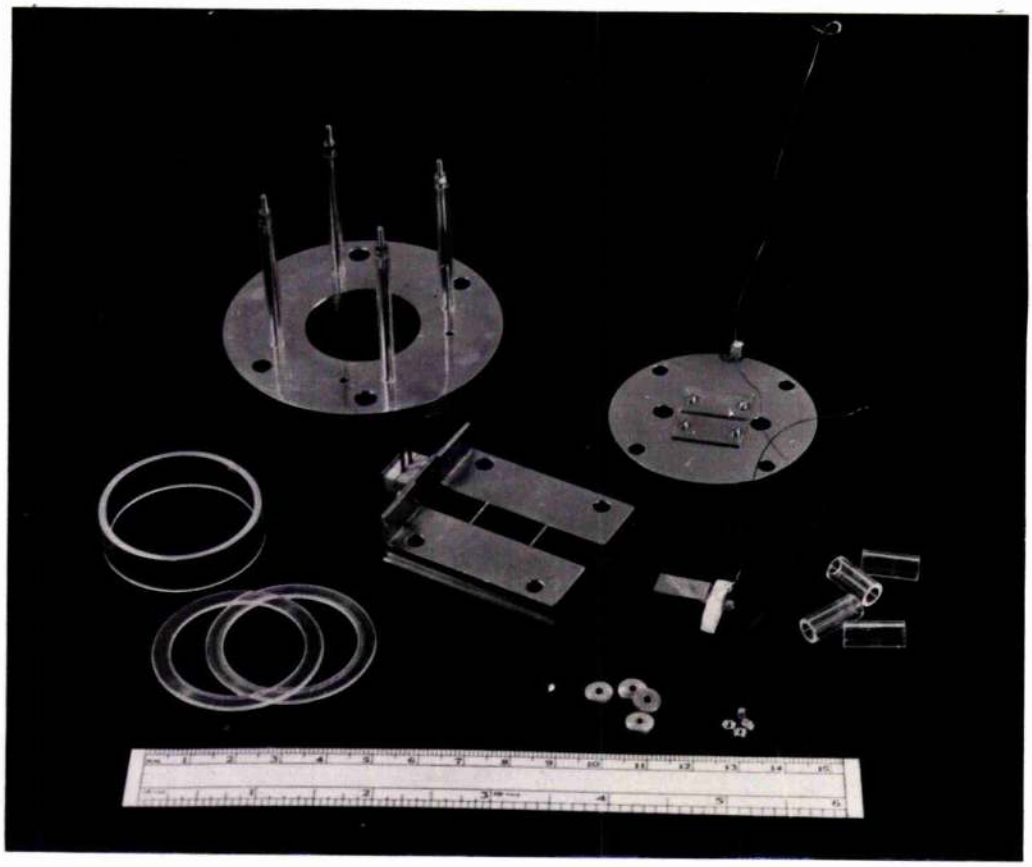

Specimen components used in the source.

sealed the region surrounding the filament from the rest of the atmosphere in the tube, giving the facility of differential pumping. For ease of assembly the stack is built as a demountable unit, whose base is a ring of inconel, B. The various plates are located on stainless steel rods screwed into this ring and from which they are insulated by thin glass tubes. The whole unit is supported in the head by four $\frac{1}{4}$in. inconel rods, A A^1. Electrical leads to supply the various source potentials are brought in through commercial metal/glass seals, P. The general construction of the source can be seen by reference to Figs 6, 7 and 8.

THE MAGNET.

The analyser consisted of a magnet of the 60° sector type, and was made on the premises with the exception of the winding of the coils. The yolk was formed from rough slabs of Low Moor iron, bolted together at milled bearing faces. The end planes of the cylindrical cores and the sector pole caps were made parallel by turning and surface grinding respectively, while the inner faces of the yolk were milled to the same tolerance of 0.001 in. These components, together with the coils, were then bolted rigidly together. In order to allow for movement of the magnet during the focussing/

focussing operation, the lower surfaces of the sides of the yolk were milled parallel and fitted with guides for roller bearings. The horizontal position of the magnet is controlled by means of screwed rods. The general construction and mounting of the magnet can be seen by reference to Fig.9. Current through the coils can be varied giving rise to fields of up to about 5000 gauss with a pole gap of 9/16 in. In order to prevent distortion of the pole gap due to the mutual attraction of the pole faces at high field strengths, a small brass spacing ring was placed in the gap.

COLLECTOR ASSEMBLY

The general method of construction of this unit resembled that of the ion gun consisting of stainless steel plates built up from an inconel ring on stainless steel rods protected by glass insulators. As before, the stack was mounted on inconel rods springing from the lower main flange. The appropriate ion beam is selected by an earthed collector slit usually 0.030 ins. wide and falls on to a collector plate, secondary emission from the latter being prevented by the insertion of a suppressor electrode carrying a negative potential of 50 volts. The design of the collector slit resembles that of the exit slit in the source, and its width is variable from 0 - 2 m m. For the work on appearance potentials,/

potentials, an aperture of 0.030 in. was used. Since the ion currents under investigation may be as small as 10^{-14}amp. the insulation of the lead from the collector to the input of the D.C. amplifier demands special care. The connection was carried through the main flange by means of a large metal to glass seal designed in such a way as to reduce the leakage to a negligible amount.

The housing for the input grid leak resistors and the electrometer valve was bolted rigidly to the other side of the flange, in order to prevent vibration giving rise to capacity effects. It was made of metal to screen the circuit from electrostatic fields, and was completely closed to prevent photoelectric effects and thermal drift. Moisture condensation on the high value grid resistors was eliminated by the use of silica gel, and a small heater built into the wall of the box the keep the ambient temperature of the enclosure slightly above that of its external surroundings. In addition, the resistors were coated with a silicone varnish. The electrometer valve was spring mounted to reduce microphony, and the size of the input resistor was controlled by a switching device mounted on the end of an insulating glass rod actuated from outside the enclosure.

FIGURE 9.

Fig. 9.

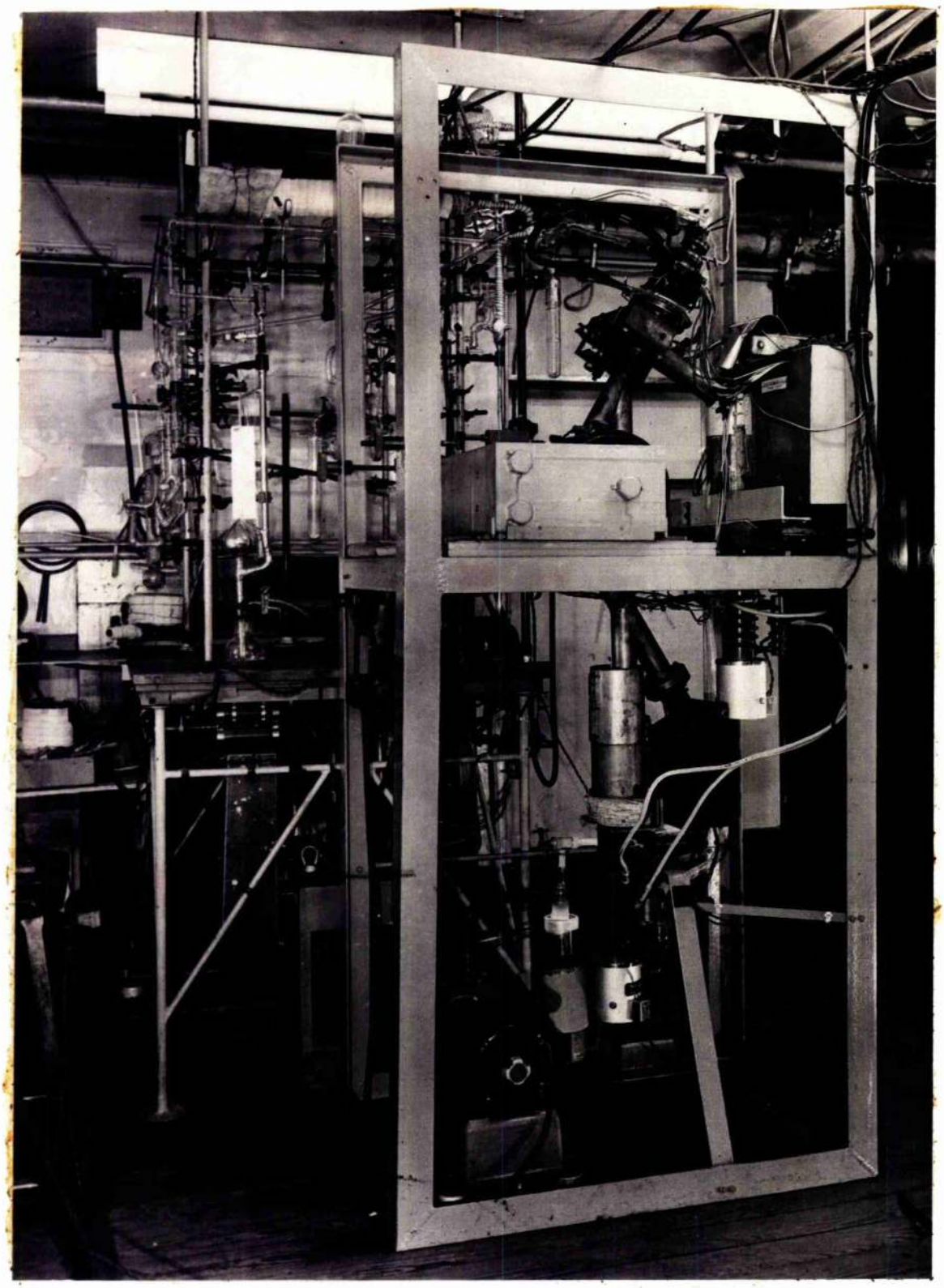

Tube in position, showing pumping system and magnet.

GENERAL CONSTRUCTION

The mass spectrometer tube was made of inconel, with the exception of the bend, which was formed of flattened copper tubing. The nickel alloy was chosen for its mechanical strength, freedom from occluded gases, heat resistance, and nonmagnetic properties. All the joints were sealed by hard solder. The general design of the instrument is evident from Fig 9.

Efficient pumping of both ends of the analyser tube was obtained by by-passing the impedance of the narrow copper bend by a 2 in. dia. inconel tube. The lower end of this tube was attached to a metal cold trap, mounted above the diffusion pump. A second pumping lead with an independent cold trap and diffusion pump gave the facility of differential pumping of the filament region. Originally, two Metrovac oil diffusion pumps, Type 0.3.B were installed, backed by an 0.2 diffusion pump and a D.R.1. rotary oil pump. Oil diffusion pumps were chosen because at that time it was planned to study the electron impact behaviour of mercury alkyls. In addition, no mercury diffusion pumps of comparable speed were commercially available. At a later stage it was found that contamination of the source was occurring from traces of diffusion pump oil, and they were

subsequently/

subsequently replaced by Edwards Speedivac mercury diffusion pumps, Type 2M3./. These gave excellent service, and after their installation, no further contamination troubles arose. In order to reduce the amount of rotary pump oil vapour back-diffusing into the mass spectrometer, a glass trap cooled by solid CO_2 was interposed in the backing line. This also served to reduce the amount of mercury vapour escaping into the rotary pump.

The gaskets used as seatings for the various flanges L, L^1 Fig. 5, consisted of Fluon (P.T.F.E.) rings T.5 which were turned from discs on a lathe. They were 1/16 in. thick and $\frac{1}{8}$ in. wide and when inserted in carefully mated seatings gave excellent service. A Penning gauge was fitted to the side pumping lead to indicate the vacuum conditions in the tube. Although less sensitive than an ionization gauge it gave adequate service, having the compensation of simplicity and greater robustness.

The high vacuum standard which is required for the satisfactory operation of a mass spectrometer demands stringent control in the fabrication of the components, and leak testing becomes an occupational hazard. Each component was examined individually, before incorporation in the final assembly, with the help of a special vacuum system containing both Pirani and Penning gauges. The method of searching for/

for a leak depended on its size. The larger holes were found by noting the effect of a suitable probe liquid such as CCl_4 on the discharge produced by a high frequency spark coil. A more sensitive method employed the response of a Pirani guage to a hydrogen probe. Minor flaws were detected by coupling the vacuum line to the mass spectrometer already existing in the Department. When the tube was completed and capable of operating as a mass spectrometer it was made to find its own leaks, and a number of micro holes were detected by the use of H_2 or CO_2 as a probe gas, in this way.

Electrical leads to the source were brought into the vacuum by commercial metal to glass seals soft soldered into seatings in the main flange, that had been wiped previously with silver solder. These soft soldered joints proved most unsatisfactory and some 50 unsuccessful attempts to produce a series of tight joints were made, using a variety of fluxes and soldering techniques. In desperation the whole area was coated with Araldite cement and baked, but after a time cracks developed under the latter, and finally the seals had to be replaced completely. The second batch were soft-soldered to short lengths of Nilo K. tubing which had been brazed onto the main flange. This arrangement proved fairly satisfactory and had the advantage that seals could be replaced individually if necessary.

The/

The tube was clamped to the main supporting framework at three places by means of two pieces of angle girder, bolted to the bottoms of the metal traps in the two pumping leads Fig. 9. Since each of these points of suspension could be adjusted vertically and independently of each other, the orientation of the tube could be adjusted with respect to that of the magnet, the movements being complementary to those produced by horizontal movement of the latter.

ASSOCIATED GAS HANDLING SYSTEM

The essential features of the apparatus used during the measurement of appearance potentials are included in Fig. 23 and call for little comment. In order to avoid the absorption of organic materials by tap grease, the reservoir J holding the mixture under examination is sealed by a mercury cut-off I. Gases were stored in large glass bulbs F, F^1 from which they were abstracted via a gas burette G. Liquids were introduced in a controlled manner from micro-burettes through a glass sinter O covered with mercury. Samples of solid materials could only be inserted by letting the system up to atmospheric pressure followed by a little glass blowing, for the small number of such substances did not warrant the design of a more elaborate arrangement. In order to gain sufficient sensitivity on the mass spectrometer, a sample pressure/

pressure of about 1-2 mm. was required, and to attain this in the case of the less volatile materials it was necessary to lag the whole of the reservoir system M, and wind the exterior with heating tapes by which the temperature could be controlled. In the case of benzyl iodide, the above system had to be modified since this compound will react with mercury vapour from the cut-off. This substance was placed in a separate container, which after evacuation, was sealed off from the rest of the apparatus, apart from its own leak into the mass spectrometer inlet tube. The partial pressure of these less volatile compounds was kept constant by immersing a short length of tube without lagging in a vapour bath, L.

The leak into the mass spectrometer consisted of a piece of grade 4F Metrosil, K, sealed into glass tubing. Later experiments employed a twin Metrosil system for reasons already explained, and this had the additional advantage that the relative pressures of the two substances under investigation were adjusted more easily. The tube containing the leak was connected to the source of the spectrometer by a metal to glass seal, and a stainless steel bellows for flexibility. The source could be removed by unbolting a small flange with Fluon gasket. In order to prevent condensation of less volatile or polar materials, the whole of the inlet line was lagged/

lagged with heating tape. The inflowing gases were led into the ionization chamber by a glass tube whose lower end was constricted slightly to seat in a hole on the top of the ion box.

The two reactor furnaces which were constructed for the examination, by electron impact, of the products of the pyrolyses of organic compounds will be described in the section dealing with the work in question.

ELECTRONIC CIRCUITRY

Circumstances dictated that part of the electrical supplies of the existing mass spectrometer should be shared with the new instrument. The common units consisted of the magnet supply, a stabilized 2 kV. supply for the ion gun, and a range change unit associated with the output meter, in the form of a Brown Recorder.

THE EMISSION STABILIZER

Regulation of the conditions existing in the source is achieved by control of the total emission from the filament with the unit shown in Fig. 10. This is based on a circuit which is described elsewhere (51).

Power is supplied to the filament in the form of D.C. by the rectification and smoothing of the square wave output of a multivibrator comprising V_1 and V_2. The emission

current/

FIGURE 10.

Fig. 10.

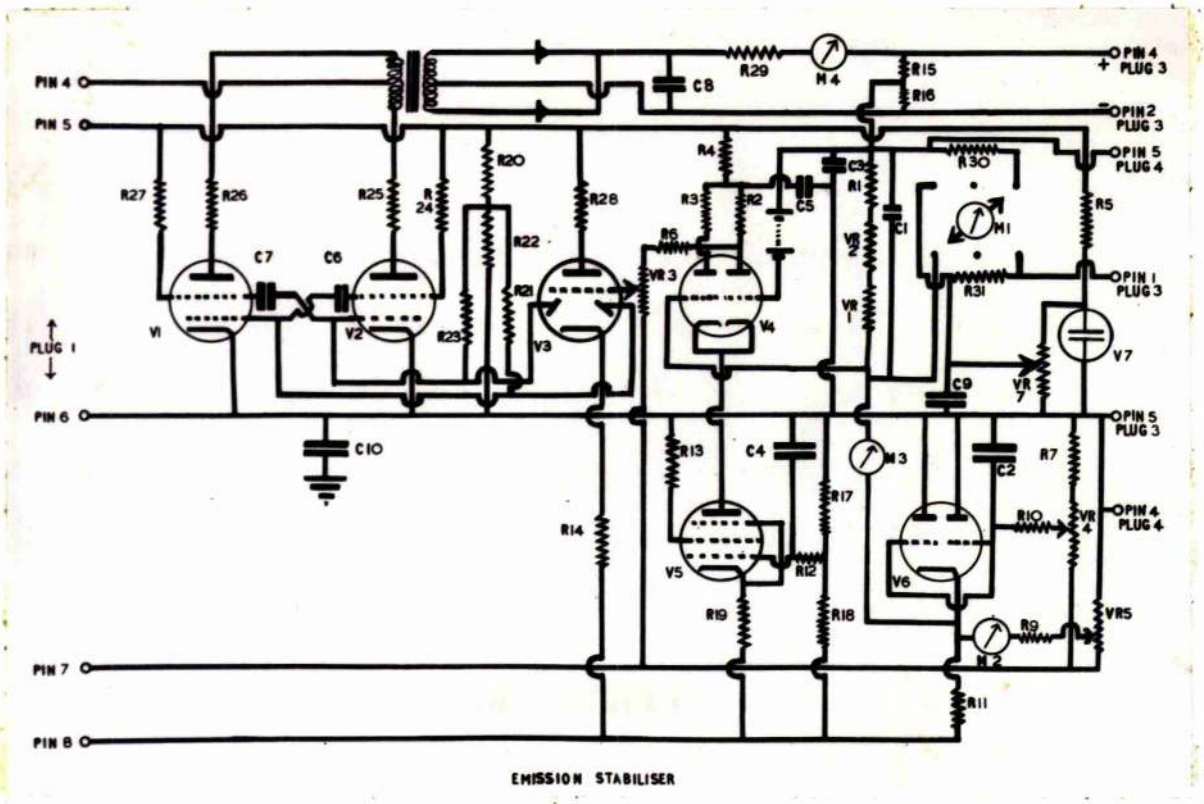

R.1	15k	R.23	470k	V.1	12E1
2	47k	24	10k	2	12E1
3	47k	25	33ohm	3	DH63
4	27k	26	33ohm	4	ECC35
5	25k	27	10k	5	EF37
6	470k	28	1.2k	6	ECC91
7	8k	29	0.4ohm	7	85A1
9	2M	30	2M		
10	470k	31	8.2k	C.1	0.01 µF
11	50k			2	0.1 µF
12	470k	VR.1	1M	3	1.0 µF
13	1k	2	50k	4	0.1 µF
14	100k	3	1M	5	4.0 µF
15	18ohm	4	25k helipot	6	470 pF
16	18ohm	5	200k	7	470 pF
17	330k	7	50k	8	150 µF
18	33k			9	1 µF
19	10k	M.1	50 µa	10	1 µF
20	47k	2	50 µa		
21	470k	3	1ma	B.1	50v
22	47k	4	5a		

current flows along a resistor chain formed by R_1, VR_2 and VR_1, generating a voltage which is backed off by a reference battery of 50 volts. This is achieved by applying the two voltages to the grids of a double triode V_4 whose cathodes are coupled as a long tailed pair, drawing constant current from the anode of the pentode V_5. Any difference between these two signals is amplified and fed back with the correct sign to the multivibrator through the cathode follower V_3, whose diodes are connected to the grids of V_1 and V_2 respectively.

The potential existing between the filament and the ionization chamber is varied by connecting a cathode follower V_6 to the negative end of the VR_1. The resultant voltage is controlled by the setting of the helipot VR_4. Any ripple otherwise appearing on this potential is suppressed by the addition of a condenser C_1.

By means of a suitable selector switch, the meter M_1 can display either the trap current, the current flowing to the repeller plate when this is made largely positive, or the voltage across $R_1 + VR_2 + VR_1$, thus indicating whether or not the circuit is stabilizing correctly.

In this form the unit gave reliable service, allowing variation of the emission current from 0.1 to 1.0 ma., the electron accelerating potential from 5 to 95 v., and the trap/

FIGURE 11.

Fig. 11.

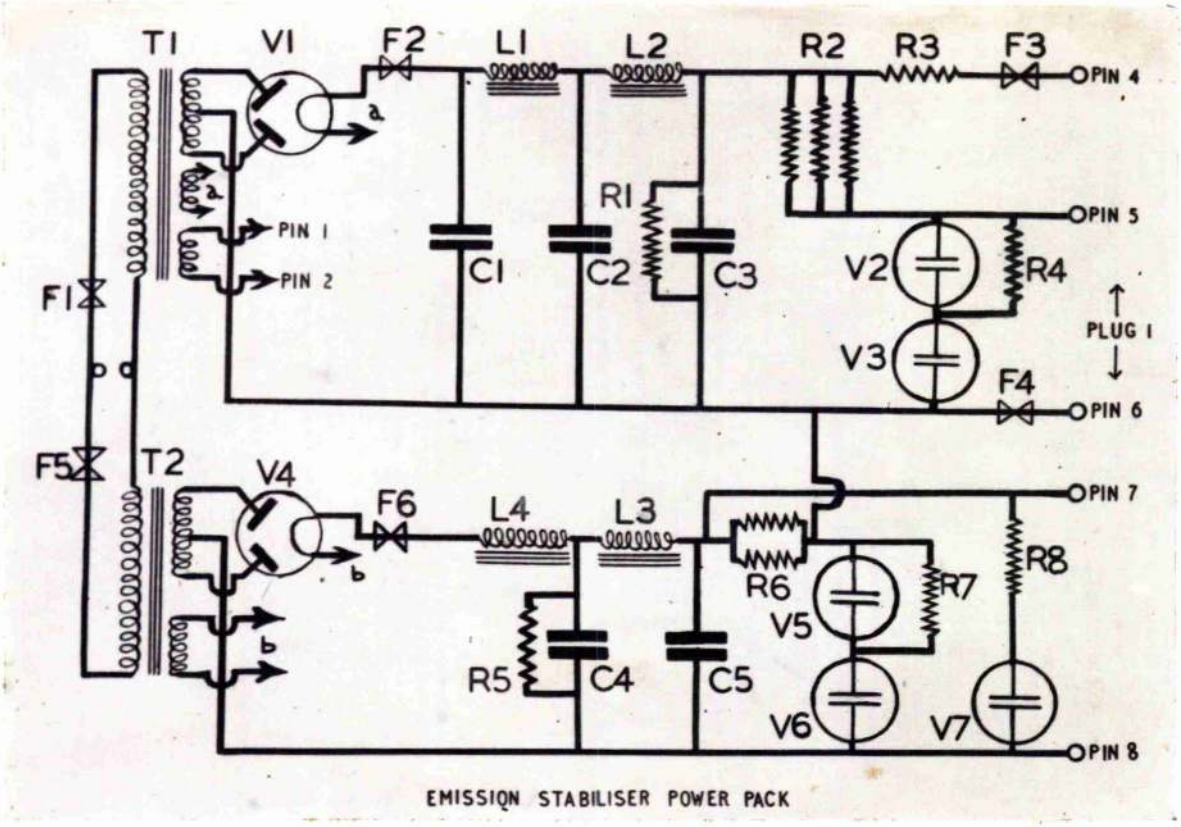

R.1	470k	C.1	6 µF
2	25k//25k//8k	2	24 µF
3	680ohm	3	30 µF
4	1M	4	6 µF
5	470k	5	6 µF
6	20k // 4k		
7	1M	F.1	3a
8	25k	2	1a
		3	250ma
V.1	FW4-500	4	500ma
2	VR105	5	1.5a
3	VR150	6	250ma
4	5Z4G		
5	VR150	T.1	500-0-500, 250ma
6	VR150		6.3v, 5a
7	VR150		4.0v, 4a
L.1	5H	T.2	400-0-400v, 100ma
2	50H		5v, 3a
3	10H		
4	5H		

FIGURE 12.

Fig 12.

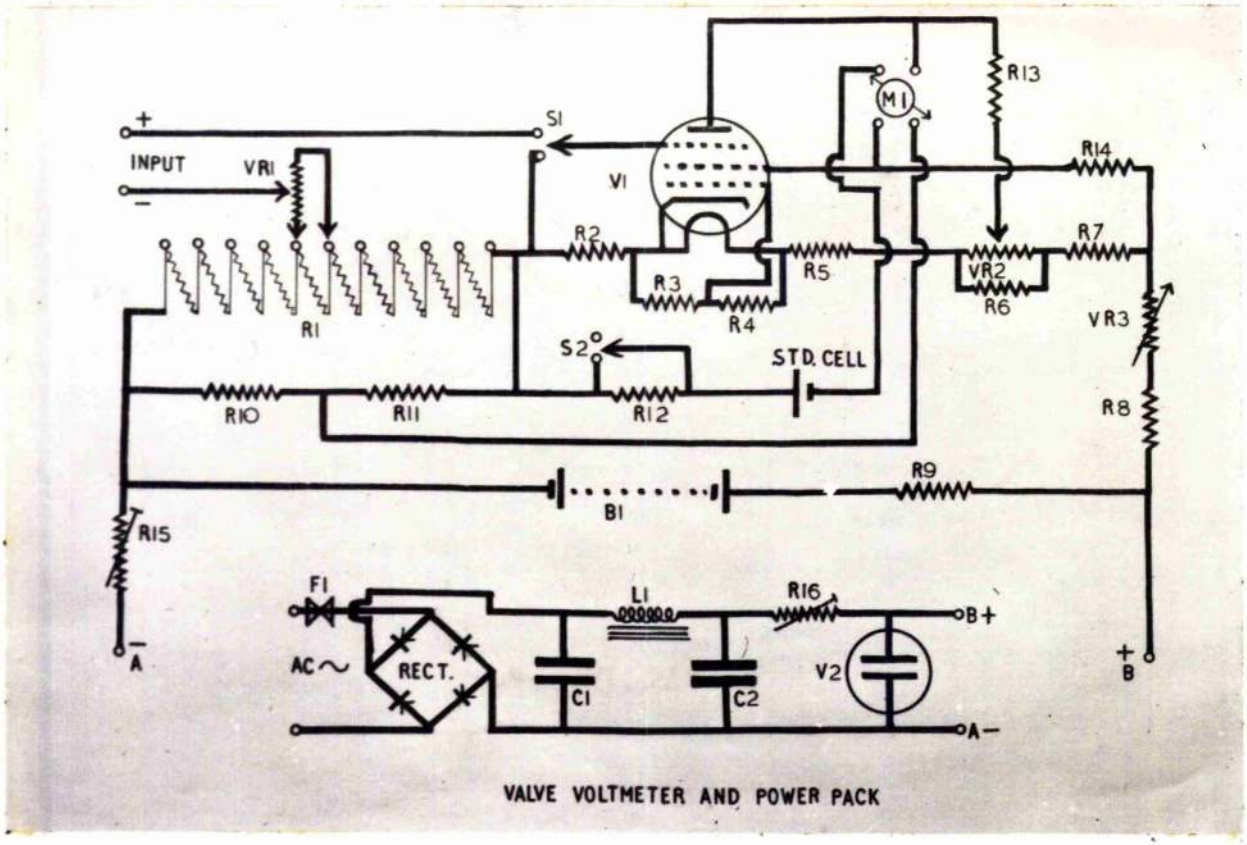

VALVE VOLTMETER AND POWER PACK

R.1	10x(100±0.1)ohm	VR.1	100k helipot
2	25ohm	2	100ohm
3	22k	3	100ohm
4	10k		
5	110ohm	V.1	954
6	5ohm	2	VR105
7	15ohm		
8	18ohm	M.1	30-0-30 μa
9	3x240ohm in//		
10	237.3±0.2ohm	L.1	10H
11	12.73±0.01ohm		
12	2.7k	B.1	Weston cell
13	20k variable		
14	20k// 100k	F.1	1a
15	2x300ohm		
16	3x300ohm		
C.1	24 μF		
2	24 μF		

trap box voltage of 0 to 80 v. The current supplied to the filament could be varied between 5½ and 5½ a. and load matching was achieved by the suitable choice of the resistor R_{29}. A.C. ripple in the output was of the order of 0.1%. Voltage supplies are provided by a stabilized power pack of conventional design as shown in Fig. 11.

VALVE VOLTMETER

The accurate measurement of the energy of the electrons entering the ion chamber requires a voltmeter of high input impedance, and a suitable valve voltmeter was designed and built to serve this purpose. Fig.12. It employs an 'electrometer connected' 954 acorn pentode (52) with an associated balancing network of the Barth type (53) to make the system insensitive to changes of filament temperature. The directly heated filament is under-run and fed by a current, set to a predetermined value by the rheostat VR_3 in conjunction with a standard cell in a potentiometer network. Since this current feeds the potentiometer R_1, a drop of exactly 80 v. across this resistor chain is ensured. The instrument is of the null type, the output of the valve being displayed by the microammeter M_1. The voltmeter is set by connecting the control grid of the valve to the positive end of the potentiometer and adjusting the tapping point of VR_2/

VR_2 until M_1 reads zero. If the unknown voltage is applied to the grid with the correct polarity, the initial conditions may be restored by backing off with a corresponding drop in potential along the potentiometer.

The input impedance of the circuit is between 10^{13} and 10^{14} ohm and the sensitivity at balance is 0.02 volt/div. All the resistive components of the potentiometer were wound to an accuracy of better than 0.1%. Power supplies were derived initially from the mains through a stabilized power pack as shown in the diagram, but owing to the difficulty of preventing A.C. signals from being transmitted to the emission stabilizer during measurements, this was replaced by a 50v. storage battery.

H.T. SUPPLIES FOR THE ION GUN.

The stabilized H.T. unit used to feed the mass spectrometer already existing in the Department provided a potential variable from 1 - 2 kV. This supply was fed into a suitable switch and resistor network from which the various voltages for the ion gun were tapped off. The potential of the repeller plate could be varied from -8 to 12 v. with respect to the ion box, while the focus plates, one of which was strapped to the drawout plate, could be altered independently from 0 to -300 v.. Both halves of the/

the beam centring plates were kept at earth potential unless maximum sensitivity was required, in which case one of them could be altered from 0 to 300 v. A large potential of about 1 kV could also be applied to this plate when it was necessary to observe the amplifier zero. The H.T. supply was capable of continuous variation over a small range to make provision for electrostatic scanning, should this be required. The super-imposed A.C. ripple was of the order of 10 mv.

MAGNET CURRENT.

The existing stabilized supply for the other mass spectrometer could be utilized by means of a suitable switching device. The current could be varied from 4-135 ma at which value the magnet was approaching saturation. The size of the ripple on the output was about 0.2v.

D.C. AMPLIFIER.

This unit, together with the housing for the electrometer valve, was built originally by Mr. R.C. Naylor, to a design which has appeared elsewhere in the literature (54). It is double sided, of the balanced type to ensure minimum temperature drift, and employs 100% feedback with a voltage gain of 1. The electrometer valve has an amplification of rather/

FIGURE 13.

Fig. 13.

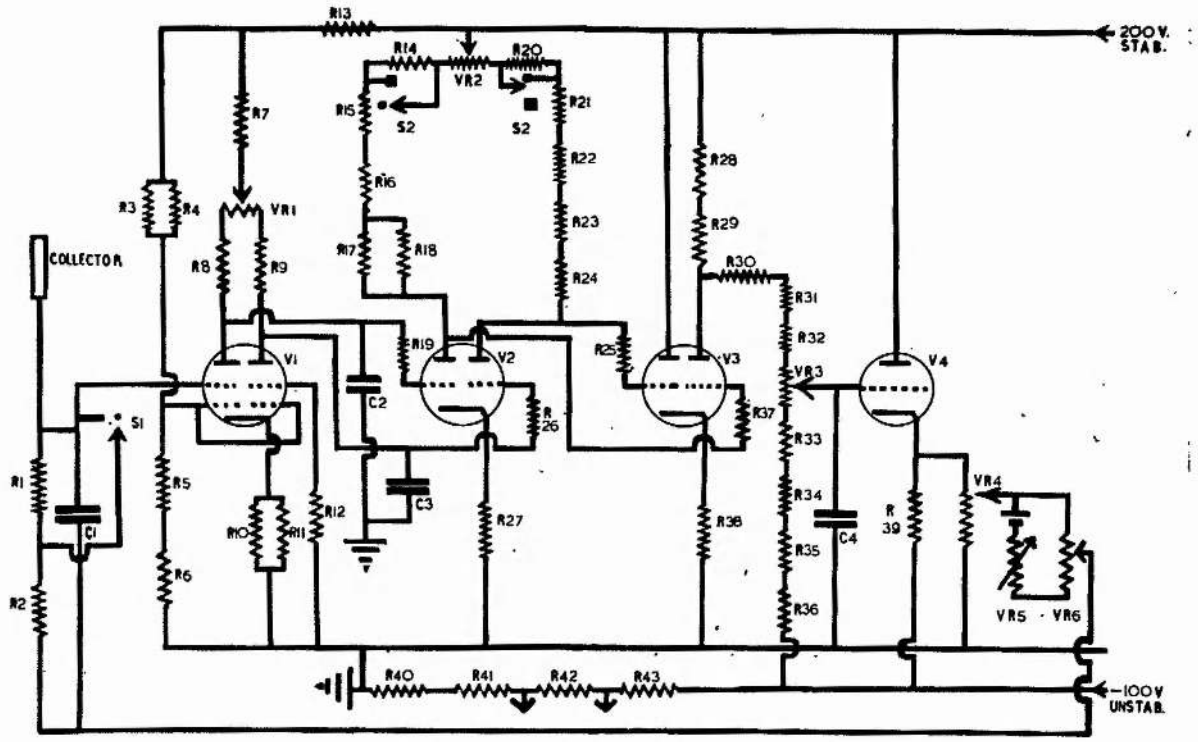

D.C. AMPLIFIER.

R.1	2×10^{11} ohm	R.21	100k	R.41	24k
2	3×10^{10} ohm	22	100k	42	650k
3	3.3k	23	100k	43	780k
4	2.2k	24	100k		
5	470ohm	25	100ohm	VR.1	100k
6	33ohm	26	100ohm	2	50k
7	60k	27	10k	3	100k step
8	100k	28	100k	4	25k
9	100k	29	100k	5	1M
10	15k	30	100k	6	50k
11	15k	31	100k		
12	1M	32	1M	V.1	BDM20
13	15k	33	100k	2	12SC7
14	50k	34	100k	3	12SC7
15	100k	35	330k	4	12J5
16	100k	36	330k		
17	100k	37	100ohm	C.1	30 pF
18	47k	38	68k	2	0.01 μF
19	100ohm	39	20k	3	0.1 μF
20	50k	40	24k	4	0.01 μF

rather less than unity, while the loop gain provided by the two double triodes is about 400. The output of the second of these valves is single ended and is fed into a cathode follower. By this means the current magnification is increased to 10^7 enabling the output to be fed into a low impedance meter. For preliminary work a Simpson meter (sensitivity 5000 ohms/volt) proved useful on account of its robustness, but accurate measurements were made with a Brown recorder (10 mv. 5 sec.) fed through a matched attenuator.

However, in its original form the noise level was too high to achieve the sensitivity needed for the accurate measurement of the lower portion of appearance potential curves, and a considerable amount of time was spent in improving the performance of this unit prior to commencing the investigation.

The original electrometer valve type DHM8A was replaced by BDM20 necessitating small alterations to the supply voltages. Although the rate of drift was as small as 1-2mv./hour, the noise level was objectionable and several steps were taken to minimise this. The high value grid resistor in the compensating side of the electrometer valve was replaced by a 1 megohm grid leak while the signal side was provided with a small condenser of 30 pf. in parallel with the/

the 2×10^{11} ohm resistor used throughout the work. This condenser was constructed specially to possess the necessary inter-plate insulation, and its value represented a compromise between adequate damping of the noise, and an undue increase in the time constant for the input signal. In addition, a small amount of A.C. ripple was removed from the H.T. supply by the inclusion of a suitably connected triode. In this way the noise level was reduced from 5 - 10 mv. to less than 2 mv. During the measurement of small signals, further accuracy was obtained by replacing the Brown recorder by a Tinsley spot galvanometer of high sensitivity, which had been suitable damped. The final form of the circuit is shown in Fig.13..

A further source of trouble arose from slight modulation of the -100 v. supply which was used to feed a voltage on to the suppressor plate in the collector assembly. This in turn induced a signal on the collector plate by a capacitive effect and caused a disturbance of 5 - 10 mv on occasions. Thereafter the electrode was fed from a battery.

After these modifications, the amplifier gave satisfactory service within these limits and had a linearity of response of 0.1% over a range of input signals of 0 - 18 volts, apart from effects arising from the voltage coefficient of the input grid resistor.

PART 3

SOME MATTERS AFFECTING THE PERFORMANCE OF THE MASS SPECTROMETER.

RESOLUTION

When the mechanical construction of the tube had been completed, the next step was to achieve the best possible resolution of which the instrument was capable.

The position of best focus was achieved by making small alterations in the orientation of the tube with respect to the main magnet, and observing the effect on the peak shape. The relevant adjustments may be considered in terms of the three co-ordinates.x, y and z where z is the field direction and y the axis passing through source and collector. Motion along the x. axis and about the y. axis is achieved by manipulation of the screwed rods which locate the horizontal position of the magnet with respect to the frame. On the other hand, movement along the y axis, and about the x and z axes is obtained by means of the adjustable clamps by which the tube is located in the supporting framework. The relative importance of these movements is discussed by Barnard (48) the most critical being the motion along the x axis.

When the resolution had been improved somewhat, xylene was introduced as a test substance, since the twin peaks at mass 105 and 106 to which it gives rise, enable an estimation of the resolution to be made by simple inspection of the spectrum. It soon became apparent that adjustment

of the magnetic field was insufficient to produce the expected improvement, and that some other disturbing factor was present which prevented attainment of the theoretical performance. Consequently a comprehensive series of checks was carried out to identify and correct the disturbance.

The electrical supplies for the ion gun and the analyser field were monitored for the presence of A.C. modulation, but the amount found was insufficient to cause trouble. The geometry of the ion gun and the collector assembly were checked, both intrinsically, and in relation to the tube, but all parallelisms were correct to within $\frac{1}{2}^{o}$. Special attention was paid to cleanliness during source assembly, and a number of different methods were tried using a variety of A.R. solvents, aqueous detergents and distilled water. By means of batteries and potential dividers, it was possible to investigate the effect of source potentials on resolution. The effect of alterations in the strength and position of the auxiliary collimating magnet was examined, but although these changes appeared to affect the resolution somewhat, the improvement was small and no useful conclusions could be drawn from them.

On further consideration, some of the results obtained in all these experiments did suggest that the resolution deteriorated over a period of time, but that it could be partially/

FIGURE 14.

Fig. 14.

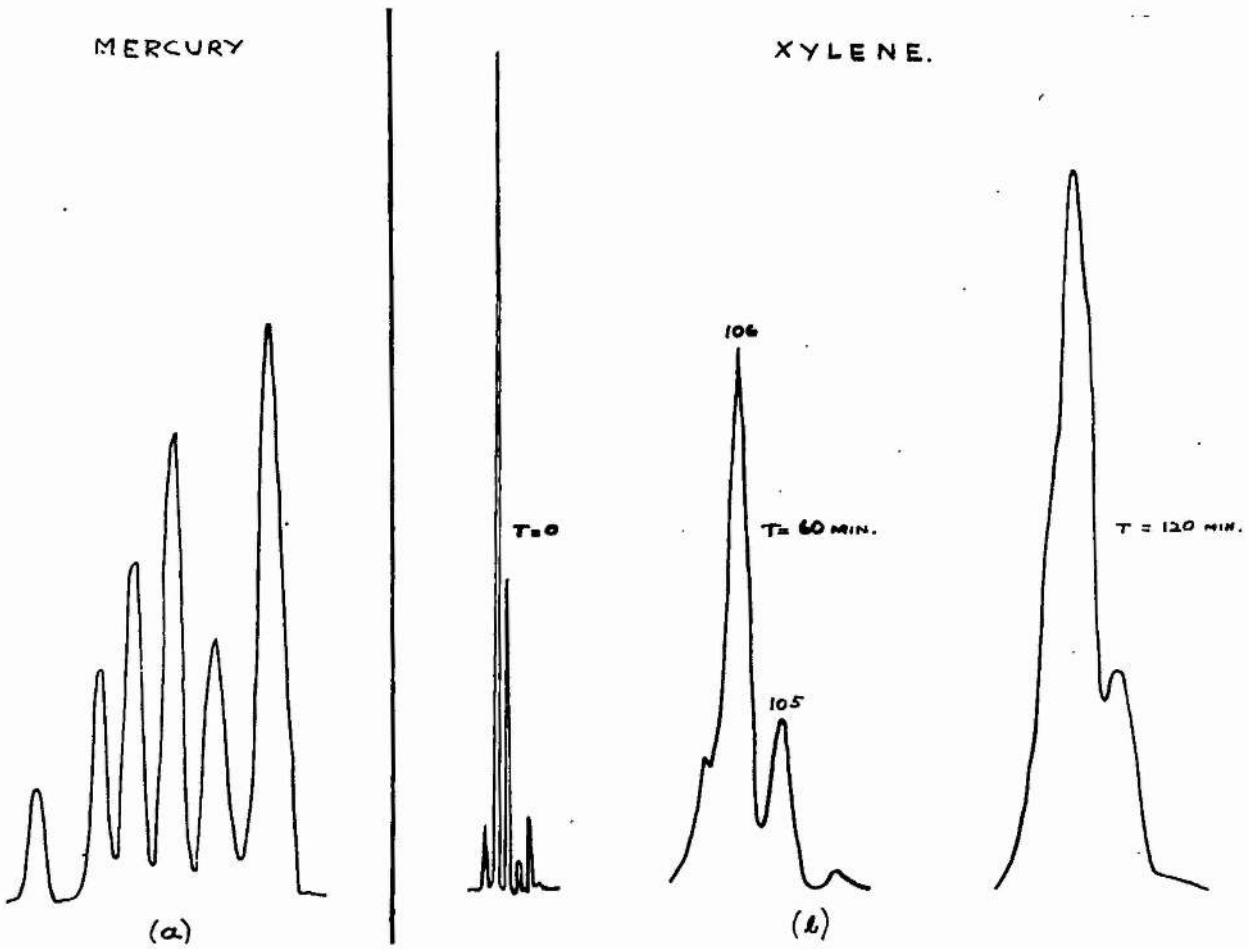

Resolution of the instrument.

(a) Spectrum of the mercury isotopes (doubly charged ions)

(b) Effect of xylene upon the resolution.

partially restored by readjustment of the focus voltages or the position of the collimating magnet. From this it was inferred that charges were building up on dirt layers in the source. In view of the care taken to cleanse all parts of the stack during assembly, these could come only from the diffusion pump oil or the xylene which was injected as the test substance. The latter material was proved to be the culprit by scanning the spectrum with a clean source immediately after the introduction of the substance. By this means excellent resolution was obtained while repeated scanning at increasing intervals of time showed a striking deterioration in the spectra as shown in Fig. 14(b). Since it had been the practice during all previous work to allow the system ample time to achieve equilibrium before commencing readings, this initial behaviour had passed unnoticed. Whether the effect was due to p-xylene polymerising (55) or to some other impurity was not pursued; it sufficed that a similar experiment with toluene showed no deterioration of resolution with time.

The experience which had been gained from the above work regarding the effect of the various source potentials was sufficient to assess the flexibility required to achieve optimum performance. At this stage a potential divider was built capable of supplying all the necessary voltages when/

when fed from the H.T. unit mentioned in Part II. With the aid of this unit a definitive procedure for focussing the instrument was worked out. Maximum resolution was found to coincide with maximum sensitivity for a particular value of the repeller voltage, but that undue increase of this parameter had an adverse effect on the ultimate resolution. In practice, the repeller was operated at a potential of about +2 volts. With the focus plates shorted together, the voltage difference between the draw-out plate and the ion box was increased until maximum beam size was obtained under which condition the focus plates were freed, and a bias voltage applied until maximum sensitivity was again achieved. At this stage the instrument was ready for operation, but when maximum sensitivity was required, the beam centring plate was given a small bias to achieve this.

The resolution provided by the spectrometer under these conditions is illustrated by Fig 14a which shows the spectrum of the doubly charged ions of the mercury isotopes. This behaviour approaches the theoretical limit of the instrument and was more than adequate for the later measurements on benzyl ions.

DIFFERENTIAL PUMPING

The/

DIFFERENTIAL PUMPING

The need for differential pumping to prevent contamination of the spectrum by fragment ions produced by pyrolysis on the filament was pointed out by Stevenson (18) who showed that $A(C_3H_6^+)$ in the spectrum of di-methyl butane = I(propylene).

Time did not permit an exhaustive examination of the effectiveness of the steps taken to achieve differential pumping nevertheless results were obtained which suggested that the design of the source was successful in this respect. Precise comparisons between the performances of different instruments are impossible owing to the dependence of cracking pattern on temperature, mass discrimination and other factors. However, the cracking pattern of the major peaks of toluene differed from the published figures by an amount greater than is likely to be accounted for by such effects, and in a direction corresponding to a decreased production of the fragment ion. These findings are summarised in the following table:-

92 /91

0.90	Mean of 16 determinations at different times under a variety of source conditions in the range 40--95 eV. with full differential pumping.
0.86	Mean of nine consecutive determinations at steps of 5 eV./

5 eV. in the range 40--80 eV. with full differential pumping.

0.83 Mean of nine similar determinations after the bellows and large glass spacing ring had been removed.

0.78 Mean of 6 published values in the range 50--75 eV.(56)

It is interesting to note that the one experiment in which the peaks of xylene were resolved satisfactorily, yielded a value of 0.37 for the ratio 105 /106 , whereas the weighted mean of the published figures (allowing for the isomeric composition) is 0.44. This again indicates a decreased abundance of the fragment ion.

THE BEHAVIOUR OF THE ELECTRON GUN

If a true measurement of the ionization cross section is to be made, the electron density of the source must be kept constant. Barnard (48) has discussed the relative merits of systems employing stabilization of the trap, emission or filament current to achieve this end. The behaviour of the electron gun was in some degree anomalous due to the unusually long distance between the filament and the ionization chamber, and occasionally to layers of dirt which were deposited on the edges of the slits. It was found over a range of electron voltages that the beam size was not always linearly dependent on the trap current. A better/

better relation existed with the current flowing to the repeller plate, when this was made largelynpositive, although this is an inconvenient parameter to use in routine work, since the ionization process is disturbed. In addition, the stabilisation of the emission current caused considerable variation in the trap current when the accelerating voltage was altered, owing to its effect on the angular distribution of electrons leaving the filament, complicated by the effect of the collimating field. Several small modifications were made to the electron gun in an attempt to simplify this behaviour, including variation of slit sizes and shapes, and the insertion of copper gauze in the first slit. However, these experiments were not pursued very far since it was found that suitable adjustment of the collimating magnet yielded trap currents which remained essentially constant over the range of voltages for which the ionization efficiency curves were measured. This is illustrated by the following set of figures taken from experiment 37.

eV.	18	17	16	15	14	13	12	11	10	9	8	7
i_t	21⅓	23⅓	24⅓	21⅓	21½	23	23	22⅓	22.	22	22	22 x 2 μa

It was therefore unnecessary to correct the peak heights which resulted from alterations in the electron accelerating voltage with a stabilized value of i_e... The validity of this reasoning was endorsed by comparing the value of an appearance/

appearance potential measured in this way with the value obtained from an experiment in which the total emission was altered manually to maintain a constant trap current. No significant difference could be detected. The effect of trap volts on the measured appearance potential was investigated during the preliminary experiments with krypton, which are described in Part 4. In experiments 33 and 34 V_t= 80v while in experiment 35 V_t= 0. No difference between the results could be detected.

OPERATIONAL FAULTS

During the experiments which have just been described, the trap current was observed to suffer from periods of instability, which also appeared to affect the filament current to a proportionately smaller extent. By substituting a battery for the filament supply, the fault was localized in the filament itself. A number of new filaments were tried, some of which reproduced the fault while others behaved normally. Examination under a microscope showed the existence of transverse flaws in just those filaments which had proved unsatisfactory, and also in the ribbon from which they had been cut initially. By selecting new filaments from portions of the ribbon which were free from these imperfections no further trouble was encountered.

Another/

Another fault associated with the filament assembly was the breakdown of the insulation of the ceramic supports for the filament leads due to the deposition of a surface film. The symptom was a steady disappearance of trap current, and the cause was not at first obvious since break-down occurred only when the insulator was hot. In all but the most severe cases the insulator had to be tested within seconds of removing the filament current, otherwise it appeared to behave normally. The only cure was the regular replacement of the ceramics.

Previous mention has been made of the replacement of the original oil diffusion pumps with comparable mercury types. This was done as a result of the persistent deterioration in the resolution of the instrument with use. The experience gained with xylene pointed to dirt layers of an organic nature, while comparison with the behaviour of the other instrument in the department suggested diffusion pump oil as the culprit. The non-recurrence of the trouble after the change amply justified the extra outlay.

PART 4

MEASUREMENT OF THE APPEARANCE POTENTIALS OF SOME SIMPLE IONS.

EXPERIMENTAL PROCEDURE

The energy of the electrons entering the ionization chamber may not correspond exactly to the voltage which is applied between the filament and the ion chamber owing to the existence of contact potentials in the source region, the potential drop along a directly heated filament, and to the effects of Maxwell-Boltzmann energy spread. This means that the energy scale of an ionization efficiency curve must be calibrated by some independent method, if a reliable estimation of the appearance potential is to be made. This is achieved by the simultaneous admission of some standard substance whose ionization process is studied at the same time.(5). Under these conditions, any uncertainties in the energy scales apply to both curves, and although the voltages obtained by extrapolating the curves individually have no significance, their differenceis real. Thus if the energy associated with the ionization process undergone by the standard, is known from other data it is possible to derive an absolute value for the appearance potential of the ion under investigation. In most cases the standard substance consists of one of the rare gases, - usually argon - whose first ionization potential is known accurately from spectrosopic measurements.

In order to check that residual peaks from the gas already present in the mass spectrometer do not contribute to the measured/

measured current, the background spectrum must be examined at the mass numbers of the ions under examination. If these are of reasonable size, their appearance potentials must be measured to ensure that they provide a negligible contribution to the ion current at the voltages employed in the determination.

In the ideal case, the ionization potential of the standard should coincide with that of the unknown in order that any persistent errors connected with changing source conditions should affect both curves and thus cancel out. The effect of change in filament temperature on the energy spread of the incident electrons has been noted already and has received attention elsewhere (57). Argon has rather a high ionization potential in this respect, but it was selected for the following reasons. It was readily available in a pure form, and was singularly free from interference with other ions of the same mass; it is also the most widely used standard, consequently, comparisons with other published data would achieve greater significance. However, in a few of the later experiments, benzene was used as a secondary standard.

The method of making a measurement was as follows. The gas handling system Fig 23 was evacuated and a sample of the substance admitted to the reservoir. The manner in which this was carried out depended on the nature of the substance, as discussed previously. A quantity of argon was then added by means/

means of the gas-burette sufficient to yield an ionization efficiency curve whose linear portion was roughly parallel with that of the test substance. In order to homogenise the two substances, use was made of the small mixing volume H, in cases where the other substance was a gas. When argon had to be added to a liquid, previously injected through the sinter, the mixture was allowed to stand for at least half an hour to achieve equilibrium, use being made of this period to condition the source, by bleeding in the sample. The large expansion ratio helped to speed up the mixing process, and checks were made with the mass spectrometer to ascertain that this had been completed. Towards the end of the work it proved possible to install a second Metrosil leak thus enabling the two substances to be isolated in separate containers. Not only were equilibrium conditions achieved much more rapidly but the relative concentrations could be adjusted with ease.

After the zero of the amplifier had been set and the valve voltmeter standardised, the appropriate ion was focussed by means of the magnet sweep control. The voltages in the source were then adjusted to provide maximum sensitivity and resolution as described in Part 3. The ion current was then noted for each of a series of values of the electron accelerating voltage. This was achieved by setting the potentiometer/

potentiometer of the valve voltmeter to the required value, and altering the accelerating potential by means of VR_4, Fig.10. until a null reading is displayed by the valve voltmeter. Under these conditions the voltage applied to the electron gun is equal to the setting of the potentiometer. The separation between readings varied in different parts of the curve, and observations were made at intervals of 0.1 or 0.2 volts in the lower section, whereas steps of 0.5 or 1.0, volts usually sufficed for the linear part of the curve. The beam was kept in focus by making small alterations in the magnet sweep control when necessary. When the size of the ion current approached the limit of detection, the beam was suppressed and the amplifier zero rechecked, after which the electron accelerating voltage was readjusted to reproduce the initial reading, in order to ensure that conditions had remained constant throughout the course of the measurement. Without any alteration in the voltages in the ion gun, the beam of singly charged argon ions was brought into focus by magnetic scanning and the whole procedure repeated. Throughout all these readings the source was operated under the condition of constant emission, note being taken of the trap current to ensure that it remained reasonably constant over the range of accelerating voltages used. Occasional checks were made to see that the repeller current behaved in a similar manner as described in Part 2.

The/

The sets of readings thus obtained were treated in the following way. After subtraction of the amplifier zero, the upper parts of the curves were plotted in order to determine the ratio of the linear slopes. This quantity was used as a multiplying factor to normalise one curve with respect to the other as explained in Part 1. The corrected ion currents were then plotted as ordinate against the corresponding electron voltage, on enlarged scales, and the appearance potential deduced by the Warren method. The sensitivity of the instrument was such as to allow measurement of ion currents less than 0.1% of the signal corresponding to 50 eV., and in practice the Warren extrapolation was only carried out for currents below about 1% of this value. Unless otherwise stated, values for appearance potentials quoted in this thesis have been obtained in this way, as is illustrated in the following example (Expt 37)

Process $Kr \longrightarrow Kr^{+} + e$

eV.	Rec^{r} Read^{g}.	Range.	Volts.	Corrected for amp.zero	Normalized value
17.5	30.3	10v.	3.03	3.03	(Ratio of
17.0	91.0	3v.	2.73	2.73	slopes 0.797)
16.5	78.2		2.35	2.35	A/Kr
16.0	65.5		1.97	1.97	
15.5	51.7		1.55	1.55	(Amp^{r} zero
15.0	41.5		1.25	1.25	20mv.)
14.5	30.5		0.915	0.915	
14.2	74.0	1v.	0.74	0.74	Normalized
14.0	61.5		0.615	0.615	Value
13.8	50.0		0.500	0.500	(mv.)
13.6/					

eV.	Recr. Readgs.	Range.	Volts.	Corrected for amp.zero	Normalised value.
13.6	39.5		0.395	0.395	
13.4	30.0		0.300	0.298	238
13.3	85.0	300mv.	0.255	0.253	202
13.2	69.2		0.207	0.205	164
13.1	55.0		0.165	0.163	130
13.0	44.5		0.134	0.132	105
12.9	54.5		0.104	0.102	81
12.8	80.0	100mv.	0.080	0.078	62
12.7	59.0		0.059	0.057	45.5
12.6	45.0		0.045	0.043	34.5
12.5	35.0		0.035	0.033	26
12.4	79	30mv.	0.0237	0.0217	17
12.3	61		0.0183	0.0163	13
12.2	45		0.0135	0.0115	9
12.1	35		0.0108	0.0088	7
12.0	80	10mv.	0.008	0.006	5
11.8	49		0.005	0.003	2
--					
17.5	31.0	10v.			

Multiplication of the figures in the last column by 0.5×10^{-14} gives the ion current in amps since the input grid resistor is 2×10^{11} ohms

Process $A \longrightarrow A^+ + e$ $\qquad I_s(A) = 15.77eV \quad (58)$

eV	Recorder Reading	Ion Current. Range	Volts	Corrected for amp. zero.	
18.0	58.0	3v.	1.74	1.74	
17.5	48.5		1.455	1.455	
17.0	39.2		1.176	1.176	Ampr. zero 30mv.
16.5	89.7	1v.	0.897	0.897	
16.0	62.2		0.622	0.622	
15.5	35.5		0.355	0.355	
15.4	31.5		0.315	0.312	
15.3	89.5	300mv.	0.2685	0.2655	
15.2	75.5		0.2265	0.2235	
15.0	55.0		0.165	0.162	
14.9	45.5		0.1365	0.1335	
14.8	37.5		0.1125	0.1095	
14.7/					

FIGURE 15.

Fig. 15.

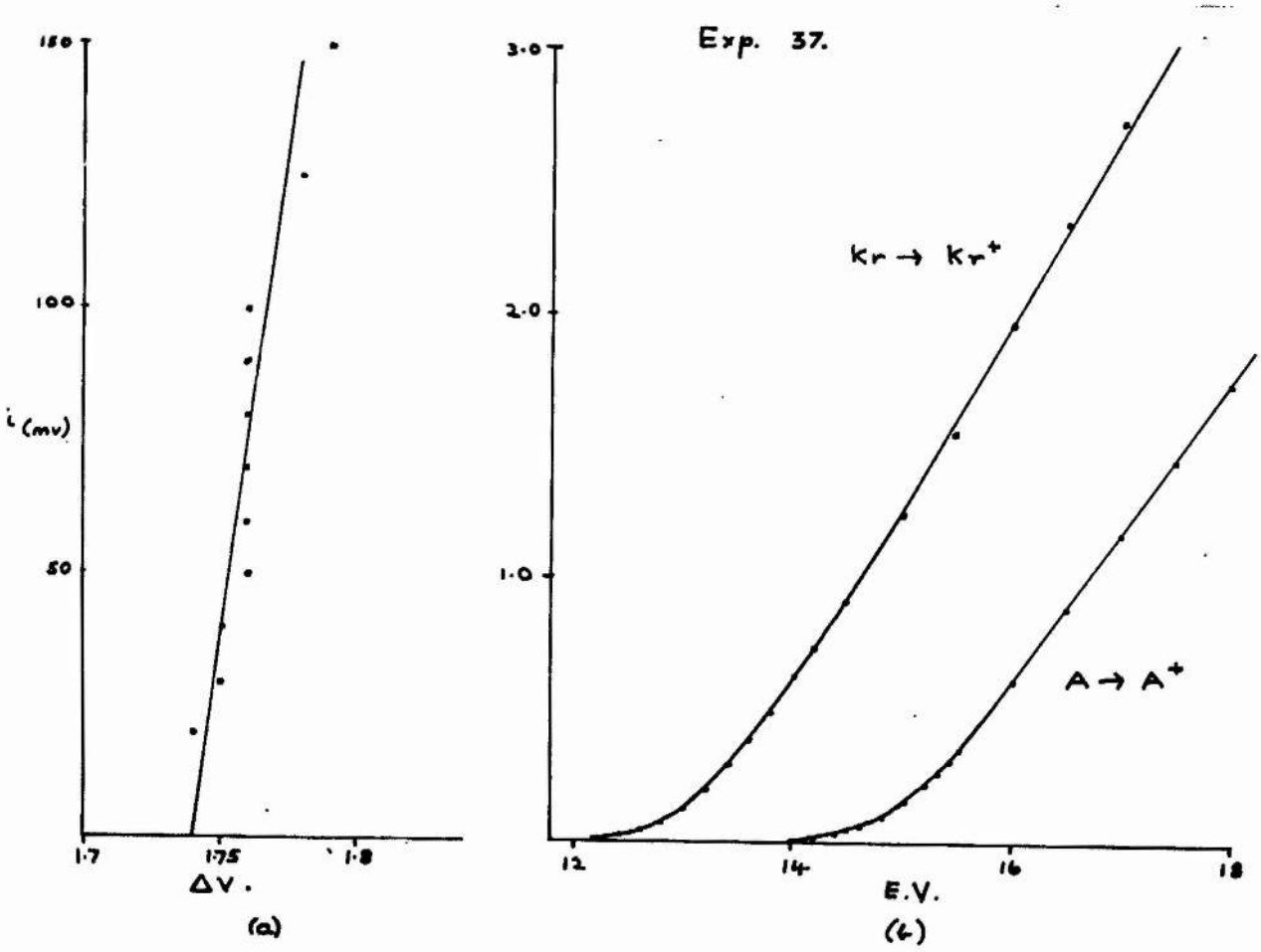

Experiment 37.

(a) Warren extrapolation of the ionization efficiency curves.

(b) Ionization efficiency curves of argon and krypton.

FIGURE 16.

Fig. 16.

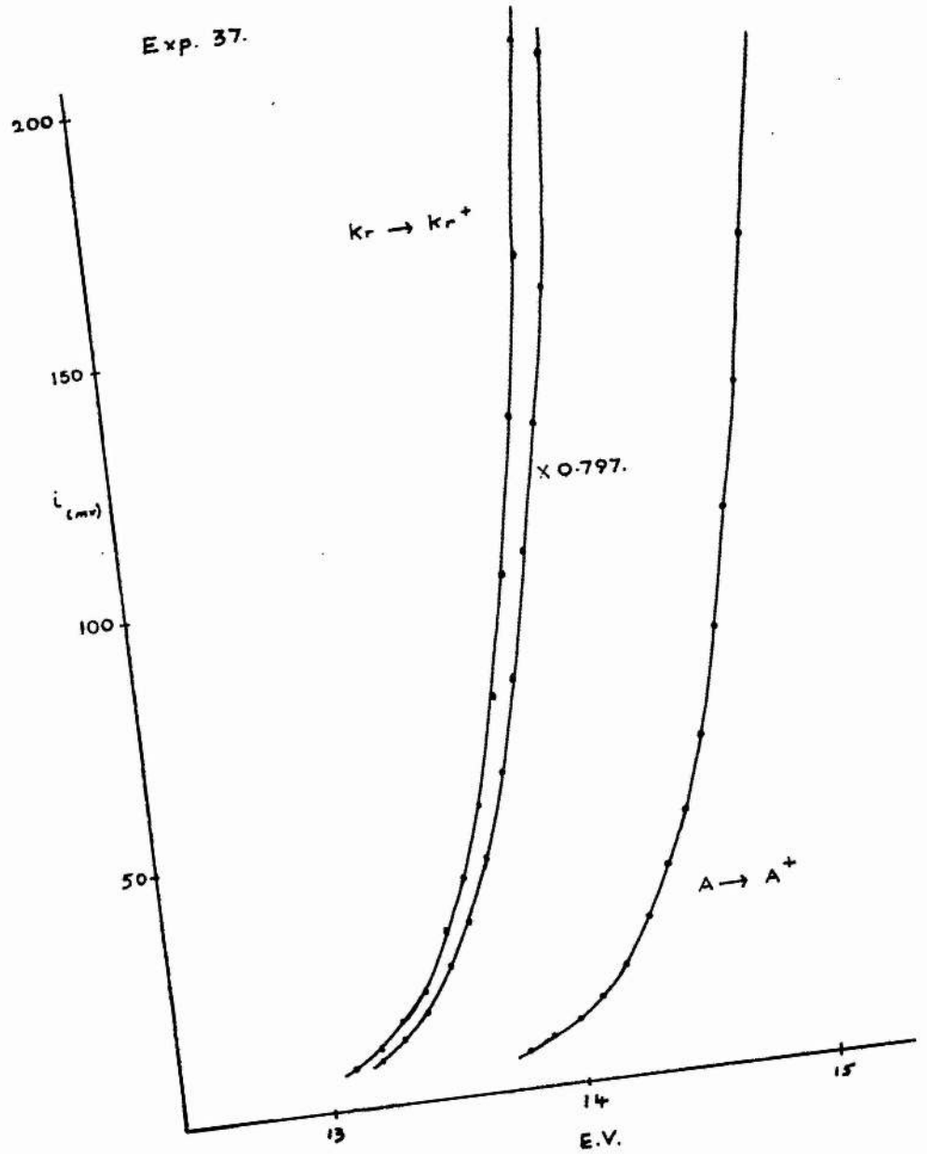

Lower part of the ionization efficiency curves of argon and krypton (exp. 37) on an expanded scale.

FIGURE 17.

Fig. 17.

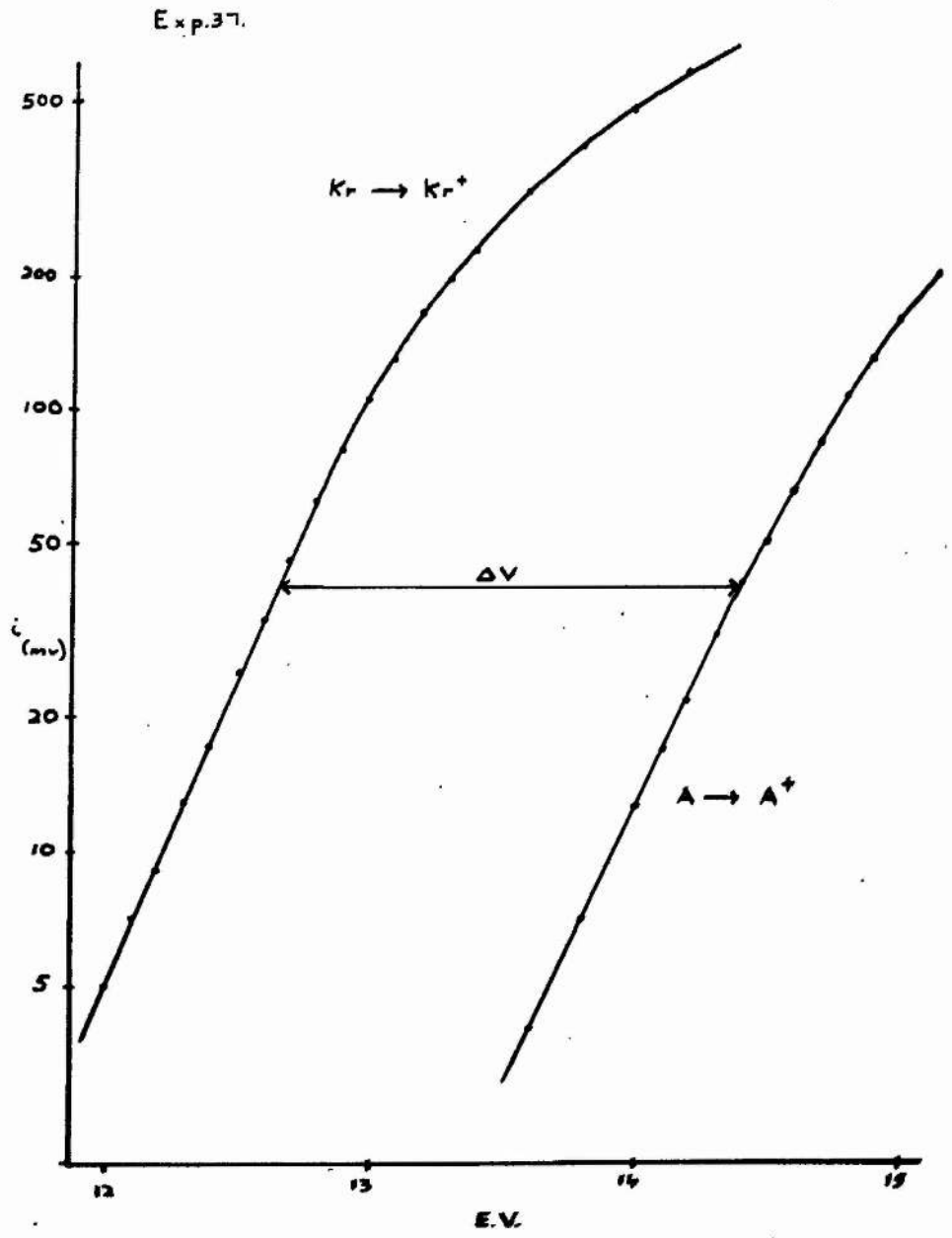

Semi-log plot of the results of experiment 37, showing Morrison's empirical method for obtaining dV.

eV.	Recorder Reading	Ion Current. Range	Volts	Corrected for amp. zero.
14.7	89	100mv.	0.089	0.086
14.6	68		0.068	0.065
14.5	54		0.054	0.051
14.4	44		0.044	0.041
14.3	34		0.034	0.031
14.2	83	30mv.	0.025	0.022
14.1	66		0.020	0.017
14.0	53		0.016	0.013
13.8	35		0.0105	0.007
13.6	67	10mv.	0.0067	0.004
13.4	60		0.006	0.003
--				
18.0	57.5	3v.		

Multiplication of the last column by 0.5×10^{-11} gives the ion current in amps.

The graphical representation of these results can be seen in Figs. 15(b) & (16), the latter consisting of the lower part of the curve on an enlarged scale. From them, values of dV were measured for a range of ion currents, enabling the ionization potential to be obtained by a Warren extrapolation Fig.15(a). The extrapolated voltage difference at i=0 is 1.74 volts corresponding to an ionization potential of 14.03 volts for the process $Kr \longrightarrow Kr^{+} + e$.

On a number of occasions, Morrison's method of extrapolation was applied, the semi log plot of ion current against electron volts yielding a series of straight lines corresponding to the exponential tails of the curves. Fig.17 shows the results of experiment (37) plotted in this way.

Although/

Although the measurement of dV was made easier, this method of displaying the results tended to disguise peculiarities in the curves as the limit of sensitivity was approached, and for this reason, Warren's method was the one usually adopted.

THE IONIZATION POTENTIAL OF KRYPTON

In order to test the reproducibility and accuracy of the experimental procedure which has been described in the previous section, measurements of the ionization potential of krypton were made, since the energy of this transition is known from spectroscopic data. The results of these experiments are tabulated below.

Experiment	Ionization Potential	
	Lin. Extrap.	Warren Extrap.
22	14.05	13.96v
23	14.17	14.07
24	14.02	13.96
25	14.05	13.99
26	13.97	13.79
27	14.02	14.01
33		14.00
34		13.98
35		13.99
36	14.02	14.01
37	14.02	14.03

The mean of the linear extrapolations is 14.04 v. while that of the Warren extrapolations is 14.00± 0.03v (excluding that of expt.26) which differs from the rest by more than five standard deviations. The spectroscopic value is 14.02v (58).

It/

It must be emphasized that the accuracy quoted for this value for the ionization potential is the standard deviation of the set of results, and therefore does not include the effect of any persistent errors. Many of the accuracies quoted in the literature are misleading in this respect, and purport to assign an absolute error to the experiment when in fact they represent simply the consistency of the procedure for a small number of runs repeated under identical conditions. Since both curves are of the rare gas type, it is not surprising that the two methods of extrapolation give similar values for the ionization potential.

THE IONIZATION POTENTIAL OF ACETYLENE

Several measurements of this quantity were made at different times, mainly in the very early stages of the work. The results are tabulated below with an assessment of their reliability.

Experiment	Warren Extrapolation	Reliability
93	11.42	Fair
98	11.57	Poor
100	11.47	Fair
77	11.45	Good
78	11.64	Poor

Spectroscopic value 11.41 eV. (59)

Independent E.I. Value 11.43 eV. (5)

Only experiment 77 can be considered to be really reliable, but/

but the general measure of agreement is quite good.

THE IONIZATION POTENTIAL OF WATER

A single determination was made on this substance with the following result:-

Experiment	Ionization Potential	Spectroscopic
180	12.7eV.	12.62eV.

Spectroscopic value 12.61 eV. (60)

Independent E.I. (Morrison) 12.76 eV. (11)

PART 5.

THE APPEARANCE POTENTIALS OF SOME AROMATIC IONS.

CHOICE OF COMPOUNDS

Over a period of years, a team of research workers at St. Andrews has been investigating the behaviour of a series of aromatic molecules under conditions leading to their thermal decomposition. Reactions whose kinetics have been studied involve toluene, dibenzyl, diphenyl-methane, phenyl iodide and benzyl iodide, and an accurate evaluation of the strengths of several bonds has been obtained from the activation energies involved in these processes. It was felt desirable to estimate these bond energies by an independent method, and as the fragmentation of this class of compound had not been studied by electron impact, it was decided to use this technique for the purpose.

At a later stage in the work, several papers appeared, notably those by Lossing (21)(22)(61), Field & Franklin (62) and Kandel (30), which discussed some of the ionization processes undergone by these substances, but it was evident that the various sets of figures contained serious anomalies. For instance, the data by which Schissler & Stevenson seek to verify Szwarc's value of 77.5 Kcal for D(Ph.CH_2-H) in toluene imply that the ionization potential of the benzyl radical is 8.45 eV. whereas Lossing (21) claims to have obtained the much lower figure of 7.73 eV. by direct measurement.

In/

In the event, ionization processes were studied which involved the following parent molecules: benzene, toluene, ethyl benzene, dibenzyl, diphenyl-methane, phenyl iodide, benzyl chloride and benzyl iodide, In addition, a direct measurement of the ionization potential of the benzyl radical was successfully carried out, and will be described in Part 6. The following pages include details of the methods by which these compounds were purified, together with an account of the experimental results obtained for each compound. The reliability of each set of figures is discussed, and compared with any published values which have lately appeared. The remainder of this part of the thesis consists of a discussion of the significance of these estimates of the appearance potentials for the various processes. The related nature of the compounds allows cross checks to be made, and bond energies are determined by both the direct and indirect methods. In this way reliable values obtained by one technique may be used to verify less reliable estimates made by the other. These findings are used to assess the general applicability of the electron impact method to aromatic molecules.

PURIFICATION OF MATERIALS

BENZENE: A small quantity of analar benzene was redistilled from sodium.

TOLUENE:/

TOLUENE: Two different samples were used, the first of which consisted of toluene which had been distilled, and twice pyrolysed - a treatment suggested by Szwarc as a means of preparing samples suitable for kinetic studies. In view of the unsatisfactory nature of the results, a small quantity of toluene was obtained from the bank of pure hydrocarbons controlled by the D.S.I.R.

ETHYL-BENZENE: Commercial ethyl benzene was fractionated in a Fenske column, 18 in. long, and closely packed with small glass rings. The portion passing over at 135 ± 0.25°C. was collected and subjected to further purification, as follows. The sample was placed in a small test tube, supported by a larger tube immersed in liquid air. By this means, freezing took place slowly from the bottom upwards, and after about ¾ of the contents had solidified, the supernatant liquor was decanted away. After the frozen material had melted, the process was repeated three times (63).

DIBENZYL: A sample of the compound (prepared initially by the reduction of benzil) was freed from traces of stilbene by recrystallizing thrice from alcohol. The melting point of the product was 51.9°C.

DIPHENYL-METHANE: A fairly pure sample was distilled under vacuum, and the product which passed over at 185.5°C, under a pressure of 12mm. was collected and subjected to fractional freezing/

freezing, repeated twice. The melting point of the product was 26·4°C.

PHENYL-IODIDE: Material previously purified for kinetic experiments was redistilled, and the fraction collected between 188°-9°C was retained, and stored over mercury.

BENZYL-IODIDE: 100gm of sodium iodide were dissolved in the minimum quantity of ethyl alcohol, to which were added 63 gm of benzyl chloride. After refluxing for 1 hour, the mixture was poured into 1500 cc of water, when the product separated as an oil. This was collected and solidified by immersion in an ice/salt bath, and the solid product filtered off by an ice-cold filter. Final purification was effected by recrystallizing twice from alcohol, giving a product which melted at 24°C.

BENZYL-CHLORIDE: A commercial sample was fractionated in the Fenske column, used for the purification of ethyl-benzene, and the fraction which passed over at 179 ± 0.5°C was retained, and subjected to three successive applications of fractional freezing.

The ARGON used as a standard in these experiments was obtained from the same source as that employed in the experiments described in Part 4., and consisted of B.O.C. cylinder gas, purified from organic contaminants by passage through a liquid air trap.

(The/

(The author's thanks are due to Dr. R.B. Cundall and Mr. R.N. Pittilo, for the gift of samples of pyrolysed toluene and dibenzyl, and to Mr. J. Gow for help in the preparation of the benzyl iodide.)

BENZENE.

$C_6H_6 \dashrightarrow C_6H_6^+ + e$

Three measurements of the ionization potential of benzene were made with the following results:

Expt.	$I(C_6H_6)$	
164	9.53 eV.	I(A) = 15.77eV
165	9.50	
166	9.53	
Mean	9.52 ± 0.02 eV.	

Since benzene was used as a secondary standard in the measurement of the ionization potential of the benzyl radical, described in Part 6. it is important to consider this result in the light of other values which have been ascribed to it, and which include:

9.24 eV.	Spectroscopic,	Price & Wood	(64)
9.3	Electron Impact	Nief	(65)
9.45		Honig	(5)
9.52		Field & Franklin	(62)
9.54		Morrison	(6)
9.52		Higasi et al	(66)
9.52	Theoretical;	Franklin	(43)

The/

The difference between the value obtained spectroscopically, and the majority of the electron impact methods, is good evidence for the correctness of the claim that significant differences between vertical and adiabatic ionization potentials have been detected. These results have been correlated by Fox & Hickman (67) in a paper describing the application of their pulsed ion source to a study of the ionization processes in benzene. The greater refinement of their experimental technique brings to light the existence of fine structure near the foot of the curve, corresponding to energy levels near the ground state. If the ionization potential is deduced from their plot by linear extrapolation, a value of 9.59 eV. is obtained, whereas extrapolation of the curve itself through the fine structure gives a value of 9.21 eV. in good agreement with the spectroscopic value of Price & Wood. The variation among the results of the electron impact experiments can be explained in terms of these energy levels, and the differing sensitivities of the instruments employed by the authors concerned. In view of the agreement between the results obtained by the author and those of Morrison, Field and Franklin, and Higasi, this value will be taken as an accurate calibration of the apparatus when benzene is used as a secondary standard.

$$I(C_6H_6) = 9.5 \text{ eV.}$$

$$C_6H_6 \dashrightarrow C_6H_5^+ + H + e/$$

$C_6H_6 \longrightarrow C_6H_5^+ + H + e$

Seven determinations of the appearance potential of the phenyl ion by this process were made on two different occasions. These are indicated by grouping the results within the column, and this procedure will be followed in subsequent cases.

Expt.	$A(Ph^+)$
122	14.11 eV.
123	14.07
124	14.13
125	14.11
164	14.11
165	14.13
166	14.13
Mean	14.11 ± 0.02

The last three of these measurements were made conjointly with the determination of the ionization potential of benzene, described above, and this is added confirmation of their correctness. Two other estimates of this appearance potential have appeared in the literature, namely:

14.54 ± 0.02 eV. Kandel (30)

14.30 ± 0.18 Field & Franklin (62)

Kandel/

Kandel claims that no excess energy was detected in association with the phenyl ion, but by the conservation of momentum, the limit of detection for the process is $2\frac{1}{2}$ eV. The value obtained by the author lies within the precision of the second of the two values quoted above, and will be taken as correct

$$A(Ph^+)_{PhH} = 14.1_1 \text{ eV.}$$

TOLUENE.

$PhCH_3 \dashrightarrow PhCH_3^+ + e$

Expt.	$I(PhCH_3)$
49	9.21 eV.

This result shows excellent agreement with other published E.I. values.

9.23 eV.	(Electron Impact)	Honig	(5)
9.23	"	Morrison	(6)
9.20		Higasi	(66)
8.77	Spectroscopic	Price & Walsh	(68)

The value of the experiment is as a check on the performance of the instrument at low values of electron energy.

$$I(PhCH_3) = 9.2_1 \text{ eV.}$$

$PhCH_2\text{-}H \dashrightarrow PhCH_2^+ + H + e$

The energetics of this process were of considerable interest, since it was hoped to deduce a value for $D(PhCH_2\text{-}H)$ from the data./

data. For some unexplained reason, the reproducibility of the extrapolated values of the energy term obtained from different sets of experiments were not as good as with most of the other processes studied. In all, fifteen determinations were made:

Expt.	$A(PhCH_2^+)$	Sensitivity
14	12.49 eV	0.7(arbitrary units)
15	12.57	0.7
16	12.23	0.75
20	12.24	0.7
38	12.42	0.53
39	12.41	0.45
40	12.62	0.55
46	12.56	0.71
47	12.60	0.71
49	12.43	0.86
53	12.31	2.12
54	12.40	2.54
55	12.30	2.2
61	12.43	0.34
62	12.34	0.38
Means	12.34 $\pm$ 0.12	

Experiment/

FIGURE 18.

Fig. 18.

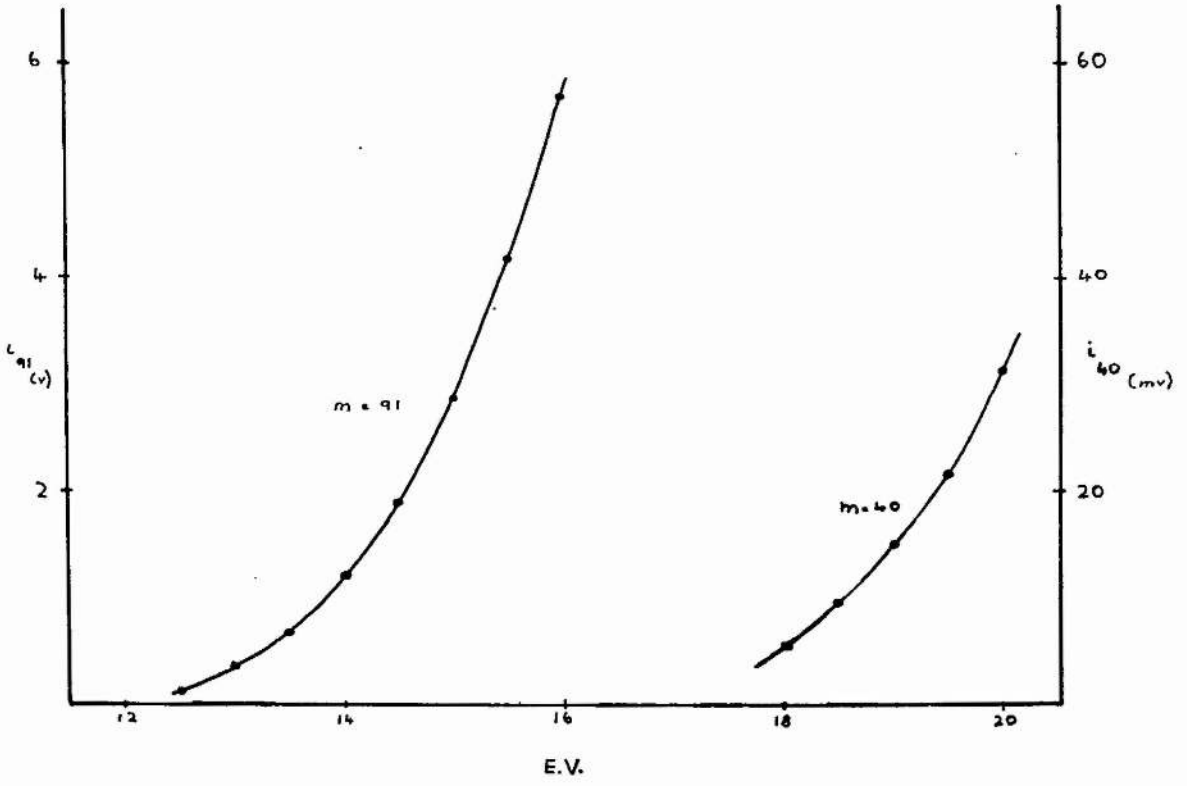

The contribution of a fragment at mass 40 from toluene, to the argon peak.

Experiment 49 includes the reliable estimate of the ionization potential of toluene, and was carried out with a sensitivity suffieient to allow extrapolation from ion currents down to 0.1% of the value at 20 eV. The mean of the 15 determinations coincides with the value obtained in this experiment. No correlation exists between the derived value of the appearance potential and the ion beam size.

$$A(PhCH_2^+)_{PhCH_2-H} = 12.4 \pm 0.15 \text{ eV}.$$

The only other published figure is one of 11.8 ± 0.1 eV. in a paper by Schissler & Stevenson (69), the discrepancy outside the limits of precision being 0.35 eV.

Three errors which may arise in the measurement of ionization efficiency curves are lack of sensitivity in detection, poor resolution and contamination of the peak of the standard gas by background ions or by a fragment of the molecule under investigation. The last of these effects was eliminated from consideration be measuring the ionization efficiency curve for the mass 40 fragment from toluene. The result is plotted in Fig 18 which shows conclusively that the contribution of this ion to the argon beam is negligible. Poor resolution could cause contamination of the peak at mass 91, by ions of the parent molecule, leading to a low value for the appearance potential, by reason of the smaller energy required for its fragmentation; this might be the explanation/

explanation of Stevenson's low value. On the other hand, poor sensitivity would lead to the opposite effect, but for reasons already stated it does not seem likely that the results quoted in this thesis should suffer from this error, and it is likely that the appearance potential for this dissociation process contains a considerable excess energy term. The relative masses of the two fragments prevents the presence of kinetic energy being observed, and the point corresponding to the benzyl ion falls on the graph shown in Fig 4 (b).

ETHYL BENZENE.

$PhCH_2 - CH_3 \longrightarrow PhCH_2^+ + CH_3 + e$

The appearance potential of the benzyl radical from ethyl benzene was determined in two sets of experiments:

Expt.	$A(PhCH_2^+)$
17	11.45 eV.
18	11.23
19	11.43
56	11.51
57	11.49
58	11.45
59	11.47
Mean	11.43 ± 0.07 eV

The/

The sensitivity of the experiments was such as to allow extrapolation down to 0.05% of the ion current at 20 eV. Two values for the energy of this process have been published in the literature;

11.21 ± 0.15 eV	Field & Franklin (62)
11.2 ± 0.1	Schissler & Stevenson (69)

but the differences between these values and that obtained by the author are just on the limits of precision for the two determinations. As in the case of toluene, the process is probably associated with an appreciable excess energy term,

DIBENZYL

$PhCH_2\text{-}CH_2Ph \longrightarrow PhCH_2^+ + PhCH_2 + e.$

Expt.	A($PhCH_2^+$)		Sensitivity
64	4.66 eV	11.11	0.27 (Arbitrary units)
65	4.88		0.27
66	4.86		0.25
67	4.84		0.24
68	4.82		0.24
69	4.82		0.23
70	5.04		0.29
71	5.04		0.29
72	5.02		0.28
73	5.02		0.27

74/

FIGURE 19.

Fig. 19.

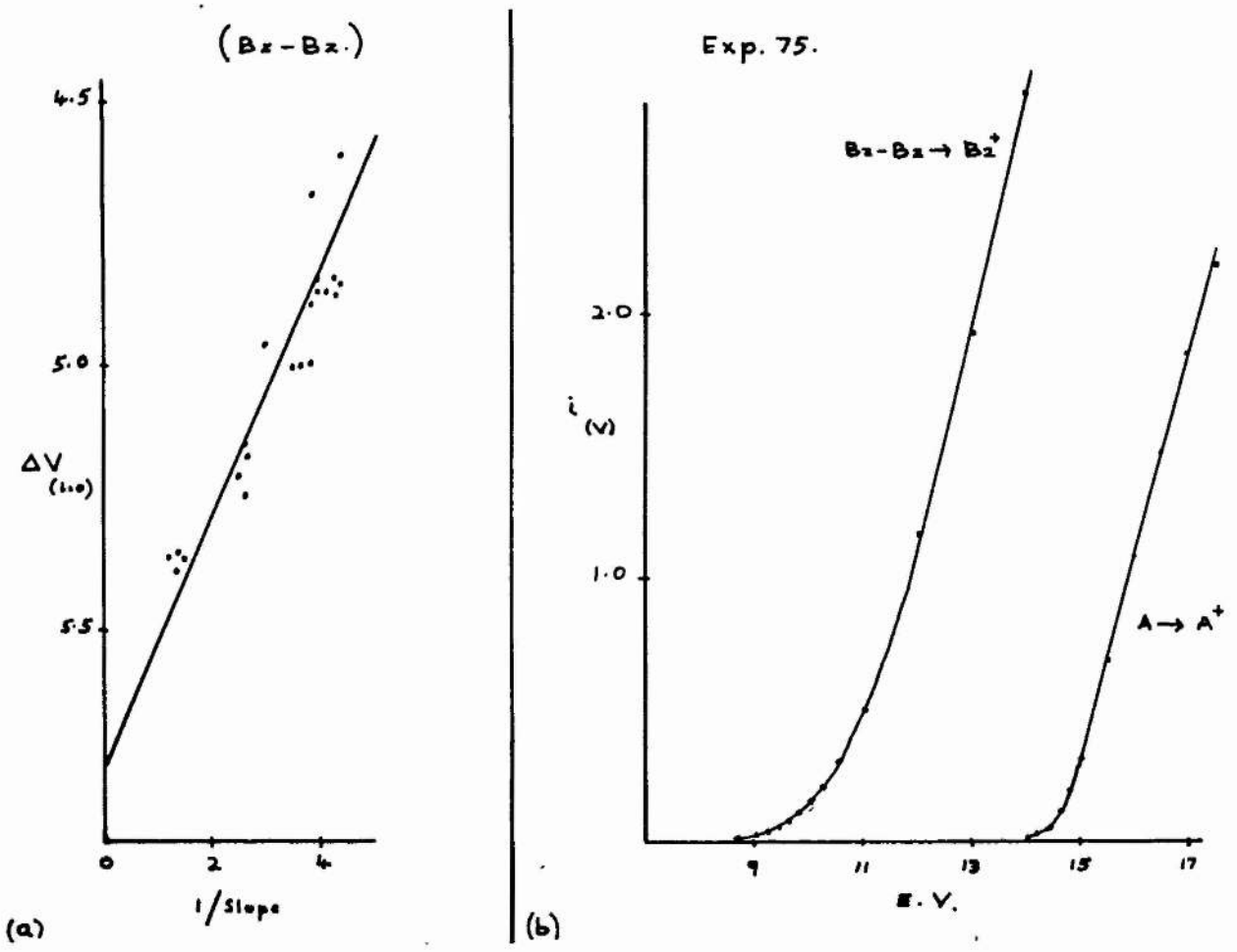

Ionization efficiency curves for dibenzyl and argon, together with the extrapolation used to combine the results of all the experiments.

Expt.	$A(PhCH_2^+)$	Sensitivity	
74	5.37	0.95	
75	5.39	0.77	
76	5.37	0.77	(0.2% of value at 20eV.
81	5.35	0.39	
106	4.98	0.35	

Inspection of these results suggests that the extrapolated value depends on the sensitivity of the measurement, and this is confirmed by plotting the results in graphical form as shown in Fig 19. In this diagram, the values of the appearance potential are plotted against the reciprocal of the concentrations, (represented as the slope of the linear part of the appropriate argon ionization efficiency curve). The intercept made by the best straight line through these points, (determined by the centre of gravity method) on the axis corresponding to (1/sensitivity = 0,)was taken as the appearance potential for the process.

$$A(PhCH_2^+) = 10.0 \text{ eV.}$$

the only other quoted figure being 10.5 $\pm$ 0.1 from the work of Schissler & Stevenson (69). Since the volatility of dibenzyl is not very great, it seems likely that the lower value obtained by the author is due to attention paid to matters of sensitivity in this work, and as the fragment under investigation forms an isolated beam, it could not be caused by/

FIGURE 20.

Fig. 20.

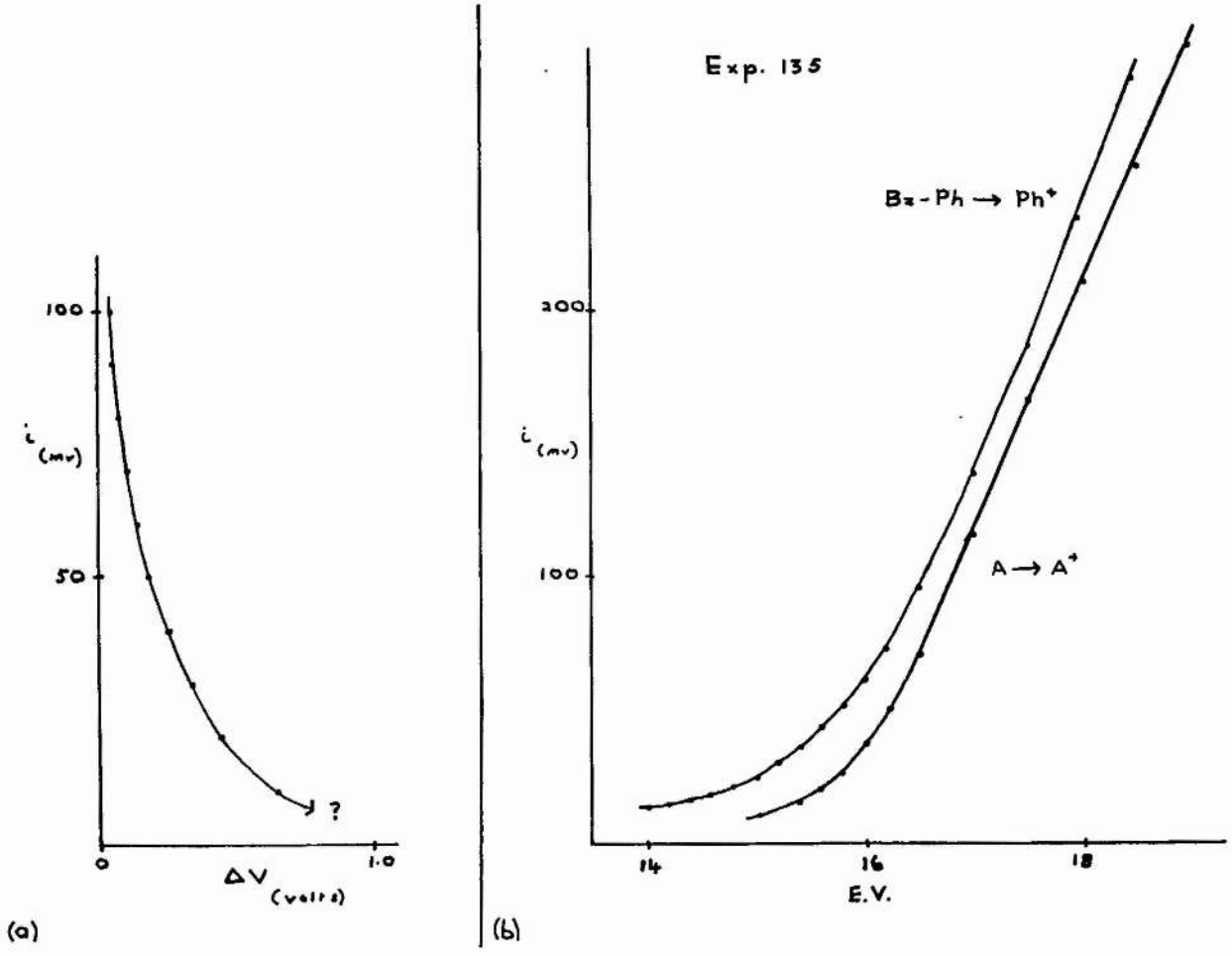

The ionization efficiency curves of diphenyl methane and argon, with a typical Warren extrapolation.

by a lack of resolution in the mass spectrometer.

DIPHENYL-METHANE.

$PhCH_2-Ph \longrightarrow PhCH_2^+ + Ph + e$

$PhCH_2-Ph \longrightarrow Ph^+ + PhCH_2 + e$

Two processes were studied, and ionization efficiency curves plotted for the formation of both benzyl and phenyl ions, but the curvature of the extrapolated voltage difference was very great. The following results were obtained for the appearance potential of the benzyl ion:

Expt.	$A(PhCH_2^+)$
111	13.07 eV.
112	12.67
113	12.77
114	12.77
Mean	12.8 ± 0.2 eV.

In the case of the second process, even a rough evaluation of the energy term is impossible as can be seen by reference to Fig 20.

BENZYL CHLORIDE.

$PhCH_2Cl \longrightarrow PhCH_2^+ + Cl + e$

Expt.	$A(PhCH_2^+)$	
50	10.61 eV	
51	10.86	Sensitivity allows
52/		

Expt.	$A(PhCH_2^+)$	
52	10.83	Sensitivity allows extrapolation to 0.05% of value at 20 eV.
Mean	10.77 ± 0.15 eV.	

Two divergent values for this appearance potential have been published, namely:

11.13 ± 0.1 eV. Franklin & Lumpkin (70)

10.35 ± 0.1 Lossing et al. (22)

Lossing suggests that the other value of 11.13 eV. is due to a lack of sensitivity in the measurement since the figure corresponds to the separation of his own curves at an ion current, 1% of that at 50 eV. The results obtained in this work confirm this explanation, but the extrapolated value obtained by measurements to ion currents 0.05% of the value at 20 eV. is still significantly higher than the figure quoted by Lossing.

$$A(PhCH_2^+)_{PhCH_2Cl} = 10.7_7$$

BENZYL IODIDE

$$PhCH_2I \longrightarrow PhCH_2^+ + I + e$$

Two sets of experiments, comprising 12 measurements, were made of this process with the following results:

Expt.	$A(PhCH_2^+)$
140	9.44 eV
141	9.55
142/	

Expt	$A(PhCH_2^+)$
142	9.62
143	9.72
144	9.61
145	9.64
146	9.74
147	9.70
148	9.55
149	9.89
150	9.66
158	9.67
159	9.65
Mean	9.65 ± 0.1 eV

The results of two other determinations of this quantity are available:

9.23 ± 0.05 eV.	Lossing et al (22)
9.68 ± 0.1	Calvert (71)

These results together with the figure for benzyl chloride quoted above, and the value of $I(PhCH_2)$ discussed in Part 6 bring to light a curious discrepancy between values obtained in this work, and those by Lossing. viz;

	This work	Lossing	Difference
$I(PhCH_2)$	8.06	7.73	0.33 eV.
$A(PhCH_2^+)_{PhCH_2I}$	9.65	9.23	0.42
$A(PhCH_2^+)_{PhCH_2Cl}$	10.77	10.35	0.42

This/

This discrepancy in the absolute values is hard to explain since the experiments have been carried out at approximately the same sensitivity. It should be noted that the last measurement of the appearance potential of the benzyl ion from benzyl chloride followed the experiment in which an excellent value for the ionization potential of toluene was obtained, and this serves to check the performance of the instrument used in this work.

PHENYL IODIDE.

$PhI \longrightarrow Ph^+ + I + e$

$PhI \longrightarrow I^+ + Ph + e$

Three measurements of the appearance potential of the phenyl ion were made:

Expt.		$A(Ph^+)$
167		11.59 eV.
169		11.72
170		11.43
	Mean	11.6 ± 0.15 eV.

However, this result is in error, since as will be shown later, I(Ph) is about 9.7 eV. which would imply a value of (11.6 ± 9.7) = 1.9 eV. for the bond energy of phenyl iodide. This quantity has been well established at 60.7 Kcal = 2.6 eV. (72) from/

from which it follows that the appearance potential of the phenyl radical measured above, is low by some 0.7 eV. Unfortunately, time did not permit the investigation of this discrepancy.

No satisfactory measurement could be made of the energy associated with the production of the I^+ ion from phenyl iodide, partly owing to its low abundance, but more because of the curvature of the Warren extrapolation, which resembled that obtained in the case of the phenyl ion from diphenylmethane shown in Fig. 20.

BOND ENERGIES DERIVED BY THE DIRECT METHOD.

In the next part of the thesis is a description of the direct measurement of the ionization potential of the benzyl radical, and anticipating the result $I(PhCH_2) = 8.0_5$ eV., it is possible to assign upper limits to the dissociation energy of the bond ($PhCH_2$-X) whenever the appearance potential of the benzyl radical from this molecule is known, since in such cases

$$A(PhCH_2^+)_{PhCH_2-X} = D(PhCH_2-X) + I(PhCH_2) + E$$

where E is a term denoting any excess energy associated with the fragments. If this treatment is applied to each of the processes of benzyl ion formation which are described above, the following upper limits may be deduced:

Toluene/

Toluene

$D(PhCH_2\text{-}H) \leq 12.34 - 8.05$

≤ 4.29 eV. (99 Kcal)

Ethyl benzene

$D(PhCH_2\text{-}CH_3) \leq 11.43 - 8.05$

≤ 3.38 eV. (78 Kcal)

Diphenyl methane

$D(PhCH_2\text{-}Ph) \leq 12.8 - 8.05$

≤ 4.75 eV. (109 Kcal)

Dibenzyl

$D(PhCH_2\text{-}CH_2Ph) \leq 10.0 - 8.05$

≤ 1.95 eV. (45 Kcal)

Benzyl chloride

$D(PhCH_2\text{-}Cl) \leq 10.77 - 8.05$

≤ 2.72 eV. (62.7 Kcal)

Benzyl Iodide

$D(PhCH_2\text{-}I) \leq 9.65 - 8.05$

≤ 1.6 eV. (36.9 Kcal)

DISCUSSION.

$D(PhCH_2\text{-}H)$

An evaluation of the dissociation energy of the benzyl - hydrogen bond was made by Szwarc (55) from a study of the pyrolytic reaction $PhCH_2\text{-}H \longrightarrow PhCH_2^+ + H$, and after further discussion of the accuracy of these results (73), the value of/

of 77.5 ± 3 kcal was confirmed. Indirect support was obtained by combining this quantity with his own figure of 63 kcal for $D(PhCH_2-CH_3)$, from which can be deduced a value of 103 kcal for the dissociation energy of methane, in good agreement with the accepted value of 101-102.kcal. On the other hand van Artsdalen favours a higher value of 89 kcal deduced from experiments on the photobromination of toluene (74). The results of Steacie et al. (75) cannot really be compared with those of Szwarc since the conditions were not identical.

In an attempt to confirm one or other of these values by an independent method, Stevenson (69) measured the appearance potentials of the benzyl ion from toluene, ethyl benzene, and dibenzyl, obtaining 11.8, 11.2 and 10.5 eV respectively. If his derived value for the toluene bond energy (77 kcal = 3.45 eV) is subtracted from the appearance potential of the benzyl ion from toluene, the difference of 8.45 eV. must represent the ionization potential of the benzyl radical. By direct measurement, Lossing (21) obtained 7.73 eV. and later (61) 7.81 eV. with a weighted mean of 7.76 eV. Suspicion was thus cast on the correctness of Stevenson's work, especially as Lossing claimed that the ionization efficiency curves for these processes possessed considerable/

considerable curvature, making extrapolation difficult. The work of the author supports Lossings claim that the ionization potential is considerably less than 8.5 eV. and that the appearance potentials quoted by Stevenson are unreliable. In the circumstance, the agreement between Stevenson's derived figure for $D(PhCH_2\text{-}H)$ and that of Szwarc must by conisdered fortuitous.

It has been shown already, that the electron impact experiments on toluene give an upper limit of 99 kcal, far in excess of either of the two postulated values. However, the measurements on dibenzyl verify Szwarc's estimate, as follows: The energy terms involved in the two processes:

$$PhCH_2\text{-}CH_2Ph \longrightarrow PhCH_2 + PhCH_2$$

$$PhCH_2\text{-}H \longrightarrow PhCH_2 + H$$

may be combined in the two equations

$$Qf(PhCH_2\text{-}CH_2Ph) + D(PhCH_2\text{-}CH_2Ph) = 2Qf(PhCH_2)$$

$$Qf(PhCH_2\text{-}H) + D(PhCH_2\text{-}H) = Qf(PhCH_2) + Qf(H)$$

and eliminating the term $Qf(PhCH_2)$

$$D(PhCH_2\text{-}H) = \tfrac{1}{2}D(PhCH_2\text{-}CH_2Ph) - Qf(PhCH_2\text{-}H) + Qf(H) + \tfrac{1}{2}Qf(PhCH_2\text{-}CH_2Ph)$$

In this way, the toluene bond energy has been expressed in terms of a bond energy derived from electron impact data, and a number of available thermochemical quantities. Now,

$D(PhCH_2\text{-}CH_2Ph) \leq 45$ kcal (see above)/

$D(PhCH_2-CH_2Ph) \leq 45$ kcal (see above)

$Qf(PhCH_2-H) = 11.9$ kcal (56)

$Qf)PhCH_2-CH_2Ph) = 29.7$ kcal (see appendix II)

$Qf(H) = 52$ kcal (76)

and substitution of these values in the last equation gives $(D(PhCH_2-H) \leq 77.4$ kcal, thus verifying the value of Szwarc.

$$\underline{D(PhCH_2-H) = 77.5 \pm 3 \text{ kcal}}$$

$\underline{D(PhCH_2-CH_2Ph)}$

A direct estimate by thermal pyrolysis was made by Horrex and Miles (77), who obtained an energy of activation of 48 kcal on the basis of a first order decomposition. It now seems that the reaction is more complex than was at first thought, and that the interpretation to be placed on this activation energy uncertain.

It has been shown that the electron impact data yield a value of about 45 kcal for the C-C bond, and that this is in agreement with a toluene bond energy of 77.5 kcal. It is therefore permissible to reverse the thermochemical cycle, and to use this value to recalculate $D(PhCH_2-CH_2Ph)$ employing thermal data only. It follows that

$$\underline{D(PhCH_2-CH_2Ph) = 45 \pm 3 \text{ kcal}}$$

$\underline{D(PhCH_2-CH_3)}$

An/

$D(PhCH_2-CH_3)$

An experimental value of 63 ± 1.5 kcal was obtained by Szwarc, based on the pyrolysis of ethyl benzene (78). No direct confirmation of this is possible by electron impact, owing to the shape of the ionization efficiency curve. However, it is now permissible to calculate it in terms of the toluene bond energy by thermochemical reasoning. The processes:

$$PhCH_2-CH_3 \longrightarrow PhCH_2 + CH_3$$

$$PhCH_2-H \longrightarrow PhCH_2 + H$$

may be represented energetically by the equations:

$$Qf(PhCH_2-CH_3) + D(PhCH_2-CH_3) = Qf(PhCH_2) + Qf(CH_3)$$

$$Qf(PhCH_2-H) + D(PhCH_2-H) = Qf(PhCH_2) + Qf(H)$$

and eliminating $Qf(PhCH_2)$

$$D(PhCH_2-CH_3) = Qf(CH_3) - Qf(PhCH_2-CH_3) + Qf(PhCH_2-H) + D(PhCH_2-H) - Qf(H)$$

Now,

$$Qf(CH_3) = 32.5 \text{ kcal (79)}$$

$$Qf(PhCH_2-CH_3) = 7.12 \text{ kcal (56)}$$

$$\underline{D(PhCH_2-CH_3) = 62.8 \pm 3 \text{ kcal}}$$

$D(PhCH_2-I)$

The earlier work of Butler and Polanyi (80) suggesting a figure of 43.7 kcal, together with a direct estimate of 39 kcal by Szwarc, has been rendered invalid by the discovery that/

that the decomposition is inhibited by the presence of iodine, thus disproving the supposed first order kinetics.

The bond energy may be derived thermochemically from that of toluene in a manner analogous with that used for ethyl benzene.

$$D(PhCH_2\text{-}I) = Qf(I) - Qf(PhCH_2\text{-}I) + D(PhCH_2\text{-}H) + Qf(PhCH_2\text{-}H) - Qf(H)$$

Now, $Qf(I) = 25.5$ kcal (76)

$Qf(PhCH_2\text{-}I) = 26.4 \pm 3$ kcal (81)

and substituting these data in the equation, $D(PhCH_2\text{-}I) = 36.5 \pm 4$ kcal. This result is confirmed by the electron impact figure of ≤ 36.9 kcal. (Lossing's data suggest about 34 kcal.) In a recent paper,(82) Graham Nichol and Ubbelohde suggest a higher figure of 43 kcal based on their own determination of $Qf(PhCH_2\text{-}I) = 18.8$ kcal. It is difficult to assess the relative merits of the two sets of thermochemical data directly, but the electron impact results of both Lossing and the author are in favour of the earlier figure for the heat of formation of benzyl iodide. Hence it will be assumed that

$$\underline{Qf(PhCH_2\text{-}I) = 26.4 \pm 2 \text{ kcal}}$$

and

$$\underline{D(PhCH_2\text{-}I) = 36.6 \pm 3 \text{ kcal.}}$$

$\underline{D(PhCH_2\text{-}Cl)}$

$D(PhCH_2-Cl)$

The decomposition of benzyl chloride has been studied by Szwarc & Taylor (83) who applied the toluene carrier gas technique, and obtained a rate equation whose A factor was rather high ($10^{14.8}$ sec^{-1}), and for which the corresponding energy of activation was 68 kcal. As in the case of benzyl iodide, the bond energy may be deduced thermochemically from the toluene data:

$$D(PhCH_2-Cl) = Qf(Cl) - Qf(PhCH_2-Cl) + D(PhCH_2-Cl) + Qf(PhCH_2-H) - Qf(H)$$

Now, $Qf(Cl) = 29.0$ kcal (76)

$Qf(PhCH-Cl) = 5.2$

(The heat of formation of benzyl chloride is calculated by (69) on the basis of the constant difference Qf(benzyl-X) -Qf(allyl-X) from data found in (84)). Substitution of these figures in the equation shows that $D(PhCH_2-Cl) = 61$ kcal. This is well supported by direct electron impact data which give a figure of $\leq$ 62.7 kcal. Similar data by Lossing give 60 kcal. for the bond energy. It will be necessary for an accurate evaluation of the heat of formation to be made before a reliable figure for the bond energy can be deduced, but it seems reasonable on the evidence quoted here, to say that

$$D(PhCH_2-Cl) = 62 \pm 3 \text{ kcal}$$

$D(PhCH_2-Ph)$/

$D(PhCH_2\text{-}Ph)$

Ionization processes involving the formation of both phenyl and benzyl ions

$$PhCH_2\text{-}Ph \longrightarrow PhCH_2^+ + Ph + e$$

$$PhCH_2\text{-}Ph \longrightarrow Ph + PhCH_2 + e$$

were studied with a view to estimating both the C-C bond energy, and the ionization potential of the phenyl radical, by the successive solution of the two equations:

$$D(PhCH_2\text{-}Ph) = A(PhCH_2^+) - I(PhCH_2)$$

$$I(Ph) = A(Ph^+) - A(PhCH_2^+) + I(PhCH_2) - E$$

The mean of this value forI(Ph) and the figure obtained from a study of the process $PhI \longrightarrow Ph^+ + I$ for which the bond energy is known accurately by kinetic measurements (72), was then to be used to calculate the Ph-H bond energy in benzene, by combining it with electron impact data for the process $Ph\text{-}H \longrightarrow Ph^+ + H$ in which case $D(Ph\text{-}H) = A(Ph^+) - I(Ph)$. Unfortunately, the electron impact data on diphenyl methane give upper limits for the benzyl-phenyl bond far too high to warrant discussion.

A value for the bond energy can be calculated in terms of the toluene bond strength, as before:

$$D(PhCH_2\text{-}Ph) = Qf(Ph) - Qf(PhCH_2\text{-}Ph) + Qf(PhCH_2\text{-}H) + D(PhCH_2\text{-}H) - Qf(H)$$

Now,/

Now, $\Delta f(Ph) = 70$ kcal (86)

$\Delta f(PhCH_2\text{-}Ph) = 33.2$ kcal (85)

$\therefore D(PhCH_2\text{-}Ph) = 74.4$ kcal

I(Ph)

No direct determination of the dissociation energy of the Ph-H bond in benzene has been made, although a number of estimates suggested 101-103 kcal as a likely figure. This has been confirmed by the recent experiments of Ladacki & Szwarc who calculate 101.4 kcal.(87). It is therefore justifiable to combine this quantity with the appearance potential of the phenyl ion from benzene, and to derive a value for the ionization potential of the phenyl radical:

$$I(Ph) = A(Ph^+)_{Ph\text{-}H} - D(Ph\text{-}H)$$
$$= 14.1 - 4.4 \text{ eV.}$$
$$= 9.7 \text{ eV.}$$

This is in good agreement with the figure of 9.9 eV obtained by Kandel (30) on the basis of electron impact work on ethyl benzene.

Conclusion.

Owing to the complexity of the ionization process in the case of aromatic molecules, it appears that the results of electron impact experiments are less valuable than those arising from thermal data, at any rate in the absence of the refinements which/

which permit the accurate measurement of kinetic energy, and the unmasking of fine structure, by the elimination of the effects of thermal energy spread. In spite of these limitations, even simple electron impact experiments may enable a decision to be made between rival values for a bond energy. The confirmed value may then be used to calculate other bond energies by means of suitable thermochemical cycles, some of which may be cross checked by direct E.I. data. For this reason, the accuracies of the derived bond energy terms are usually those associated with the thermochemical data employed, although in cases where good support is provided by direct E.I. cross checks, they may be improved somewhat.

PART 6.

THE IONIZATION POTENTIAL OF THE BENZYL RADICAL

INTRODUCTION

It was explained in Part 1, that the derivation of bond energies from electron impact data by the direct method involves a measurement of the ionization potential of the radical formed in the fissile step, and it was suggested that the experimental difficulties involved in such an experiment were so great that this energy term was usually calculated by indirect methods.

Prior to the experiment about to be described, the direct measurement of the ionization potential of a radical by electron impact had been accomplished by two research teams. In 1943 Stevenson and Hipple reported values for $I(CH_3)$ and $I(C_2H_5)$, the radicals having been produced by injecting the appropriate lead alkyl into the mass spectrometer, and decomposing it on the wall of a small furnace (88). Later $I(CH_2)$ was determined by the same method. (89). The only other contribution to this field was a paper by Lossing describing a reactor by means of which he was able to re-determine $I(CH_3)$ and also obtain values for the ionization potentials of the allyl and benzyl radicals. (21)

In view of the importance of the last of these quantities in an investigation of the general problem of bond energies among aromatic compounds, it was felt desirable to repeat the determination/

determination, and thereby confirm or refute the figure of 7.73 eV quoted in his paper.

More recently, further papers have appeared, one of them (90) describing the measurement of $I(CCl_3)$ and $I(CF_3)$, and others giving a value for $I(HO_2)$. (91) and I(OH) (92).

APPARATUS.

The original intention had been to produce benzyl radicals by the pyrolysis of dibenzyl in the reactor which is described in the next section, but owing to a delay in its construction, a simpler system was devised. The method resembled that used by Stevenson and Hipple (21) mentioned above, and details of the unit are included in the diagram of the source in Fig. 5.

The usual inlet pipe to the ion box was replaced by a quartz tube O wrapped with a coil of tungsten wire W. In order to increase the efficiency of the furnace, it was surrounded by a radiation shield consisting of a polished copper tube Q. Originally, nichrome wire had been employed for the winding, but at the temperature necessary to produce the radicals, enough nickel was vapourised to short the coils of the heater itself, and to break down the insulation of the ion gun. Rough temperature measurement was achieved by the insertion/

insertion of a themocouple (not shown) in the gas stream in the centre of the heated region.

It did not prove possible to observe benzyl radicals using dibenzyl as a source, since the temperature required to rupture the bond was high enough to cause breakdown of the glass insulators in the ionization chamber. However, the substitution of the less stable benzyl iodide reduced the wattage needed in the heater coil, and radicals were produced in abundance. The furnace temperature was held fairly constant by taking power supplies from a variac, backed by a constant voltage transformer, and high enough to cause total decomposition of the iodide; in this way small fluctuations in temperature did not affect the yield of radicals.

The associated gas handling system on the high pressure side of the inlet leak, was identical with that employed for the measurement of the appearance potential of the benzyl radical ion from benzyl iodide, including twin metrosil leaks, the partial pressure of the compound being controlled by a vapour jacket as described previously.

RESULTS

Seven measurements of the ionization potential of the benzyl radical were made, and in view of the large difference between/

between its value, and that of the ionization potential of argon, benzene was introduced as a secondary standard. The following results were obtained:-

Experiment	$I(Ph-H) - I(Ph-CH_2)$
51	1.46 eV
52	1.44
53	1.46
54	1.46
55	1.50
56	1.46
57	1.43
mean value	1.46 eV

The value ascribed to I(Ph-H) is 9.52 eV on the basis of the experiments described in Part 5, and which is in agreement with other reliable values which have appeared in the literature. From this assumption it follows that

$$I(Ph-CH_2) = 8.6_5 \text{ eV}$$

The only independent estimates have been made by Lossing et al (21) (61) who give values of 7.73 and 7.81, with a weighted mean of 7.76 eV. In view of the practical difficulties associated with the experiments, the difference between the two values is not large. It is interesting to note that a recent theoretical computation of the ionization potential/

potential of benzyl as 7.98 eV. has appeared since this work was completed (93). The implications of this determination of $I(Ph\text{-}CH_2)$ have been discussed already in Part 5.

PART 7.

DEVELOPMENT OF THE MASS SPECTROMETER FOR THE STUDY OF THE MECHANISM OF PYROLYTIC REACTIONS.

INTRODUCTION

Many of the papers published during the last two decades dealing with the mechanism of homogeneous reactions in the gas phase have served to emphasize the important role played by free radicals in such systems. This interpretation of the evidence has been gained laboriously by inductive reasoning, since the properties of these radicals do not lend themselves to direct investigation. Their short half lives preclude any method involving collection and examination in bulk, and in general their U.V. absorption spectra are not amenable to quantitative estimation. The electronic configuration of free radicals with one unpaired electron might suggest electron spin resonance as a method of detection and measurement, but although it has proved possible to design a cavity suitable for incorporation in a flow system, the signal strength is difficult to interpret in terms of concentration, as the relation is not a linear one.

The limitation posed by their short life under normal conditions of temperature and pressure, could be surmounted if the reaction were 'frozen' in some way. If at some time during the course of the reaction, a portion of the mixture is abstracted suddenly into a region of low pressure, the collision frequency will decrease concurrently, thus effectively stopping/

stopping the reaction at time t. If now this 'frozen' sample is examined by a detector of sufficiently high sensitivity in a time significantly less than that of the new half life of the reactant, even free radicals may be examined with relative ease. Its high sensitivity under conditions of high vacuum renders the mass spectrometer particularly suitable for this purpose. The first successful application of the instrument in this way was described by Eltenton (94) (95). His apparatus consisted of a reactor furnace situated above the ionization chamber of his mass spectrometer, the inlet leak comprising a small hole punched in a sheet of gold foil. He reported the presence of methyl radicals in the decomposition products of methane, ethane, dimethyl ether, and lead tetra-methyl; methylene in the decomposition of diazomethane, while ethyl and propyl radicals resulted from the reaction between methyl radicals and ethane and propylene respectively. The results of his experiments with low pressure flames suggested the existence of HO_2 in propane-oxygen flames and CHO in methane-oxygen systems.

This work has been followed by Lossing and his collaborators at the National Research Council Laboratories in Ottawa, who have studied the formation of a variety of radicals by this means. (96) (97) (99). By an ingenious development of this technique, these workers were able to make a direct assessment

of/

of the rate of recombination of methyl radicals. For a given geometry of a reactor furnace, the inlet leak, samples the products at a time t after leaving the hot zone, where t is determined by the rate of flow of carrier gas. Conversely, for constant flow of carrier gas (and reactant), t is dependent on the geometry of the system, so that if it is possible to increase the distance between the hot zone and the leak by making the furnace element retractable, the rate of disappearance of the radical with time may be measured. Details of this work may be found in (99).

By a method similar to that of Eltenton, Foner and Hudson have carried out a search for the HO_2 radical in flames (100) (101).

One or two instances are on record of decompositions being induced after the substance has entered the high vacuum system of the mass spectrometer. The work of Hipple and Stevenson (88) has been mentioned already in Part 6, while more recently, Robertson has studied the decomposition of a number of hydrocarbons on a hot wire (102). He has developed the method to study a number of simple hydroxylic compounds. (103) (104).

PROPOSED INVESTIGATION

It was intended originally that a number of reactions involving/

FIGURE 21.

Fig. 21.

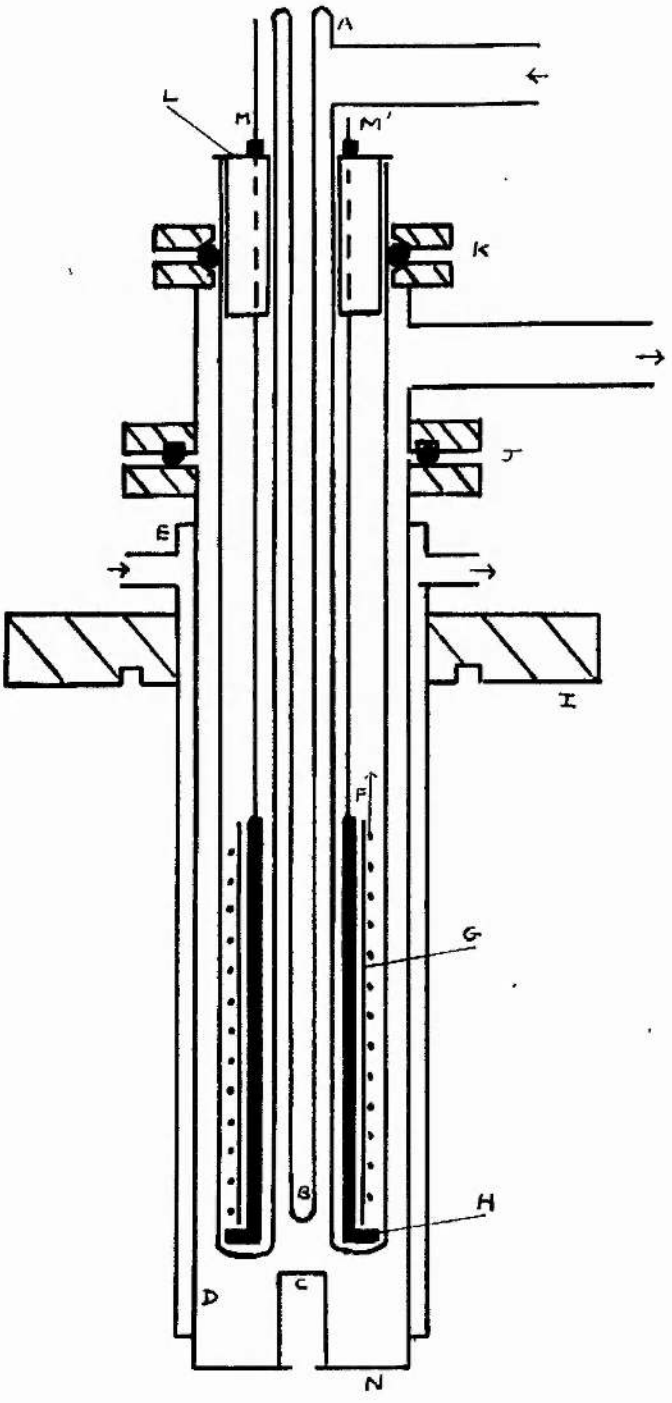

Diagram of the reactor furnace described in Part 7 used for the study of reaction mechanisms.

involving benzyl radicals should be investigated by this method. In particular, the thermal decomposition of mercury dibenzyl, and the rate of the subsequent dimerisation of the resultant benzyl radicals. The preparation and properties of this compound were studied by Calvert, (108) who showed that unfortunately it was not possible to get a sufficient quantity into the vapour phase for the investigation, due to its low vapour pressure and temperature sensitivity. This part of the work had therefore to be abandoned. Time did not permit more than a brief application of this technique, but the results obtained in the case of the thermal decomposition of benzyl iodide, serve to illustrate some of its potentialities for the elucidation of reaction mechanisms.

THE REACTOR FURNACE

This unit was designed to replace the uppermost inconel flange of the mass spectrometer supporting the normal inlet line, and its main features can be seen by reference to Figs. 21 & 22. Gas enters the hot zone along a quartz tube (a) fitted with a thermocouple well(B). After reaction the products are swept past the inlet leak (C) and are pumped away along the outside of the furnace. The outer body of the reactor (D) is composed of inconel tubing fitted with a water jacket (E). Heat is supplied by a solenoid wound

from/

from nichrome tape (F) on a former of silica tubing (G). The coils are prevented from sagging due to thermal expansion at high temperatures, by a series of minute blobs of silica produced by touching the surface with a silica rod in a hydrogen flame. An inconel sleeve (H) is interposed between the former and the furnace wall in order to achieve a more even temperature profile. By means of rods (m m') attached to this metal heat spreader, the furnace may be raised or lowered at will from the outside of the apparatus. The central quartz reactor is held along the axis of the assembly by means of a locating ring, constructed from nickel foil, surrounding its lower end. The seal between the two units is made by a rubber 'O' ring (K) protected from excessive heating by a water cooled copper block (L). The nichrome tape leading down to the solenoid is covered by ceramic insulators.

Two kinds of leak (C) were investigated, bearing in mind the necessity for withstanding temperatures approaching 1000°C. Initially, an attempt was made to simulate the quartz thimble described by Lossing (96) but efforts to produce holes in a controlled manner by means of a high frequency discharge proved unsuccessful. As an alternative, pieces of gold foil 0.001 in. thick were silver soldered to the upper ends of short cylinders of Nilo K tube. After brazing, the foil was supported on the/

FIGURE 22.

Fig. 22.

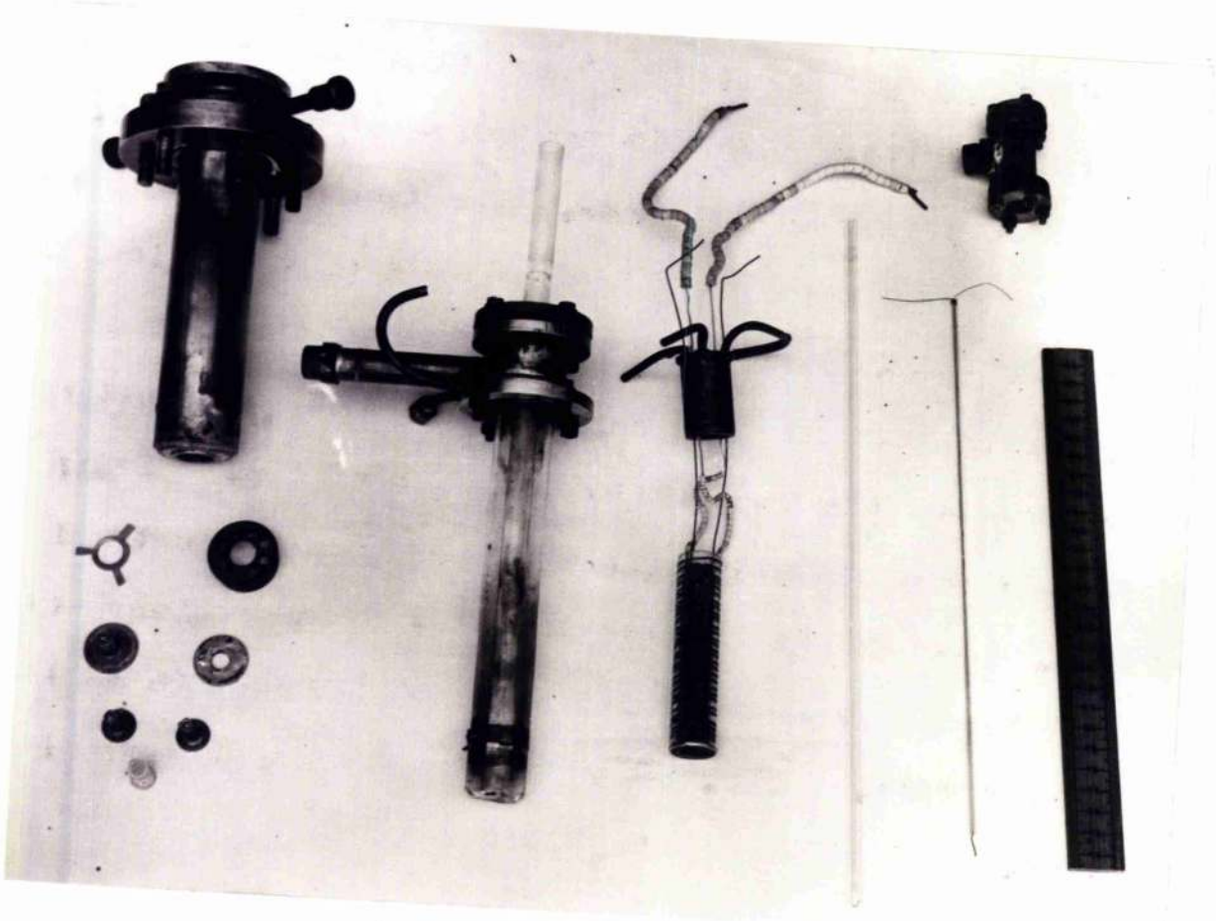

The reactor furnace dismantled.

the flat end of a centre punch covered with a single layer of tissue paper to act as a pad; a hole was then punched in the foil with the aid of a suitably sharp pointed needle. This was made by stroking the end of a heated tungsten rod with a stick of sodium nitrite. In this way holes of 0.001-2 in. diameter could be produced with ease. The leak was then fixed into position by soft soldering the other end of the Nilo K tube to a silver disc (N) with high melting point soft soldor (95% lead), the whole unit then being sealed into the bottom of the outer case of the reactor by eutectic solder. Owing to the stringent vacuum conditions required in some parts of the apparatus, a carefully devised sequence of operations was necessary for the construction, each one being followed by an appropriate leak test. Fig. 22 shows the essential components of the reactor.

ASSOCIATED FLOW SYSTEM.

Details of this part of the apparatus are shown in Fig. 23. The substance under examination was swept through the reactor by means of a carrier gas operating in a closed loop. Argon was employed for this purpose and was circulated by a mercury pump (S), traces of mercury vapour being removed by a cold trap (T) and demister (U).

The substance was injected into the gas stream in the saturator/

FIGURE 23.

Fig. 23.

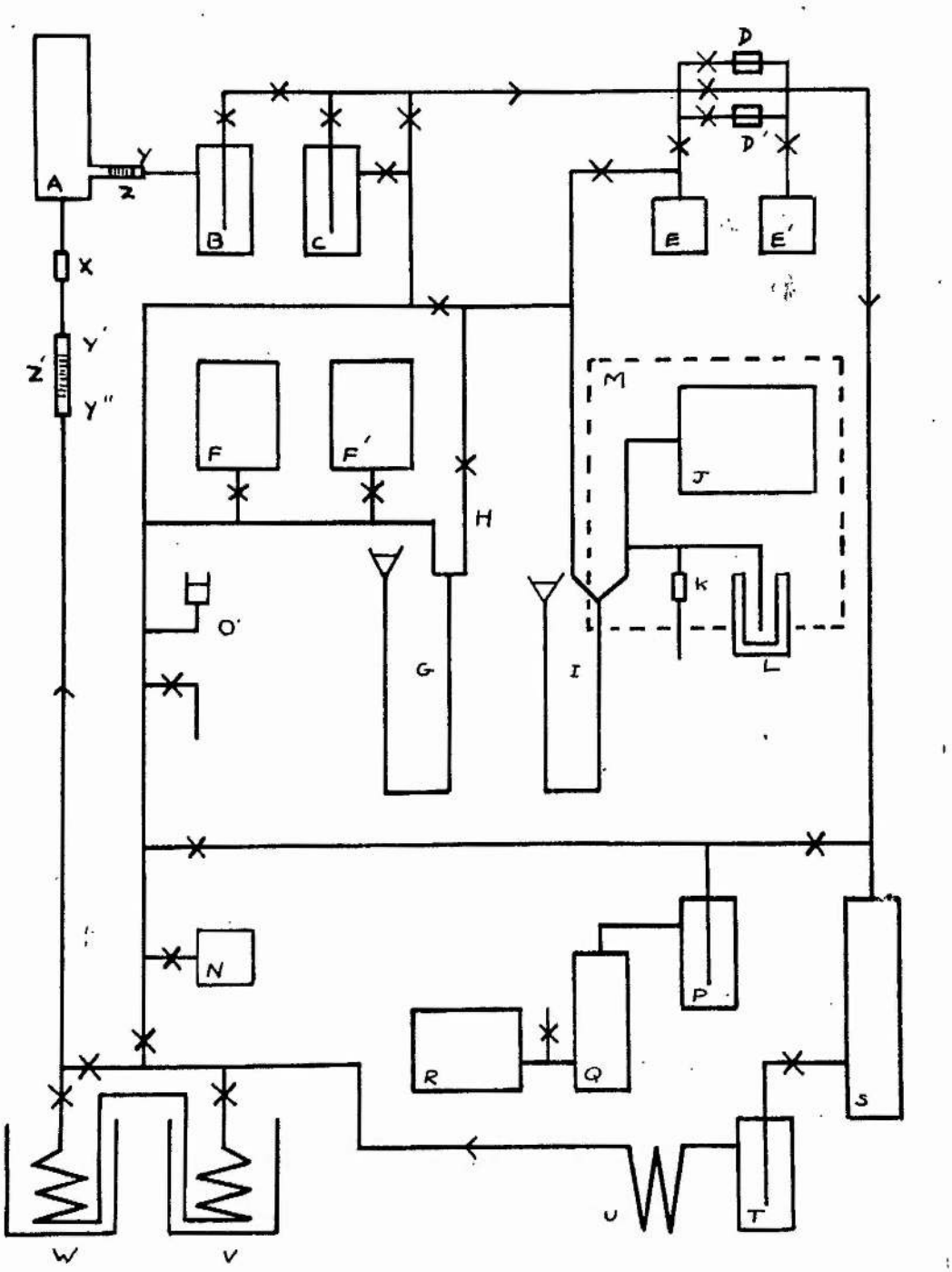

Complete gas handling system, including that used during measurements of appearance potentials, and the flow system employed for the decomposition of benzyl iodide.

saturator which consisted of two parts. In the first section (V) which was immersed in a bath some 10° higher than the temperature of that surrounding the second part (W), an excess of material was taken up into the vapour phase. Passage through the cooler chamber allowed equilibration to be achieved, corresponding to the saturation vapour pressure at the lower temperature.

The gas handling system was connected to the reactor by a silica to pyrex seal (X) and a metal to glass seal (Y). Two stainless steel bellows (z,z') offered protection against shock, the former being interposed in the glass line with the aid of two metal to glass seals (Y; Y"). Any condensible products are removed from the effluent gas by the cold trap (B) and the carrier gas is them returned to the circulating pump through the capillary tubes (D, D'), the rate of flow being indicated by the pressure drop across the appropriate capillary, as measured by the twin McLeod gauges (E, E'). Since the rate of many reactions is modified by the presence of traces of oxygen, a sodium trap (C) was incorporated, through which the carrier gas might be circulated prior to the experiment.

The vacuum tightness of the apparatus was checked by a high sensitivity McLeod gauge (N), pumping being provided by a rotary oil pump (R), mercury diffusion pump (Q), and cold/

cold trap (P). All taps and joints were coated with a rubber-based high vacuum grease, except those coming into contact with the compound under study. These were treated with the minimum quantity of a silicone preparation.

THE DECOMPOSITION OF BENZYL IODIDE.

Pure benzyl iodide was placed in the first half of the saturator, and degassed by alternate heating and cooling (CO_2/acetone) the latter operation being accompanied by prolonged pumping. The benzyl iodide was finally frozen down, while argon at 0.75 mm was circulated over hot sodium for one hour. The sodium trap was isolated from the rest of the apparatus, and baths at 20° and 10.5°C were placed round the two sections of the saturator.

The first experiment was to search for the appearance of benzyl radicals in the decomposition products, as the temperature of the reactor, through which the benzyl iodide was flowing, increased. In Patts 5 & 6 the values 8.05 eV, 9.65 eV, and 10.0 eV. have been shown to represent the ionization potential of the benzyl radical, and the appearance potentials of the benzyl ion from benzyl iodide and dibenzyl respectively. It follows, that if the electron accelerating energy is held at a value intermediate between the last two figures, the contribution to the ion current at mass 91 from benzyl/

FIGURE 24.

Fig. 24.

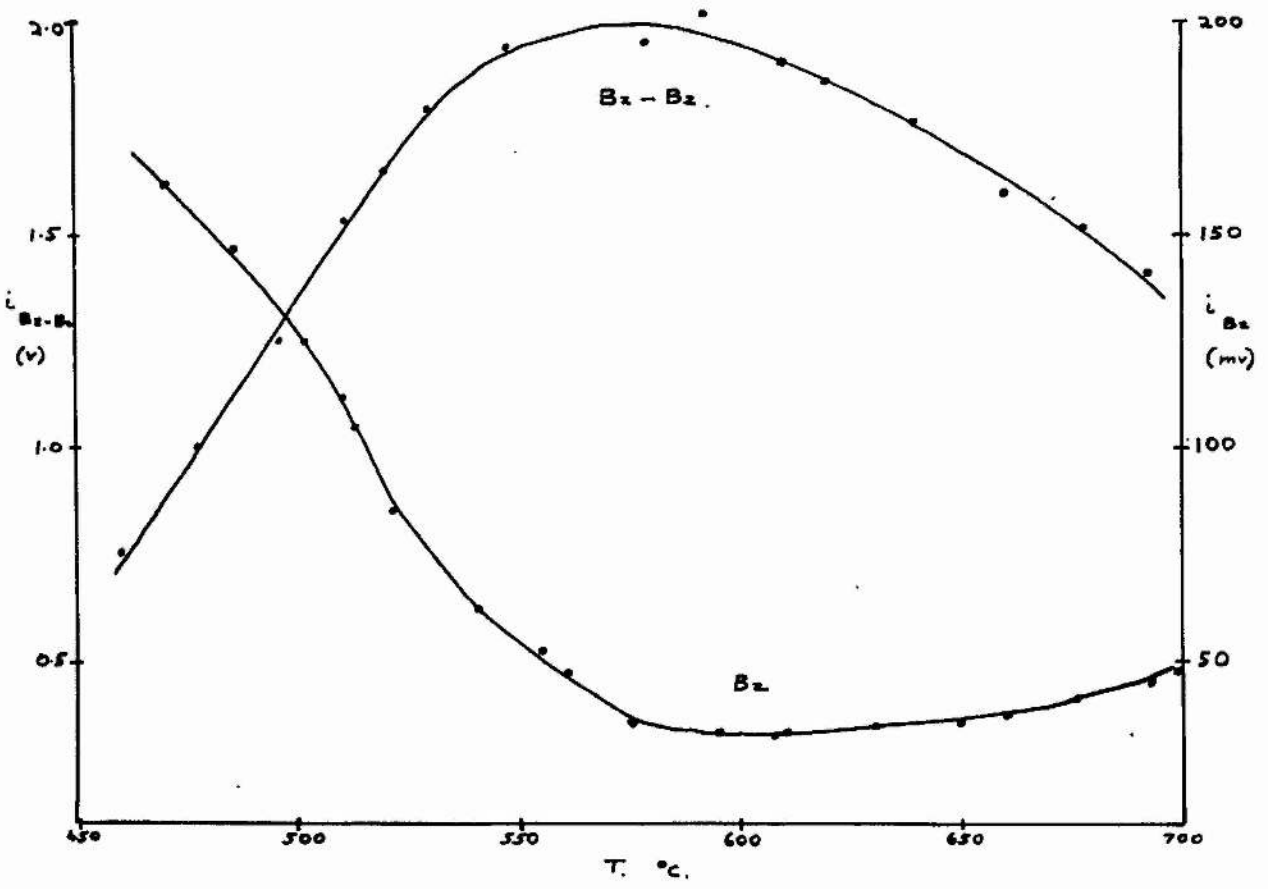

Results obtained in the experiments on the decomposition of benzyl iodide.

benzyl iodide will be small but observable, while that from dibenzyl will have vanished. On the other hand the instrument will possess a high sensitivity towards benzyl radicals.

Power was supplied to the furnace heater from a variac fed by a constant voltage transformer, and the temperature of the hot zone was recorded with the aid of a chromel-alumel thermocouple. Fig. 24 shows the variation in the size of the beam at mass 91 as a function of furnace temperature. The fall in ion current which occurs as the temperature rises, shows that increasing decomposition of the benzyl iodide is taking place, but that some mechanism is preventing any benzyl radicals formed in the process, from reaching the leak. Above 620°C. the size of the 91 peak begins to increase again. It was assumed that the results could be explained by an initial decomposition $PhCH_2-I \longrightarrow PhCH_2 + I$, followed by a dimerisation of the resultant benzyl radicals.

In order to verify this, the mass spectrometer was tuned to mass 182 (the parent ion of dibenzyl), and the experiment repeated over the same temperature range. Further reference to Fig 24 shows that there is a close correlation between the increase of dibenzyl and the disappearance of benzyl iodide. Furthermore, above 600°C. the dibenzyl itself begins to decompose, and this explains the increase of the 91 peak at higher temperatures, already noted, since the percentage decrease/

decrease and increase of the two peaks over the temperature range 600-700°C. are in agreement.

The failure to observe benzyl radicals was due simply to inadequate pumping speed through the reactor, and although attempts were made to increase it, the speed was still insufficient for the purpose. Unfortunately time was not available to effect the necessary alterations to remedy this defect.

REFERENCES & BIBLIOGRAPHY.

REFERENCES.

1. Hustrulid, Kusch & Tate, Phys. Rev. 54, 1037, (1938)
2. Franck, Trans,Far.Soc., 21, 536, (1925)
3. Condon, Phys.Rev., 28, 1182, (1926)
4. Condon, Phys. Rev., 35, 658, (1930)
5. Honig, J.Chem.Phys., 16, 105, (1948)
6. Morrison & Nicholson, J.Chem.Phys., 20, 1021, (1952)
7. Happ & Stewart, J.A.C.S., 74, 4404, (1952)
8. McDowell & Warren, Disc.Far.Soc., No.10, 53, (1951)
9. Robertson, Mass Spectrometry, Methuen, London, (1954)
10. Oldenberg, J.Chem.Phys., 13, 196, (1945)
11. Morrison, J.Chem.Phys., 19, 1305, (1951)
12. Long & Norrish, Proc,Roy.Soc., A 187, 337, (1946)
13. Morrison, J.Chem.Phys., 21, 1767, (1953)
14. Morrison, J.Chem.Phys., 22, 1219, (1954)
15. Fox, Hickam, Kjeldaas & Grove, Phys.Rev., 84, 859, (1951)
16. Fox, Hickam & Kjeldaas, Phys.Rev., 89, 555, (1955)
17. Vought, Phys.Rev. 71, 93, (1947)
18. Stevenson, Disc.Far.Soc., No.10, 35, (1951)
19. Warren, Nature, 165, 810, (1950)
20. Thorburn, Private Communication
21. Lossing, Ingold & Henderson, J.Chem.Phys., 22, 621, (1954)
22. Lossing, Ingold & Henderson, J.Chem.Phys., 22, 1489, (1954)
23. Lossing Tickner & Bryce, J.Chem.Phys., 19, 1254, (1951)

24/

24. Foner, Kossiakoff & McClure, Phys.Rev., 74, 1222, (1948)

25. Fox & Hipple, Rev. Sci.Inst., 19, 462, (1948)

26. Hagstrum, Rev.Mod.Phys., 23, 185, (1951)

27. Stevenson, J.Chem.Phys., 18, 347, (1950)

28. McDowell & Warren, Trans.Far.Soc., 48, 1084, (1952)

29. Lozier, Phys.Rev., 36, 1285, (1930)

30. Kandel, J.Chem.Phys., 22, 1496, (1954)

31. Thomson, Rays of Positive Electricity and their application to Chemical Analysis, Longmans Green & Co. London, (1913)

32. Franck & Hertz, Vert.Deut.Phys.Ges., 15, 34, (1913)

33. Aston, Phil.Mag., 49, 1172, (1915)

34. Dempster, Phys.Rev., 11, 316, (1918)

35. Smythe, Proc.Roy.Soc. A 102, 285, (1922)

36. Bleakney, Phys.Rev., 40, 496, (1932)

37. Smith, Phys.Rev., 51, 263, (1937)

38. Nier, Rev. Sci.Inst., 11, 212, (1940)

39. Nier, Rev. Sci.Inst., 18, 398, (1947)

40. Jones & Hall Disc. Far.Soc., No.10, 18, (1951)

41. Hall, Proc.Roy.Soc., A 205, 541, (1951)

42. Hall, Proc.Roy.Soc., A 213, 102, (1952)

43. Franklin, J.Chem.Phys., 22, 1304, (1954)

44. Walsh, Qu.Rev., 2, 73, (1948)

45. Barber, Proc.Leeds, Phil.Soc., 2, 427, (1933)

46. Stephens, Phys.Rev., 45, 513, (1934)

47. Herzog, Z.Phys., 89, 463, (1934)

48/

48. Barnard, Modern Mass Spectrometry, Institute of Physics, London, (1953).

49. Graham, Harkness & Thode, J.Sci.Inst., 24, 119, (1947)

50. Philips Research Report No. 9, 1, (1954)

51. Brown, Elect. Eng., 24, 171, (1952)

52. Nielson, Rev.Sci.Inst., 18, 18, (1947)

53. Penick, Rev.Sci.Inst., 6, 115, (1935)

54. Peirson, Elect.Eng., 22, 48, (1950)

55. Szwarc, J.Chem.Phys., 16, 128, (1948)

56. American Petroleum Institute, Research Project No.44

57. Waldron, Trans.Far.Soc., 50, 102, (1954)

58. Bacher, & Goudsmit, Atomic Energy States, McGraw Hill Book Co., New York (1932)

59. Price, Phys.Rev., 47, 444, (1935)

60. Price, J.Chem.Phys., 4, 147, (1936)

61. Farmer, Henderson, McDowell & Lossing, J.Chem.Phys., 22, 1948, (1954)

62. Field & Franklin, J.Chem.Phys., 22, 1895, (1954)

63. Scott & Brickwedde, J.Research, Nat.Bur.Stand., 35, 501, (1945)

64. Price & Wood, J.Chem.Phys., 3, 439, (1935)

65. Nief, J.Chim.Phys., 48, 333, (1951)

66. Higasi, Omura & Baba, J.Chem.Phys., 24, 623, (1956)

67. Fox & Hickam, J.Chem.Phys., 22, 2059, (1954)

68/

68. Price & Walsh, Proc.Roy.Soc. A, 191, 22, (1947)

69. Schissler & Stevenson, J.Chem.Phys., 22, 151, (1954)

70. Franklin & Lumpkin, J.Chem.Phys., 19, 1073, (1951)

71. Calvert, Unpublished work.

72. Cowan, Ph.D. thesis, St.Andrews. (1952)

73. Szwarc, Disc.Far.Soc., No.10, 228, (1951)

74. Anderson, Scheraga & Van Artsdalen, J.Chem.Phys., 21, 1258, (1953)

75. Blades, Blades & Steacie, Can.J.Chem., 32, 151, (1954)

76. U.S. Nat.Bur.Stand.Circular No.500, Selected Values of Chemical Thermodynamic Propoerties, Washington,(1952)

77. Horrex & Miles, Disc.Far.Soc., No.10, 233, (1951)

78. Szwarc, J.Chem.Phys., 17, 431, (1949)

79. Hartley, Pritchard & Skinner, Tr.Far.Soc., 46, 1019, (1950)

80. Butler & Polanyi, Trans.Far.Soc., 39, 19, (1943)

81. Gellner & Skinner, J.C.S., 1145, (1949)

82. Graham, Nichol & Ubbelohde, J.C.S., 115, (1955)

83. Szwarc,& Taylor, J.Chem.Phys., 22, 270, (1954)

84. Roberts & Skinner, Trans.Far.Soc., 45, 339, (1949)

85. Parks, West, Naylor, Fujii & McClaine, J.A.C.S., 68, 2524, (1946)

86. Szwarc & Williams, J.Chem.Phys., 20, 1171, (1952)

87. Ladacki & Szwarc, Proc.Roy.Soc.A, 219, 341, (1953)

88. Hipple & Stevenson, Phys.Rev., 63, 121, (1943)

89./

89. Langer, Hipple & Stevenson, J.Chem.Phys., 22, 1836, (1954)

90. Ingold, & Bryce, J.Chem.Phys., 24, 360, (1956)

91. Foner & Hudson, J.Chem.Phys., 23, 1364, (1955)

92. Foner & Hudson, J.Chem.Phys., 25, 603, (1956)

93. Tanaka & Komatsu, J.Chem.Phys., 23, 976, (1955)

94. Eltenton, J.Chem.Phys., 10, 403, (1942)

95. Eltenton, J.Chem.Phys., 15, 455, (1947)

96. Lossing & Tickner, J.Chem.Phys., 20, 907, (1952)

97. Lossing, Ingold & Tickner, Disc. Far.Soc., No.14, 34, (1953)

98. Ingold & Lossing, Can.J.Res. 31, 30, (1953)

99. Ingold & Lossing, J.Chem.Phys., 21, 1135, (1953)

100. Foner & Hudson, J.Chem.Phys., 21, 1374, (1953)

101. Foner & Hudson, J.Chem.Phys., 21, 1608, (1953)

102. Robertson, Proc.Roy.Soc., A, 199, 394, (1949)

103. Robertson, Mass Spectrometry, P.47, Inst. of Petroleum, London, (1952)

104. Robertson, Applied Mass Spectrometry P.112, Inst. of Petroleum, London, (1954)

105. Coops, Mulder, Dienske & Smittenberg, Rec.Trav.Chim., 65, 128, (1946)

106. Stuld, Ind.Eng.Chem., 39, 517, (1947)

107. Handbook of Chemistry & Physics.

108. Calvert, Ph.D. thesis.

BIBLIOGRAPHY.

Aston, Mass Spectra & Isotopes, Arnold, London, (1942)

Barnard, Modern Mass Spectrometry, Inst. of Phys. London, (1953)

Barnard, Mass Spectrometer Researches, N.P.L. publication, H.M. Stationery Office, (1956)

Cottrell, The Strengths of Chemical Bonds, Butterworths Scientific publications, London, (1954)

Dunning, Mass Spectrometry in Chemistry, Quart. Revs Vol IX P.23, (1955)

Gaydon, Dissociation Energies & Spectra of Diatomic Molecules, Chapman & Hall, London, (1947)

Hagstrum, Rev.Mod.Phys., 23, 185, (1951)

Inghram & Hayden, Mass Spectrometry, Nuclear Science Series, Report No.14, National Academy of Sciences.

Herzberg, Molecular Spectra & Molecular Structure, I, Spectra of Diatomic Molecules, Prentice Hall, 2nd Edn. New York, (1950)

Institute of Petroleum, Mass Spectrometry, London (1952)

Inatitute of Petroleum, Applied Mass Spectrometry, London, (1954)

Massey & Burhop, Ionisation & Electron Impact Phenomena, Oxford University Press, (1952)

Mayne, Mass Spectrometry, Rep. on Prog. in Phys., 15, 24, (1952)

Craggs & McDowell, The Ionization & Dissociation of Complex Molecules by Electron Impact, Reports on Progress/

Progress in Phys., 18, 374, (1955)

Robertson, Mass Spectromery, Metheun, London (1954)

Szwarc, The Determination of Bond Dissociation Energies by Pyrolytic Methods, Chemical Reviews, 47, 75,(1950)

Szwarc, Bond Dissociation Energies, Quart.Revs.Vol.V,P.22,(1951)

Thode & Shields, Mass Spectrometry, Reports on Progress in Phys., 12, 1, (1948)

Walsh, Far.U.V. Spectra, Ionization Potentials and their significance in Chemistry. Quart.Rev. Vol.II, P.73. (1948)

APPENDIX I

NOMENCLATURE

E.I.	Electron Impact.
I.E.	Ionization efficiency.
eV.	Electron-volt = 23.06 kcal.
Ph-	Phenyl group.
$A(R_1)_{R_1-R_2}$	Appearance potential of the ion R_1 in the mass spectrum of the molecule R_1-R_2.
$I(R)$	Ionization potential of the species R.
$I_s(R)$	Spectroscopically determined ionization potential.
$D(R_1-R_2)$	Dissociation energy of the bond R_1-R_2.
$Qf(X)$	Heat of formation of X for gas phase at 25°C $= \Delta Hf^{\circ}(X)$
$E(X)$	Excess energy associated with X, due to the molecule being in an excited state.
$K(X)$	Kinetic energy of the species X.
dV	Voltage difference between points on two ionization efficiency curves corresponding to the same ion current.

APPENDIX II

Collated list of thermochemical data used in this thesis.

Q_f(H)	52.0 kcal	(76)
(Cl)	29.0	(76)
(I)	25.5	(76)
(CO_2)	94.05	(76)
(H_2O)	68.32	(76)
(CH_3)	32.5	(79)
(Ph)	70.0	(86)
($PhCH_3$)	11.95	(56)
($PhCH_2CH_3$)	7.12	(56)
($PhCH_2Ph$)	33.2	(85)
($PhCH_2CH_2Ph$)	29.7	from $Q_{comb.}$ = 1805.7 kcal (105)
		L_{evap} = 13.3 kcal (106)
		L_{fus} = 5.64 (107)
($PhCH_2I$)	26.4	(81)
($PhCH_2Cl$)	5.2	(69) & (84)